Physiological involvement of presynaptic L-type voltage dependent calcium channels in GABA release of cerebellar molecular layer interneurons

Stéphanie Rey

THESE DE DOCTORAT DE L'UNIVERSITE PARIS DESCARTES

Ecole Doctorale Cerveau-Comportement-Cognition

Spécialité

NEUROSCIENCES

Présentée par :

Stéphanie Rey

Pour obtenir le grade de :

DOCTEUR DE L'UNIVERSITE PARIS DESCARTES

Sujet de thèse :

Physiological involvement of presynaptic L-type voltage dependent calcium channels in GABA release of cerebellar molecular layer interneurons

Soutenue le 13 Décembre 2013

Devant le jury composé de :

Régis Lambert, président du jury

Oussama El-Far, rapporteur

Philippe Lory, rapporteur

Rossella Conti, invitée

Anne Feltz, invitée

Claire Legay, invitée

Thibault Collin, directeur de thèse

Remerciements

Je tiens tout d'abord à remercier Alain Marty de m'avoir permis de réaliser ma thèse au sein de son laboratoire et pour son soutien durant ces trois années de thèse.

J'adresse de chaleureux remerciements à mon directeur de thèse Thibault, merci de m'avoir encadré durant ma thèse, de m'avoir guidé, conseillé et de votre aide lors de la rédaction de ce manuscrit. Je garderai toujours un bon souvenir de vos dégustations de Kusmi tea (surtout le detox).

Je tiens à remercier Philipe Lory et Oussama El-Far d'avoir accepté d'être rapporteur de ma thèse.

Merci à Régis Lambert, Claire Legay, Rossella Conti et Anne Feltz d'avoir accepté de faire partie de mon jury de thèse.

Merci à Isabel de m'avoir encouragé et soutenu pendant ces trois années et pour mes recherches de postdoc. Merci encore de m'avoir permis d'aller au Brésil.

Merci à Ali pour m'avoir initié à immunohistochimie et à la microscopie confocale. Merci encore de m'avoir soutenu et conseillé dans ma découverte de la microscopie électronique et dans la vie de tous les jours.

Merci à Alain Schimtt pour m'aidé et conseillé lors de mon apprentissage de la microscopie électronique. J'espère que nous collaborerons ……

Merci à Philippe de m'avoir prêté de nombreux articles sur la pharmacologie des canaux calciques. Ils sont été très utiles.

Merci aussi à Jacsue pour tes mots réconfortants et tes petits gâteaux qui étaient très bienvenue surtout les weekends d'écriture de la thèse.

Merci à Jonathan pour m'avoir signalé et envoyé des articles venant d'être publiés sur les canaux calciques et d'avoir corrigé ma lettre de motivation qui m'a permis d'aller au cours EMBO.

Merci à Brandon pour m'avoir aidé dans ma recherche de postdoc, pour ses corrections et ses suggestions pour mes lettres de motivation.

Je remercie Luc de m'avoir aidé avec mes problèmes d'ordinateur et surtout pour la connection à distance sur Lilith. Je reconnais qu'il n'est pas impossible qu'une partie du problème se situe entre la chaise et l'ordinateur…

Merci à tous ceux qui ont quitté le laboratoire et qui me manquent beaucoup: Gilliane, Gaelle et Pancho.

Merci à Guadalupe, Camila, Javier, Jin, Elric et Pepe pour votre bonne humeur et vos petits mots réconfortant pendant l'écriture de ma thèse.

Un grand merci à tous ceux qui ont partagé ma vie au laboratoire de physiologie cérébrale et tous ceux que je connais au St Pères : David Ogden, Céline, Sandrine, Fede, Catherine, Félicité, David Dubayle, Christophe, Visou, Paloma, David Orduz, Brice, Patrick, Patrice……

Mes remerciements les plus tendres sont pour ma mère. Merci de tout mon cœur pour ton écoute et ton soutien depuis ma plus tendre enfance.

Merci Alexis, mon amour pour ton écoute et tout ton amour.

Durant la rédaction de mes remerciements, j'ai réalisé que je viens de passer 8 ans à étudier au St Pères. Je me revois en L1 assistant au cours de Claire Legay et me rappelle de mon premier stage en laboratoire comme si c'etait hier. Le temps passe si vite…

A ma grand-mère, Thérèse

Résumé :

La libération de neurotransmetteur est provoquée par la dépolarisation de la terminaison présynaptique et l'entrée de calcium à travers les canaux calciques voltage-dépendants (VDCCs). Les VDCCs à haut seuil de type-P/Q et de type-N sont classiquement impliqués dans la libération de neurotransmetteurs et sont localisés dans la terminaison axonale près de la zone active. Deux membres de la famille des VDCCs de type-L, $Ca_v1.2$ et $Ca_v1.3$ sont connus pour être exprimés dans le système nerveux central. Dans le cortex cérébelleux, les propriétés pharmacologiques des VDCCs présynaptiques ont été examinées aux synapses GABAergiques entre les interneurones de la couche moléculaire (MLIs) et entre les MLIs et les cellules de Purkinje. Bien qu'il n'y ait aucun doute que les VDCCs de type-P/Q et de type-N sont les principaux acteurs de l'entrée de calcium présynaptique et de la libération de GABA par les MLIs, l'absence d'effet des dihydropyrines antagonistes a exclut le potentiel rôle des VDCCs de type-L (Forti et al., 2000; Stephens et al., 2001). Il est intéressant de noter que les dihydropyrines antagonistes sont très peu efficaces sur les courants calciques de type-L activés par un potentiel d'action (Helton et al., 2005), ce qui suggère que l'implication des VDCCs de type-L dans la libération de neurotransmetteur a été largement négligée.

Dans cette étude, nous avons montré que le BayK8644 (une dihydropyridine agoniste) augmente fortement la fréquence des mIPSCs enregistrés dans les MLIs et dans les cellules de Purkinje suggérant que les VDCCs de type-L peuvent être présents dans les terminaisons axonales des MLIs. Ce résultat a été confirmé par des expériences d'immunohistochimie utilisant la microscopie confocale et électronique ainsi que par des expériences d'imagerie calcique. Nos résultats démontrent que les VDCCs de type-L, souvent négligés dans les terminaisons axonales, ont un rôle crucial dans la libération de GABA par les MLIs.

Table of contents

List of abbreviations

cAMP	cyclic adenosine monophosphate
CNS	Central nervous system
DHP	Dihydropyridines
ER	Endoplasmic reticulum
EPSC	Excitatory synaptic current
HVA	High Voltage Activated
IP3R	inositol 1,4,5,-triphosphate receptor
IPSC	Inhibitory synaptic current
IV	Current-voltage
KO	knockout
LTP	Long term potentiation
LVA	Low Voltage Activated
MLI	Molecular layer interneuron
mIPSC/mEPSC	miniature IPSC/ miniature EPSC
P	Postnatal days old
PPR	Paired pulse ratio
PSD	Postsynaptic density
PTP	Posttetanic potentiation
RyR	Ryanodine receptor
SCaTs	Spontaneous calcium transients
TTX	Tetrodotoxine
WCR	Whole cell recording

List of illustrations

Introduction

Materiels and Methods

Results

Chapter 1

Introduction

1.1 Cerebellum:

Studying the cerebellum is of primary importance in the field of neuroscience. It bears a unique crystalline structure and is traditionally acknowledged to be involved in motor control although recent studies have postulated its role in several cognitive processes (Glickstein et al., 2009, 2011). Historically, the first neuron ever was observed in the cerebellum by J.E Purkinje (1837) and is referred to as “Purkinje cell” since. Moreover, the typical cerebellar circuitry inspired the “neuronal theory” to Ramón y Cajal (1894).

1.1.1 Anatomy and connections with other part of the brain.

In all vertebrates, the cerebellum is a distinct subdivision of the central nervous system (CNS) localized in the rostral roof of the fourth ventricle (Fig1). The cerebellum consists of the cerebellar cortex and cerebellar deep nuclei (fastigial, dentate and interpositus nuclei) enclosed within the white matter. The cerebellum is divided into two hemispheres connected by a central region, the vermis. Ten lobes are easily distinguished in parasagittal section and grouped in three major classes: anterior lobe (lobes I to V), posterior lobe (lobes VI to IX) and flocculonodular lobe (lobe X) (Fig 2, Palay & Chan-Palay, 1974).

Fig 1: Dorsal view of adult rat CNS including cerebellum.
Note the vermis (v), one of the two hemispheres (h) an the paraflocculus (p).
(From Palay & Chan-Palay, 1974).

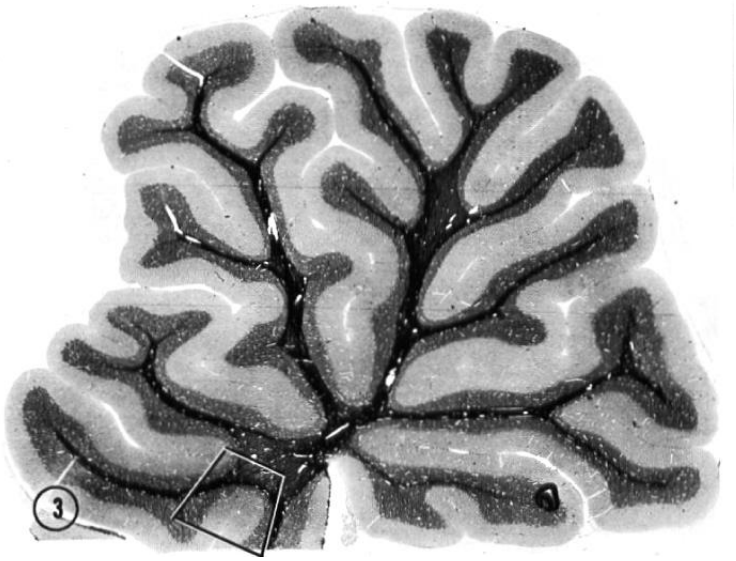

Fig 2: Parasagittal section of adult rat cerebellum.
Lobes are numbered from I to X. Note that the lobule I is cut. The three layers of the cerebellum can be easily recognized: the molecular layer (light-gray), the granular layer (dark-grey) and the white matter (black). Cerebellum is stained using toluidine blue epoxy.
(Modified from Palay & Chan-Palay, 1974).

The efferent projections of the cerebellar cortex are formed by Purkinje cell axons, the greatest number of which connects to the deep cerebellar nuclei. The cerebellum is connected to the rest of CNS by the three pairs of cerebellar peduncles (superior, middle and inferior peduncle) resulting from bundles of afferent and efferent fibers. The major output pathway of the cerebellum leaves through the superior peduncle and is composed of fibers originating from the deep nuclei. The efferent fibers of the superior peduncle contact the reticular formation, the red nucleus and the thalamus (ventrolateral and ventroanterior nuclei). The inferior peduncle carries efferent fibers coming from the fastigial nuclei and direct projections of Purkinje cells of the flocculonodular lobe to the vestibular nuclei. The afferents of the cerebellum can be divided into four groups: vestibular, ascending spinal, descending pontine nucleus (which receives input from the cerebellar cortex), olivary and reticular. The vestibular afferents reach the cerebellar cortex though the inferior peduncle; it distribute to the fastigial nucleus and to the flocculonodular lobe. Moreover, afferents from spinal cord also enter though inferior peduncle and distribute in the anterior lobe and part of the posterior vermis. Moreover, the afferents from the inferior olive and the reticular formation enter the cerebellum though the inferior peduncle. Finally, the middle peduncle only contains afferent fibers emerging from the pontine nuclei; it distributes to all the cerebellar cortex.

1.1.2 Cerebellar functions.

The first experimental approaches aiming to tackle cerebellar functions were based on animal cerebellar lesions or ablations and started in the beginning of the 19th century. Luigi Rolando observed the first motor symptoms following a cerebellar lesion in 1809 and he concluded that the cerebellum was involved in instating movement (Rolando, 1809). Thereafter, Pierre Flourens (1824) noted that a cerebellum ablation did not prevent the movements but mainly altered their coordination. At the end of the 19th century, Luigi Luciani

classified the various symptoms caused by cerebellar lesions as atonia, ataxia and loss of continuity of movement (Luciani, 1891). The involvement of the cerebellum in motor coordination was further confirmed by clinical studies over the 20th century (Sammet, 2007; Glickstein, 2009 and 2011 for review).

In recent years, it has been proposed that the cerebellum plays a role in cognitive processes. First of all, the cerebellum has been shown to be anatomically connected to prefrontal cortex (Middleton & Strick, 2001) and clinical studies have demonstrated an involvement of the cerebellum in language (Riva & Giorgi, 2000) and dyslexia (Nicolson & Fawcett, 2005). Furthermore, cerebellum seems to be involved in the pathology of autism. In fact, postmortem studies showed histoanatomic abnormalities in autistic individuals as a decrease in the number of Purkinje cells and abnormalities in deep cerebellar nuclei (Fatemi et al., 2012 for review).

1.1.3 Cerebellar cortex organization: cellular and ultrastucture description.

References used for the morphological description and organization of the cerebellar cortex are: Ramón y Cajal (1911), Chan-Palay & Palay (1972), Palay & Chan-Palay (1974), and Sotelo (2010) unless otherwise stated.

1.1.3.1 Cellular organization of the cerebellar cortex.

The cerebellar cortex bears a simple and uniform organization in three layers: molecular layer, granular layer and white matter (Fig 2). Between the molecular layer and the granular layer, the Purkinje cell layer is composed by a single row of Purkinje cell somata. Within granular and molecular layer, several types of neurons have been identified: granule cells, molecular layer interneurons (MLIs: basket cells and stellate cells), Golgi cells, Lugaro

cells and unipolar brush cells. Granule cells and unipolar-brush cells are excitatory glutamatergic neurons whereas Purkinje cells, MLIs, Golgi and Lugaro cells are inhibitory GABAergic neurons (Fig 3). Besides, astrocytes, oligodendrocytes, Bergman cells, microglia and NG2(+) cells are glial cell types commonly found in the cerebellum.

At the connectivity level, the cerebellar cortex receives two excitatory glutamatergic inputs: climbing fiber and mossy fiber, which respectively arise from the inferior olive and brainstem/spinal cord. Climbing fibers directly contact Purkinje cell somata and dendrites. Note that one Purkinje cell is contacted by only one climbing fibers but makes around 200 synapses. Mossy fibers form the major input to the cerebellum and they establish contacts with the granule cells and Golgi cell in a typical structure called glomerulus and hence make indirect contact with Purkinje cells. The cerebellum unique ouput is formed by the axons of Purkinje cells (Fig 3). These latter project through the granular cell layer into the white mater and terminate on deep cerebellar nuclei and on some brainsterm nuclei. Sometimes, Purkinje cell axons project in the molecular layer (Ramón y Cajal, 1911; Orduz & Llano, 2007).

1.1.3.2 Light and electron microscopy cell descriptions.

A czech physiologist Jan Evangelista Purkinje described the first neuron in 1837: it was a rather large neuron of the human cerebellar cortex (Fig 4). In 1873, Camillo Golgi developed selective silver staining of neurons which allowed the observation of the neurons and their processes in black in a clear background. He was the first to report the Purkinje cell dendritic tree and the axon description. In the beginning of 20th century, Ramón y Cajal proposed a definitive picture of the cellular organization and connectivity of the cerebellar cortex arises through the use a refined Golgi's method. In addition, two types of interneurons were introduced after the Cajal period namely Lugaro cells and unipolar brush cells. The development of electron microscopy techniques in the 1950s brought up the ultrastructural

description of cerebellar cells and synapses beautifully summarized in the work of Palay and Chan-Palay (1974).

A

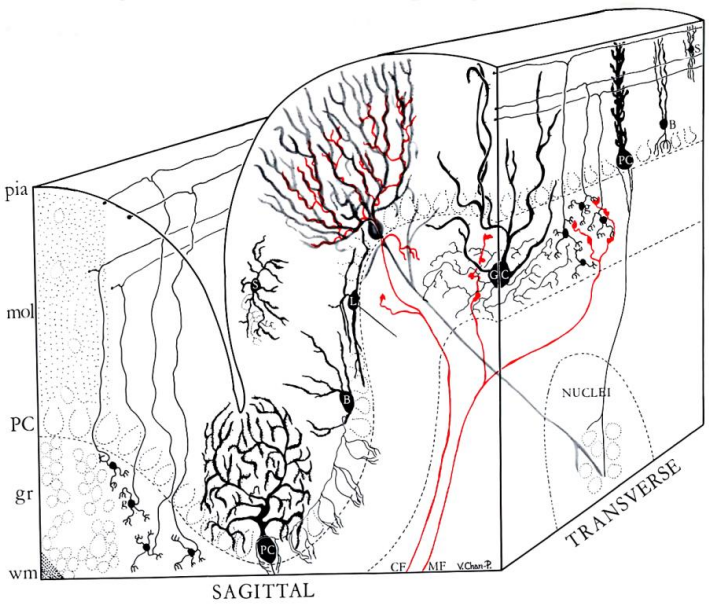

B

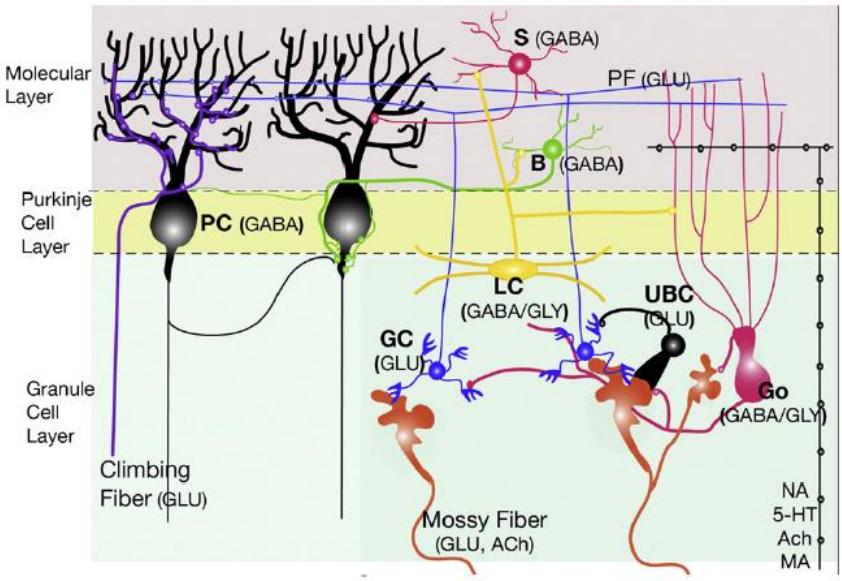

Fig 3: Cerebellar cortex organization.

A) Drawing from Palay & Chan-Palay (1974) represents the cellular and synaptic organization of the cerebellar cortex in parasagittal and transverse plan.

B) Drawing from Sotelo (2011), includes the two new types of interneurons, Lugaro cells and the unipolar brush cells and also neurotransmitters for each neuron.

Legends for Palay & Chan-Palay: pia (pial surface), mol (molecular layer), PC (Purkinje cell), gr (granular layer), wm (white matter), S (stellate cell), B (basket cell), GC (granule cell), CF (climbing fiber, red), MF (mossy fiber, red).

Legends for Sotelo 2011: S (stellate cell), PF (parallel fiber), B (basket cell), LC (lugaro cell), UBC (unipolar-brush cell), GC (granule cell), GO (golgi cell), GLU (glutamatergic cell), GABA (GABAergic cell), GLY (glycinergic cell), Ach (cholinergic), NA (noradrenalin), 5-HT (serotonin), MA (monoaminergic neurons).

Purkinje cells

The cell body of Purkinje cell appears globular or ovoid and is on average 21 µm in diameter and 25 µm in length. The dendritic tree of the Purkinje cells projects in the molecular layer in the parasagital plan and originates from one of four primary dendrites (Fig 3A, 4 and 5). Each primary dendrite is divided in secondary dendrites and tertiary dendrites that split into three to five branches themselves holding abundant thorns (around 7500 per Purkinje cell). The dimensions of these thorns (1.5 to 2 µm long and a head around 0.45 µm in diameter) make them easily observed in electron microscopy. Note that they are free of mitochondria and characterized by cisternaes of agranular endoplasmic reticulum (Fig 6).

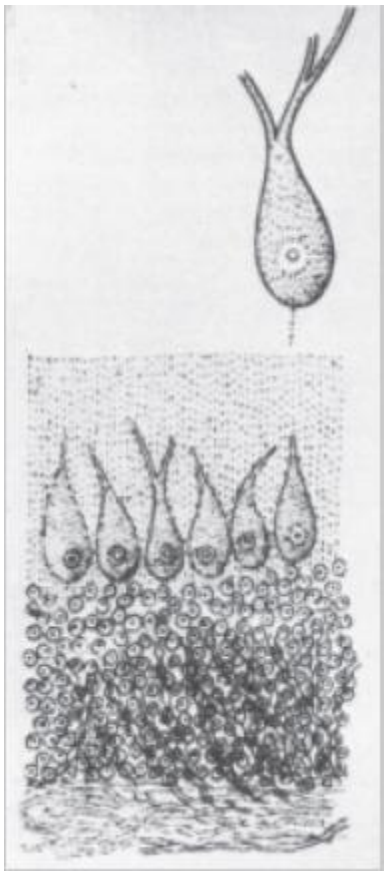

Fig 4: First Purkinje cell illustration.

First representation of Pukinje cell presented to the Congress of Physician and Scientist in Prague in 1838. He described «a great number of similar corpuscles, which surround the yellow substance [...] its two prologations get lost in the grey substance near the outer periphery, where this is covered by the meninges». yellow substance: granular layer, grey substance: molecular layer.

Fig 5: Purkinje cell drawing.

Human Purkinje cell drawing. a: axon, b: collateral, c: blood vessel holes, d: basket cell hole. (From Ramón y Cajal, 1911).

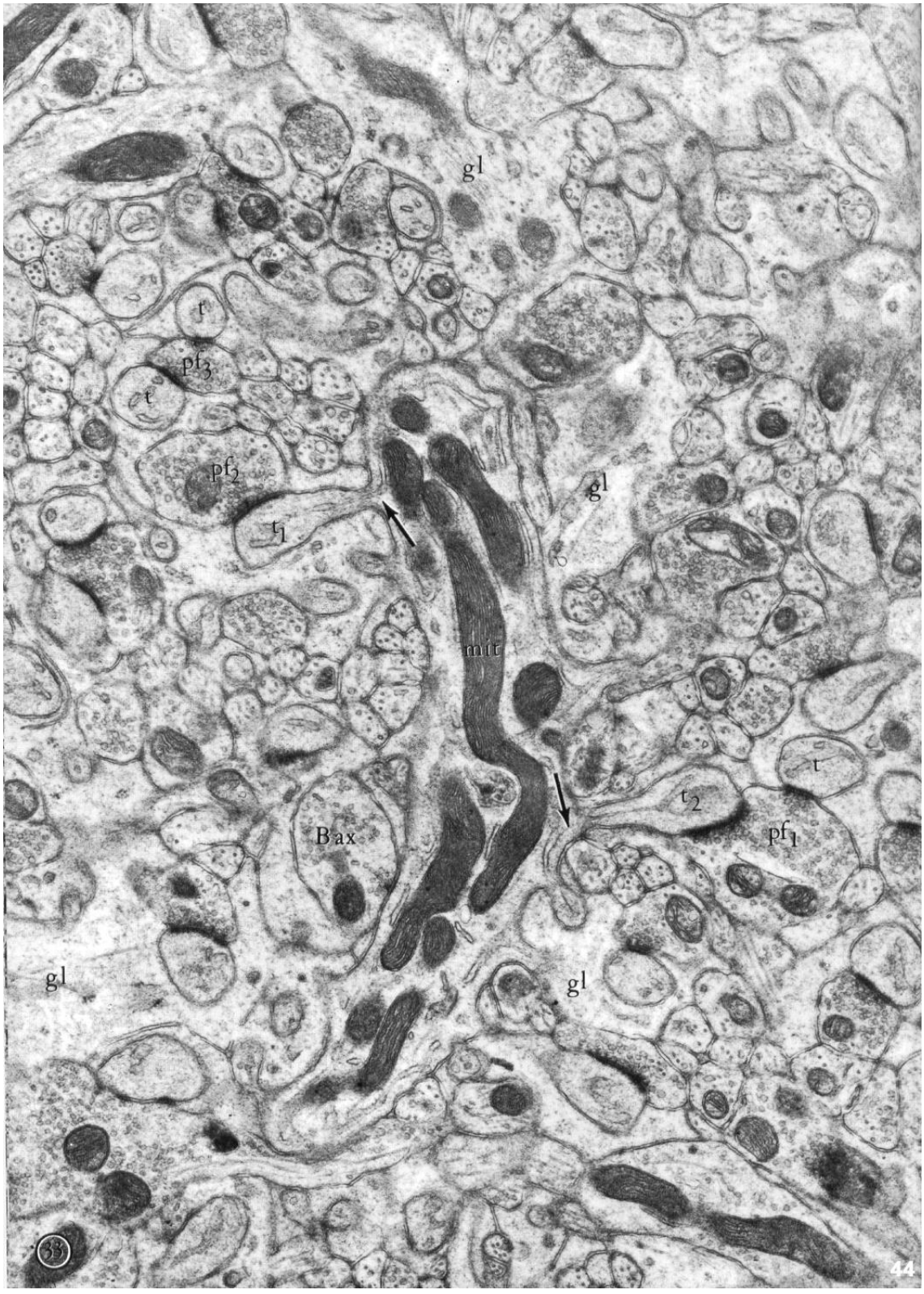

Fig 6: Electron micrograph of Purkinje cell dendrites and synapses.

Purkinje cell dendrites and its torns (t_1 and t_2) make synapses with two parallel fibers ($pf_1$and pf_2). Neuroglias (gl) cover Purkinje cell dendrite. A basket cell axon (B ax) synapses directly the Purkinje cell dendrite. Several mitochondria (mit) are found in the Purkinje cell dendrite but not in thorns. Two parallel fibers (pf_1 and pf_3) connect two Purkinje cell thorns (t and t_2). Note that cisterna of agranular endoplasmic reticulum from the dendrite goes through the thorns (arrows).
Magnification: X19000.
(Modified from Palay &Chan-Palay, 1974).

Climbing fibers

Climbing fibers originate from the inferior olive, across the granular layer and enter obliquely or vertically in the molecular layer (Fig 3A). They are small myelinated fibers of 1-2 µm in diameter which divide in thin branches of 0.1 µm diameter in the molecular layer. The climbing fiber axonal varicosities are fully filled with spherical synaptic vesicles of 40 to 100 nm in diameter and eventually contain mitochondria (Fig 7). They form synapses with Purkinje cell somata and thorns (Fig 3A and 7).

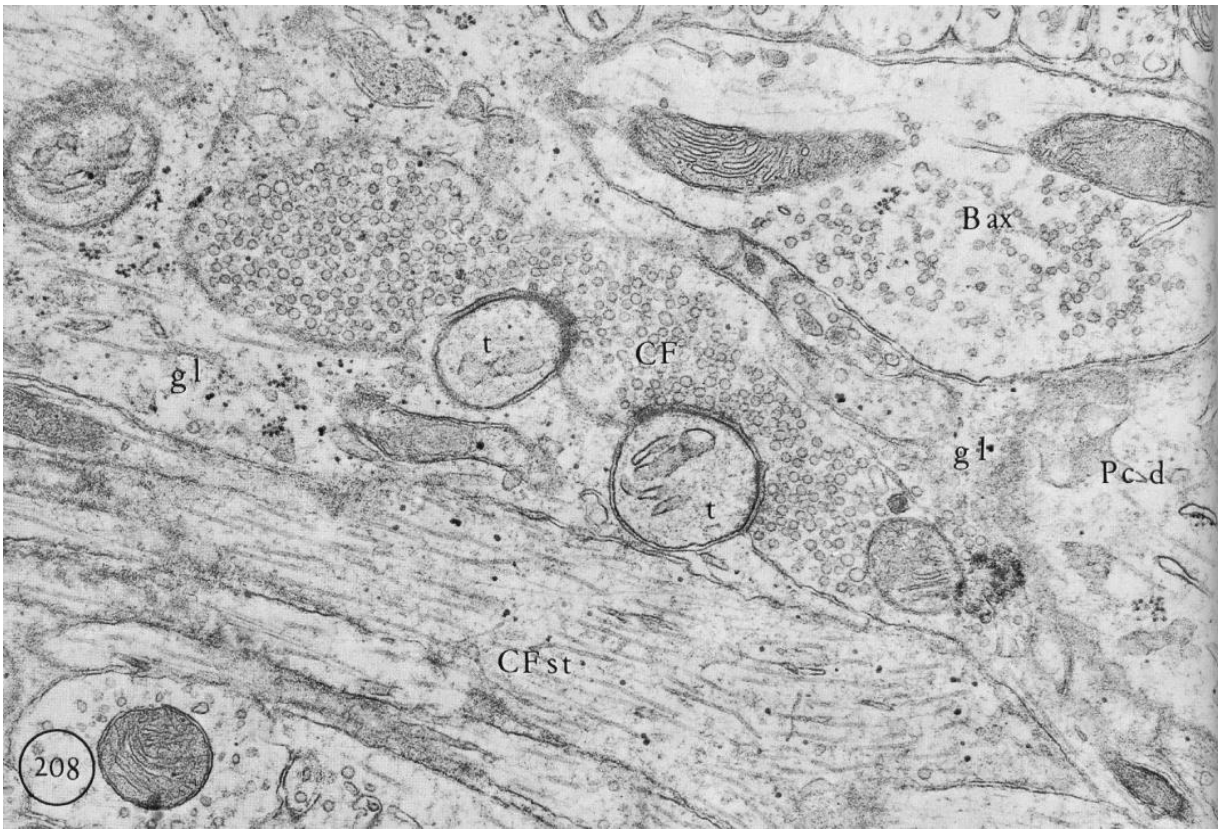

Fig 7: Electron micrograph showing climbing fiber synapses on Purkinje cell thorns.
Climbing fiber stem (CF st) is recognized by its small diameter. Climbing fiber termini (CF) fully filled with round synaptic vesicles makes synapse with two Purkinje cell thorns (t). Moreover a basket cell axon (B ax) can be distinguished as well as neuroglia (gl) and Purkinje cell dendrite (Pc d). Magnification: X39000.
(From Palay & Chan-Palay, 1974).

Mossy fibers

Mossy fibers are thick (0.4 – 1.5 µm) and myelinated axons which enter in the granular layer from the white matter. They divide in 20 to 30 collaterals in the granular layer.

Granule cells

Cerebellar granule cells have a globular cell body of 5-6 µm, they are amongst the smallest neurons in the brain. They are also very numerous and their juxtaposition in one layer results in the granular aspect of the so-called granular layer (Fig 3). Granule cells usually emit three or four short dendrites. Their unmyelinated axon projects in the molecular layer where it bifurcates giving rise to a T-shape in the coronal plan (Fig 3A). The ensemble of these axons builds a parallel network named “parallel fibers” after Ramón y Cajal. Before the bifurcation, granule cell axon is 0.1-0.3 µm whereas the parallel fibers are 0.1-0.2 µm in diameter. Parallel fibers cross over Purkinje cell dendritic tree and make synapses on Purkinje cell thorns (Fig 6). They also contact MLIs (Fig 9) and Golgi cells. Parallel fiber termini (usually containing one or two mitochondria) are filled with round vesicles of 26 – 44 nm that are often aggregated at one side of the fiber opposite to a thorn or a dendrite (Fig 6 and 9). Therefore, these synapses are characterized by their asymmetric nature. The parallel fibers endings are concave and the synaptic cleft is widened (30 nm). On the postsynaptic side, a postsynaptic density is found (PSD, Fig 6 and 9).

Molecular layer interneurons

Two types of MLIs are classically distinguished according to their localization in the molecular layer and their connectivity to the Purkinje cell. At first glance, basket cell somata are localized in the lower third of the molecular layer close to Purkinje cells whereas stellate

cells sit in the outer two third of the molecular layer (Fig 3). Nevertheless, MLIs can be considered as a varying single class of cells (Fig 8; Ramón y Cajal, 1911; Rakic, 1972; Sultan et Bower, 1998) for many types of studies including the ones I am describing hereby. For anatomical reasons, I chose to develop the formal description of Palay & Chan-Palay (1974) which served as a reference for my electron microscopy experiments. Basket cell body is roughly triangular or ovoid (10 µm) and their dendritic tree extends in the parasagittal plane (Fig 3A). Their straight dendrites display an irregular contour and their mitochondria become elongated from 6 to 7 µm with increasing distance from the soma. Synapses between parallel fibers and basket cell dendrites are asymmetric: parallel fibers endings show round vesicles aggregated close to the active zone and a PSD is usually observed (Fig 9). In addition, axons of other basket cells or stellate cells can make synapse with basket cell dendrites. These synapses are characterized by a symmetrical profile as well as by the elliptical and dispersed nature of the vesicles (Fig 9). The unmyelined axon of basket cells runs horizontally in the parasagittal plane among the lower dendrites of Purkinje cells (Fig 3) and projects descending, ascending and transverse collaterals. Around the Purkinje cell body, basket cell axons elaborate a characteristic terminal plexus initially referred to as basket, hence the name of "basket cell". This plexus continues until the initial segment of the Purkinje cell axon resulting in an axo-axonic synapse named "pinceau". Basket cells axoplasm is easy to recognize because it is rather poor in organelles including a few mitochondria of 0.3-1 µm in diameter. Basket cell axons (the largest axons of the molecular layer with a diameter from 1 to 3 µm) make *en passant* synapses with dendrites and somata (Fig 10, example for Purkinje cell somata). The synapses between basket cells and Purkinje cell somata or dendrites are symmetrical. More or less elliptical vesicles of 40-60 nm in diameter appear dispersed and loosely aggregated at basket cell termini. At the actual "basket", axons are around 0.5 to 3 µm in diameter and they follow Purkinje cell soma for about 15 µm (Fig 10).

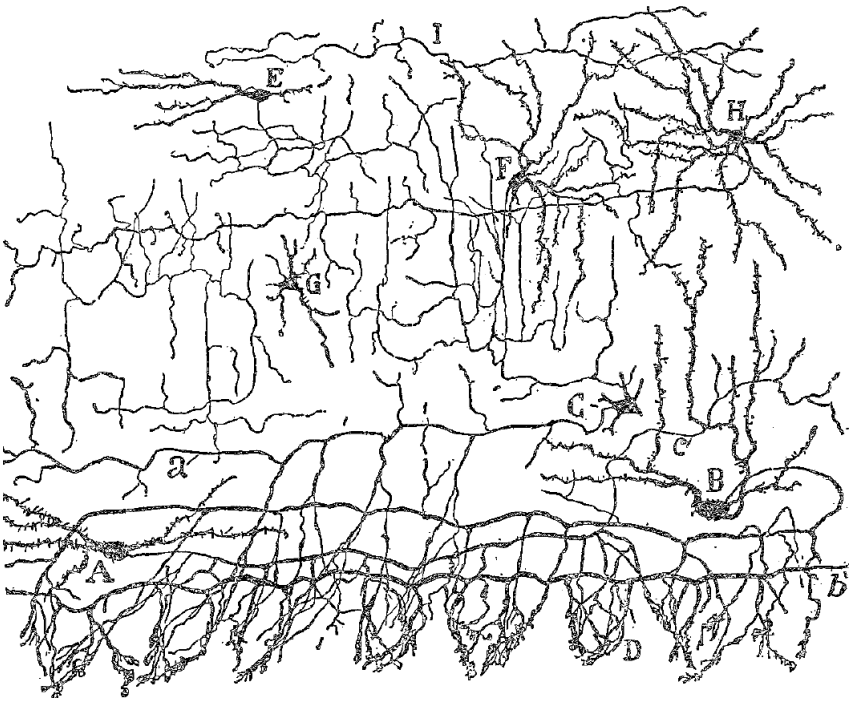

Fig 8: MLIs from rabbit cerebellum.

Drawing shows many different MLIs morphology. A,B: basket cells, E: stellate cells, F-G: intermediate morphology, a: axon, b: basket.
(From Ramón y Cajal, 1911).

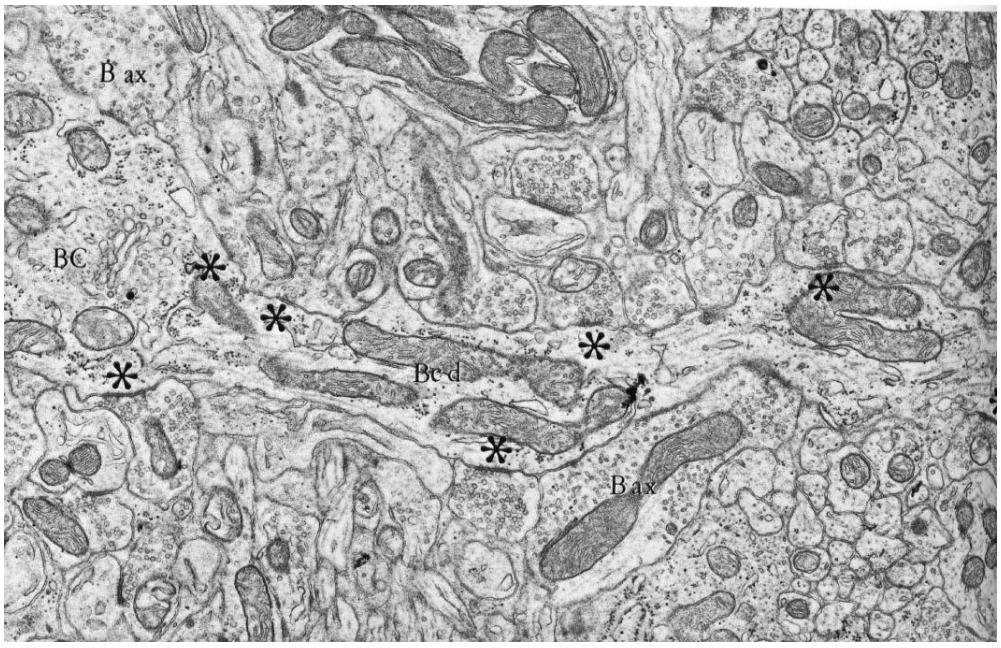

Fig 9: Micrograph of synapses on basket cell dendrite.

A dendrite (Bc d) emerges from basket cell somata (BC). Six synapses formed by parallel fibers (*****) and two by a basket cell axons (B ax) were detected.
Magnification: X 25500
(From Palay & Chan-Palay, 1974).

Palay & Chan-Palay (1974) described two classes of stellate cell namely superficial short axon cells and deeper long axon cells. Superficial short axon cells are the only neurons located in the upper part of the molecular layer. Their ovoid somata exhibit a diameter of 5-9 µm, their short dendrites as well as their short and branched axons (40 µm) project under the pial surface. Similarly to basket cells, their dendrites and axon are comprized in the sagittal plan. Deeper long axon cells stand in the middle third of molecular layer bear somata of around 12 µm in diameter. They have very long axons (450 µm), which run in the parasagittal plan and go through Purkinje cell dendritic trees. They can establish synapses with Purkinje cell somata and contribute to the pericellular basket. Their dendrites are contacted by parallel fibers and other MLIs. Interestingly, parallel fiber synapses are eventually found on stellate cell somata. Their axonal varicosities (about 0.1 µm in diameter) contain small elliptic vesicles make synapses with Purkinje cell thorns and somata, Golgi cells and other stellate and basket cells. The structure of the synapse is always symmetrical with unaggregated vesicles (Fig 11). In comparison to basket cell, deeper long axon cells exhibit contorted dendrites and a long thin axon with collaterals close to the origin.

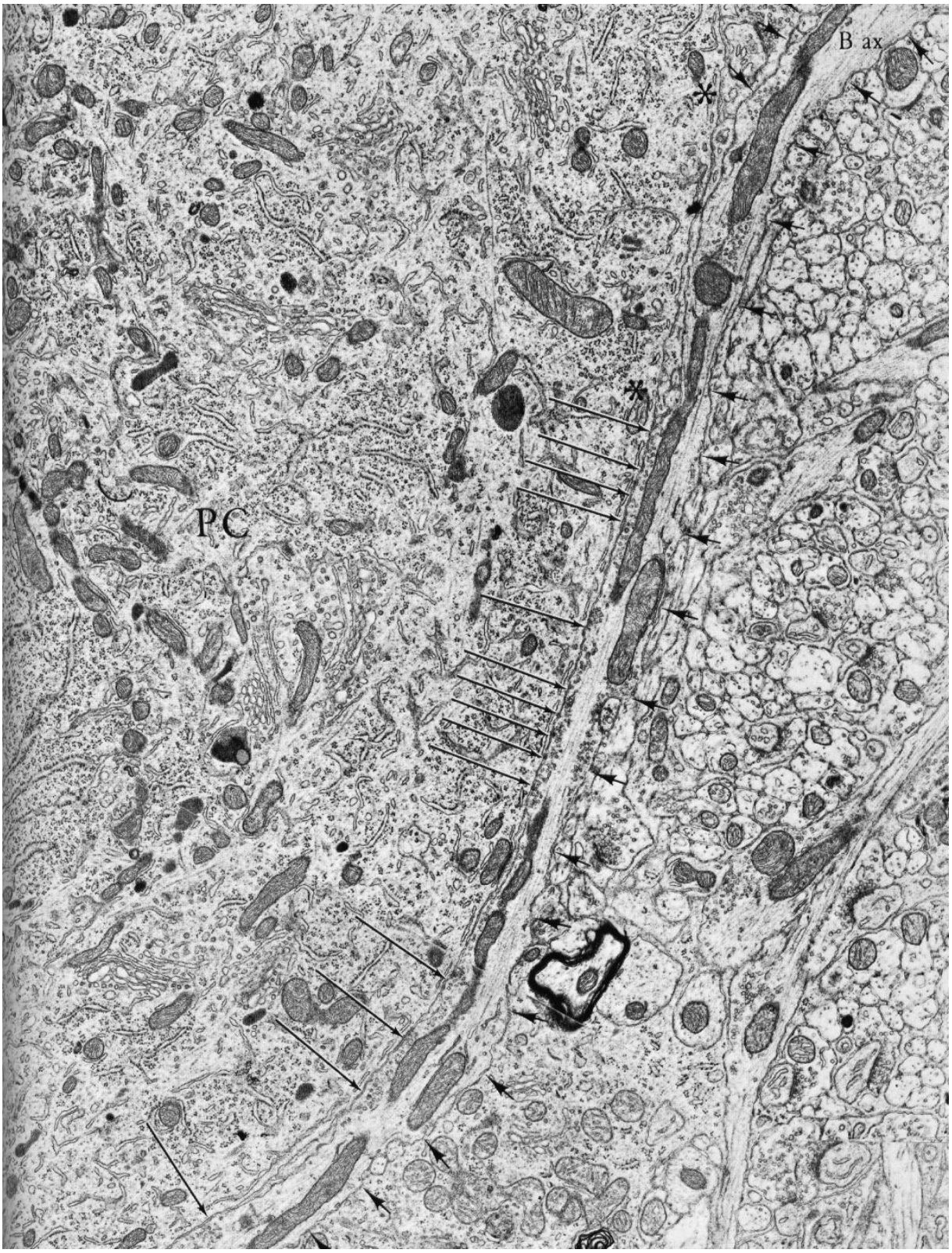

Fig 10: Micrograph showing basket cell axon around Purkinje cell somata.

Basket cell axon (B ax, arrowheads) in contact with Purkinje cell somata (PC) make *en passant* synapses. GABAergic synapses are symmetrical and have dispersed elliptical vesicles (arrows). Axons can be separated from the Purkinje cell somata by neuroglia (*).
Magnification: X 17000
(From Palay & Chan-Palay, 1974).

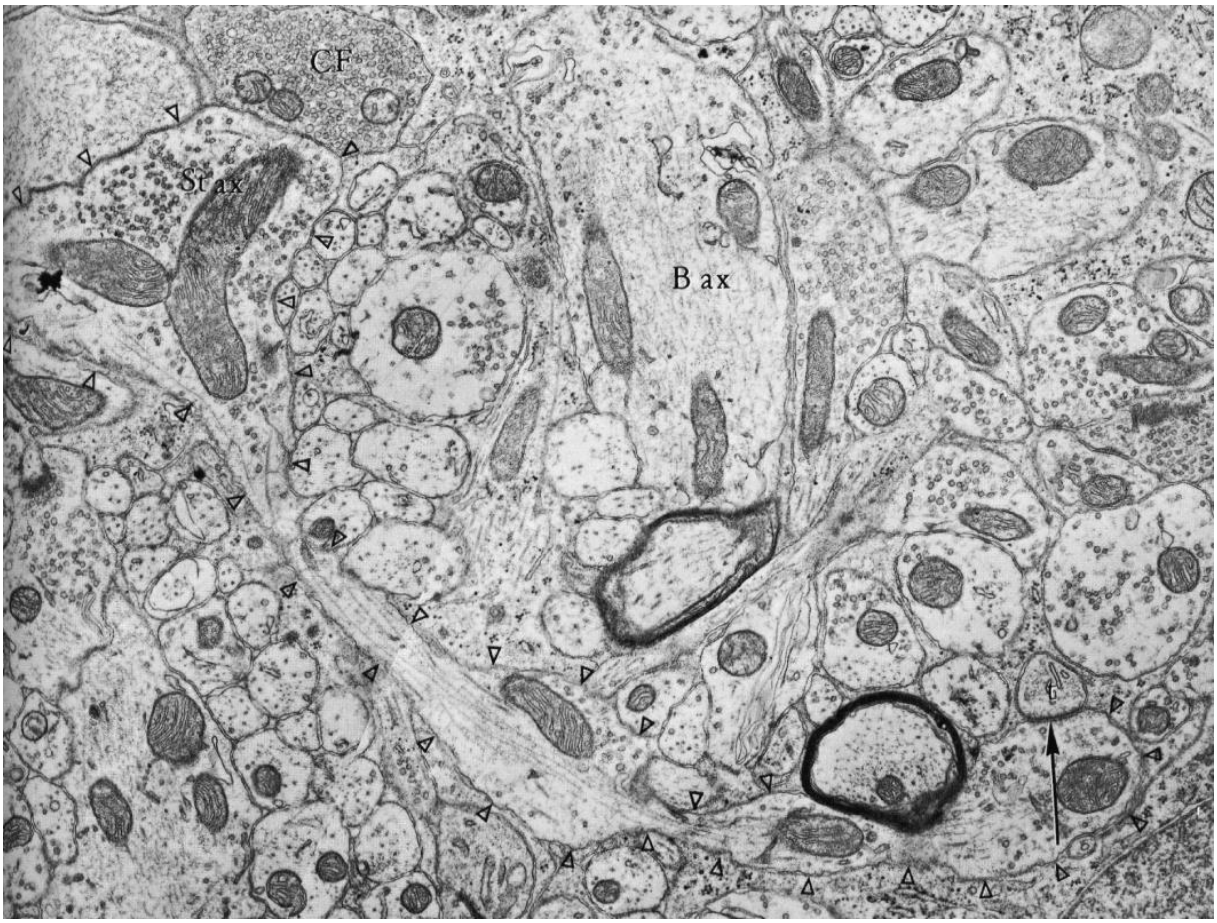

Fig 11: Micrograph representing stellate cell and basket cell axons in molecular layer.
Stellate cell axon (St ax, Δ) can be recognized in comparison to climbing fiber (CF) and basket cell axon (B ax). Here the stellate cell axon makes a synapse with a Purkinje cell thorn (t, arrows).
Magnification: X 14500
(From Palay & Chan-Palay, 1974).

Golgi cells

Golgi cells are situated in the granular layer just below the row of Purkinje cell somata. Their somata is roughly 15 μm in diameter and gives rise to two to four thick dendrites which extending in the molecular layer. The highly arborized axons of Golgi cells mostly run in the granular layer but also in the molecular layer (Simat et al., 2007).

Lugaro cells

The lugaro cell fusiform somata of 7 or 8 μm in diameter sits at the top of the granular layer and their dendrites extend horizontally below the Purkinje cell layer with a bipolar arborization. Their partially myelined (in the lower part of molecular layer) and highly branched axons project in the molecular layer in the parasagittal plan as well as in the transverse plan parallel to the parallel fibers. These axons are thicker that parallel fibers (1 μm in diameter) sometimes descend in the granular layer and go through the white matter. They bear elongated mitochondria and their termini are filled with numerous ellipsoidal and spherical vesicles. Lugaro cell axons make symmetric synapses with MLIs somata and dendrites as well as with Golgi cells (Lainé & Axelrad, 1998; Dieudonné & Dumoulin, 2000).

Unipolar-brush cells

Unipolar-brush cells are confined in the granular layer and are characterized by spherical somata smaller than golgi cells but bigger than granule cells. Their dendritic brush-like tree receives glutamatergic input from mossy fiber and their axons project on granule cells.

Glial cells

As mentioned before, five different types of glial cells are present in the cerebellar cortex including astrocytes, oligodendrocytes, Bergman cells, microglia and NG2(+).

Bergman cells also named “Golgi epithelial cell” by Palay & Chan-Palay, have their irregular spheroidal cell body in the Purkinje cell layer between two Purkinje cells. They have ascending and irregular branches projecting horizontally in the molecular layer and they sheath Purkinje cell dendritic tree, somata and axon initial segment. Only synaptic sites are not sheathed by Bergman cell process. Their cytoplasm is pale and homogenous with dense spherical granule of about 25 nm in diameter (Fig 12).

Two different types of astrocytes are present in the cerebellar cortex: velate protoplasmic and smooth protoplasmic astrocytes. The first type is located in granular layer and has branches which encircle glomeruli and partially granule cell somata. The second type is localized in molecular layer and granular layer and they have smooth, long and radiating processes.

Oligodendrocytes are mostly found in the lower part of the molecular layer as well as in the Purkinje cell layer close to Purkinje cell somata. They have small and round cell body (5-6 μm) and they are easily recognized due to their dark cytoplasm (Fig 12). The myelinated Purkinje cell axons are directly in contact with the oligodendrocyte cell bodies.

NG2(+) cells share a common shape with stellate cells showing a small ovoid cell body ($53 \pm 18\ \mu m^2$); they are frequently found in the molecular layer. Their thick processes radiate from the cell soma (Levine & Card., 1987).

Finally, microglia are found in the perivascular tissue.

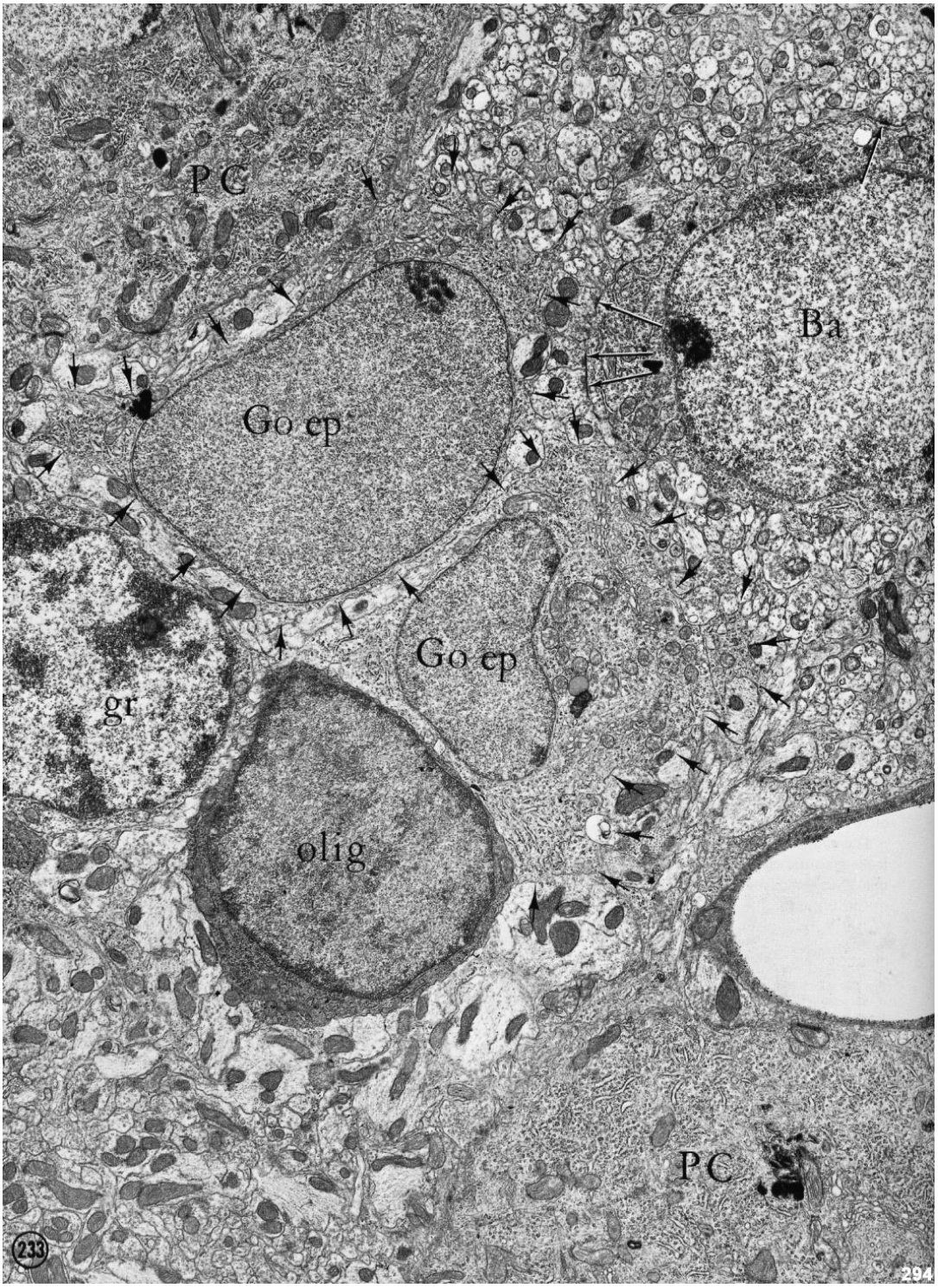

Fig 12: Electron micrograph showing Bergman cells and oligodendrocyte close to Purkinje cell somata.

Bergman cells (Go ep, arrowheads) can be recognizable by their thin nucleoplasmm. Their cytoplasm has neuropil (arrowheads). One oligodendrocyte with dark nucleoplasm and cytoplasm is in the field. Granule cell somata (gr) can be recognized by their localization and their dispersed chromatin. Two Purkinje cell somata (PC) and basket cell somata (Ba) are also present. Note synapses on basket cell somata (arrows).

Magnification: X 11000.

(From Palay and Chan-Palay, 1974).

1.1.3.3 Neuromodulative innervations.

Five different neuromodulative innervations enter the cerebellar cortex. During my PhD, I only focused on the noradrenergic innervation. Noradrenergic innervations have been discovered with radioautoradiographic and fluorescence microscopy studies these latter being performed after microinjection of a tracer in the locus coeruleus. Noradernergic axons enter the cerebellar cortex via the superior peduncle and project in the molecular layer and around Purkinje cells (Olson & Fuxe, 1971; Pickel 1974a,b) where they make asymmetric synapses on MLIs. They have been visualized in electron microscopy on adult rats using an antibody against dopamine-beta-hydrolxylase (noradrenaline synthesizing enzyme; Olschowka et al., 1981). Noradrenergic axons are unmyelined and have two different profiles: thin axon of 0.45 µm in diameter without vesicles and thicker axon of around 1 µm in diameter with two types of vesicles, large granular vesicles (85-105 nm diameters) and agranular vesicles (35-55 nm diameters).

Briefly, other neurotransmitters involved in cerebellar modulations are: serotonin, acetylcholine, dopamine and histamine. Their inputs arise from reticular formation, raphe, basal ganglia, ventral tegmental area and tuberomammillary nucleus (Schweighofer et al., 2004) respectively.

1.1.4 Cerebellar cortex post-natal development.

The experiments enclosed in this PhD thesis were performed on young rats (P11-P16) and older rats (P17-26) for reasons of convenience and homogeneity with previous studies of the laboratory such as Forti et al. (2000).

Cell localization and synapses set up progressively in the postnatal cerebellum. MLIs arise from dividing precursors initially sitting near the fourth ventricle as Purkinje cells and

Golgi cells. Purkinje cells are present at birth, they move to create the single row of Purkinje cells until P4 and their dendritic tree grows from P7 up to P30 (Altman, 1972b). Immature MLIs migrate through the white matter and granular layer to the molecular layer until P20 (Zhang & Goldman, 1996). Basket cells are the first to reach their final position in the molecular layer and to contact Purkinje cells. Furthermore, granule cell precursor located in the thick external granular layer progressively exit the cell cycle and then migrate from the external granular layer through the molecular layer to generate the granular layer from P0 until P21 (Altman, 1972a).

GABAergic synapses are detected at P12 between basket and Purkinje cells and at P15 between stellate and Purkinje cell. Vesicular GABAergic transporter (VGAT) expressing synapses appear in the molecular layer and on Purkinje cell at P5 and they massively increase during the second and the third postnatal week (Takayama & Inoue, 2004). Glutamatergic synapses between climbing fibers and Purkinje cell somata are detected at P7. Moreover, glutamatergic synapses made by parallel fiber on Purkinje cell dendritic tree are found at P12 (Altman, 1972b). Interestingly, different subtypes of vesicular glutamatergic transporters (VGLUT1 and VGLUT2) were identified in the cerebellar cortex (Fremeau et al., 2001; Ichikawa et al., 2002). During the postnatal development, expression of VGLUT1 is replaced by VGLUT2 after P10 in parallel fiber termini (Miyazaki et al., 2003). Contrary to parallel fibers, VGLUT2 expression in climbing fiber termini is unchanged during the postnatal development.

Fig.13, adapted from Altman 1972b, summarizes the main steps of postnatal cerebellar development.

Not so many studies have described the morphology and ultrastructure of MLIs axon during post-natal development. Palay & Chan-Palay (1974) exclusively studied the adult rat. Of interest, Altman (1972b) described some basket cell termini on Purkinje cell somata at P12 and P15 (Fig 14). Moreover, Nusser and co-workers described MLIs terminals in young rat P13-P26 using $GABA_A$ receptor immunoreactivity and concluded that the presence of GABAergic synapses on MLIs is 10-fold less than that glutamatergic synapses (Nusser et al., 1997). Filling MLIs with biocytin or Lucifer yellow during whole cell recording permitted to indicate that MLIs axons have a uniform diameter and few varicosities in young rat (P11-15) *versus* older rat (P16-P21; Pouzat & Hestin, 1997)

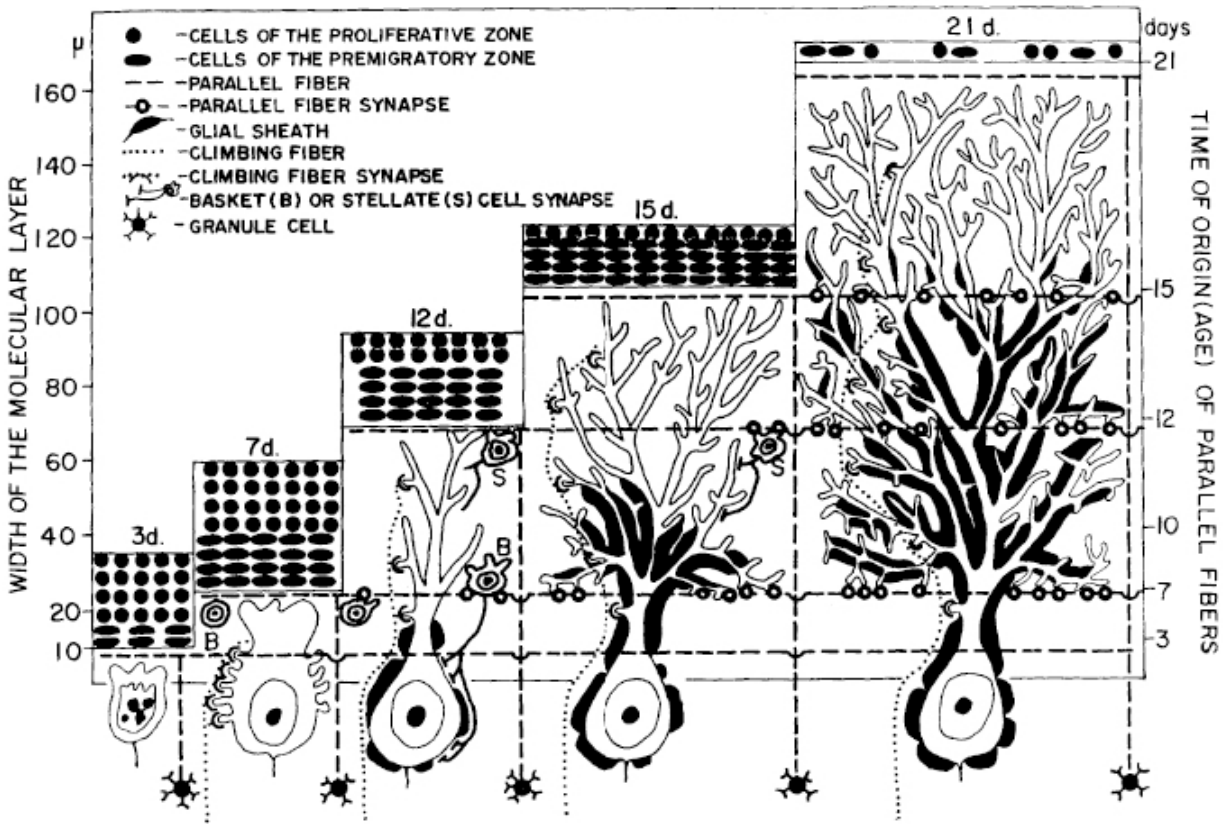

Fig 13: Rat cerebellar postnatal development.

Major events of postnatal development are represented. The width of the molecular layer (left abscissa) increases as a function of rat's age (columns, d: postnatal days). Parallel fiber time of origin (right abscissa) correspond to their age of their localization in the molecular layer. The external granular layer (here named external germinal layer) is composed of precursors of granule cells and pre-migratory granule cells.
(From Altman, 1972b).

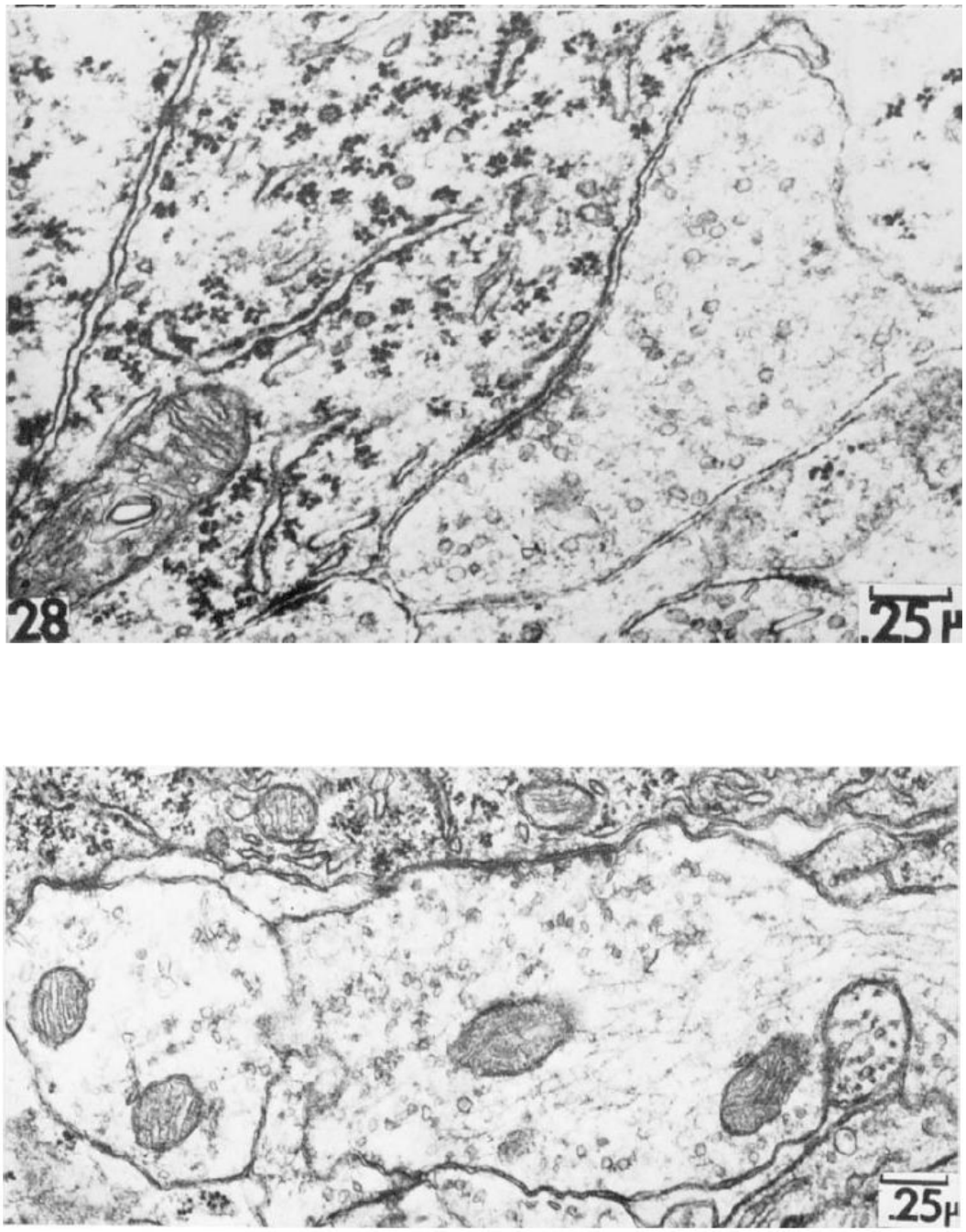

Fig 14: Micrographs of basket cell termini on Purkinje cell somata at P12 (upper panel) and P15 rats (lower panel).
Scale bars: 25 μm.
(From Altman, 1972b).

1.1.5 Characterization of synaptic current recorded in MLIs and Purkinje cells in young rats.

As it is noticed before, Purkinje cells receive inhibitory inputs from MLIs and two types of excitatory imputs namely from climbing fibers and parallel fibers. The spontaneous excitatory synaptic currents (EPSCs) are smaller than their inhibitory counterpart (IPSCs) while recorded in Purkinje cells, the former being mediated by AMPA receptors but not by NMDA receptors (Konnerth et al., 1990; see Fig. 15A).

Moreover, mean amplitude of miniature IPSCs (mIPSC) recorded in Purkinje cells in the presence of tetrodotoxine (TTX) to block action potentials is 152 ± 9 pA with high internal Cl^- soltution and their average frequency is 4.3 Hz (Llano et al., 2000).

The major excitatory input of MLIs results from parallel fibers and they receive inhibitory inputs as a result of GABA release from other MLIs. The first intracellular recordings of MLIs were performed in a study by Llano & Gerschenfeld (1993a) in which they show that IPSCs are mediated by $GABA_A$ receptors and EPSCs by AMPA receptors. These authors also documented that the IPSC decay time can be fitted by a double exponential function with time constants around 10 and 40 ms for the slow and the fast component respectively. By contrast, the EPSC decay time was fitted by a single exponential function with a time constant usually around 15 ms. Note that the average IPSC amplitude is roughly similar to what was reported for Purkinje cell recordings with high internal Cl^- solution (Fig 15B).

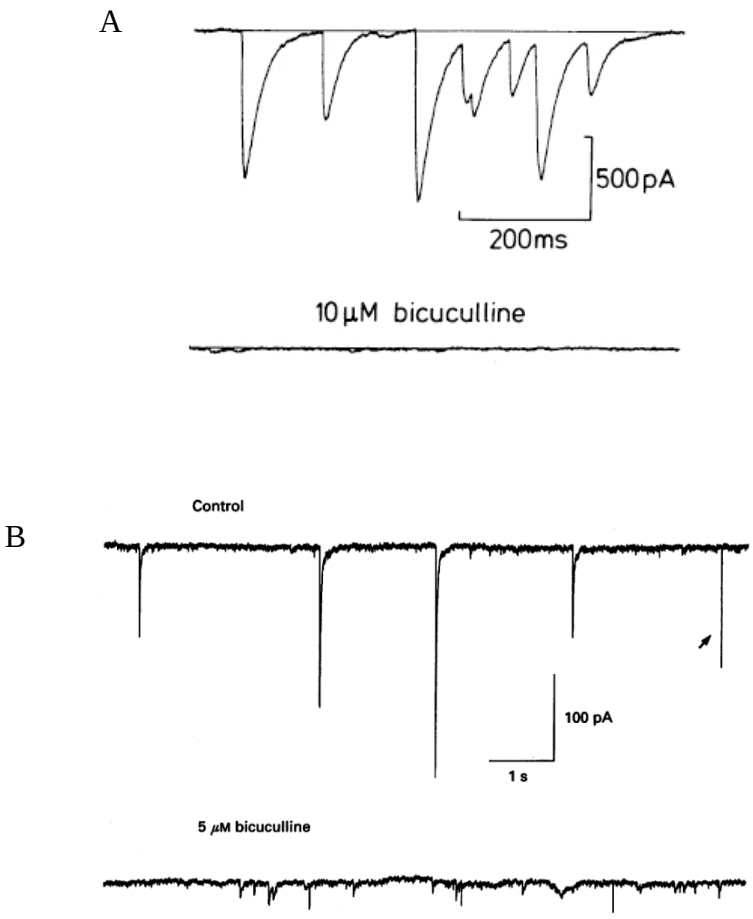

Fig 15: Spontaneous synaptic current traces recorded in Purkinje cells (A) or in stellate cells (B).
(From Konnerth et al., 1990 and Llano & Gerschenfeld, 1993a).

1.1.6 Characterization of axonal calcium transients in MLIs axons in young rats.

Axonal Ca^{2+} transients induced by propagated action potentials were first described in basket cell axons of young rats (Llano et al., 1997; Tan & Llano, 1999). They mainly consist of large Ca^{2+} increases appearing in a discrete manner along the axons. These structures were named axonal "hot spots" and are supposed to correspond to the varicosities commonly observed in morphological studies. These latter were proposed to materialize *en passant* synapses on the Purkinje cell somata and/or branching points of the axon (Fig 16). Such a balkanization of the Ca^{2+} signaling was attributed to the high parvalbumin immunoreactivity specifically found in basket cell axonal compartment (Kosaka et al., 1993). Altogether, these

data suggested that axons need an important endogenous Ca^{2+} buffering capacity associated with a high density of Ca^{2+} channels. Later, Forti et al., (2000) proposed that axonal Ca^{2+} transients in hot spots are mediated by opening of voltage dependent calcium channels (VDCCs) predominantly P/Q- and N-type VDCCs in developing MLI termini.

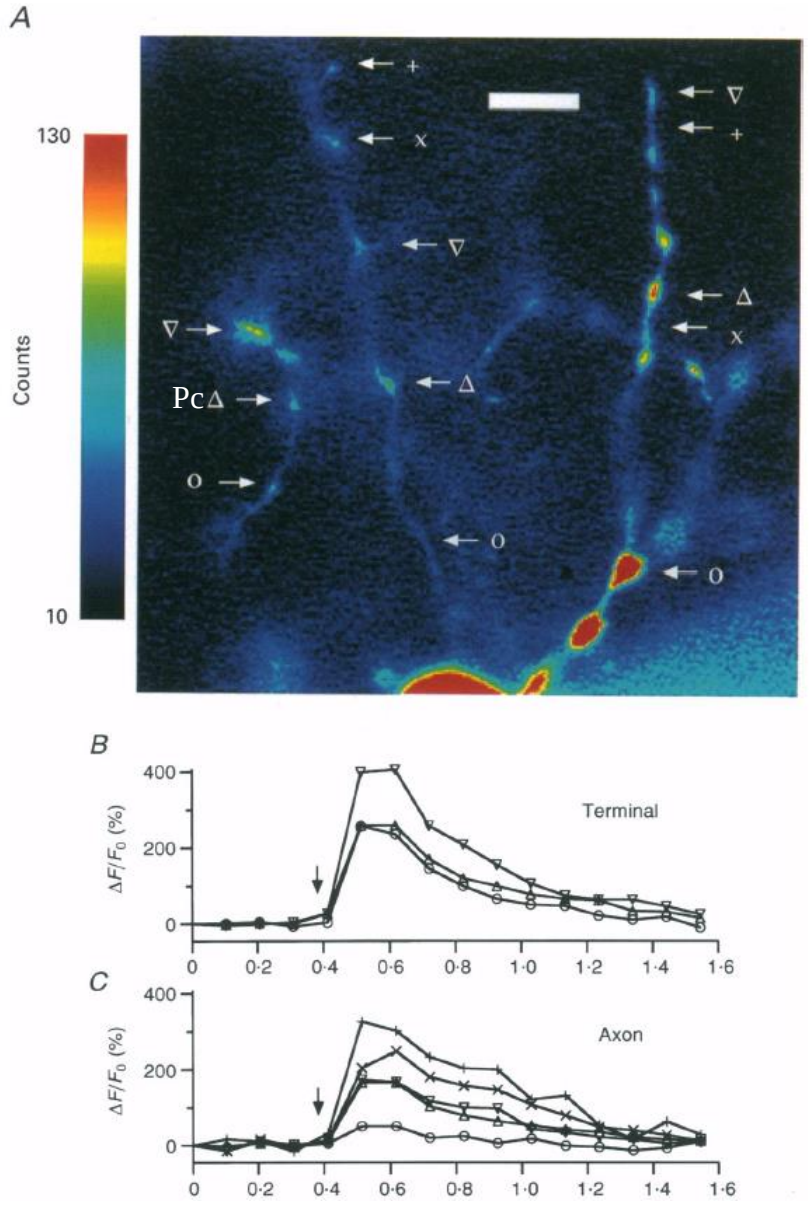

Fig 16: Axonal Ca^{2+} transients in a basket cell in response to a depolarization.

A) Change of fluorescence is measured in basket cell filled with Ca^{2+} indicator after a depolarization. Large Ca^{2+} transients are detected in hot spots (+, x, □,□).

B-C) show responses to the depolarization (arrows) in various hot spots at synaptic terminal and in axonal varicosities as a function of time (seconds).

Scale bar in A: 10 µm

(Modified from Llano et al., 1997)**.**

1.1.7 Modulation of synaptic currents and axonal calcium transients in MLIs.

The endoplasmic reticulum (ER) of neuron is a dynamic calcium stores which can be recruited by electrical or chemical signals (Berridge, 1999). Calcium release from ER can be either mediated through ryanodine receptors (RyR) or inositol 1,4,5-trisphosphate receptor (IP3R). Of interest, RyR are abundantly expressed in basket cell axon and action potential induced axonal calcium transients were found to be sensitive to ryanodine (Llano et al., 2000). Moreover, IPSCs evoked from MLIs in basket/Purkinje cells paired-recording, display an amplitude and a paired pulse ratio (PPR) that is clearly decreased by ryanodine superfusion (Galante & Marty, 2003). Finally, 'spontaneous calcium transients' (SCaTs: spontaneous variation of Ca^{2+} in axons recorded in presence of TTX) recorded in basket cells axon termini onto Purkinje cell somata are also sensitive to ryanodine (Conti et al., 2004).

Different isoforms of RyR (RyR1, RyR2 and RyR3) are known to be expressed in the cerebellum. Purkinje cell mainly expresses RyR1 whereas granular cell express RyR2 and the isoforms present in MLIs are still unidentified to date (Kuwajima et al., 1992; Giannini et al., 1995; Mori et al., 2000; Sawada et al., 2008).

Several studies have focused on the involvement of RyR in the efficiency of transmitter release but little is known about the putative contribution of IP3R in neurotransmitter release. Nevertheless, Kelm et al. (2010) indicated that IP3R is expressed in MLIs terminals and that ethanol can induce an increase in IPSC frequency onto Purkinje cell through presynaptic IP3R opening.

As mentioned earlier in this manuscript, the cerebellar cortex receives noradrenergic inputs from the locus coeruleus. Accordingly it has been shown that noradrenaline can inhibit Purkinje cell firing (Hoffer et al., 1972). It has been also reported that noradrenaline superfusion enhances the frequency of spontaneous IPSC and mIPSC recorded in stellate cells and Purkinje cell (Llano & Gerschenfeld, 1993b; Kondo & Marty, 1998; Saitow et al., 2000).

It was concluded that activation of presynaptic β2-adrenergic receptors on MLIs axons could potentiate inhibitory neurotransmission through an increase in cAMP intracellular level. Moreover, noradrenaline was reported to alter PPR of evoked IPSC recorded in Purkinje cells (Saitow et al., 2000).

1.2 Voltage dependent calcium channels.

Voltage dependent calcium channels (VDCCs) typically open in response to membrane depolarization and specifically mediate Ca^{2+} influx. Ca^{2+} ions induce and regulate many intracellular processes such as muscle contraction, cell proliferation, hormone secretion, neurotransmitter release and gene expression. Different types of VDCCs are distinguished according to their biophysical and pharmacological properties (Table 1 for pharmacology). Based on these criteria, VDCCs are classified as high-threshold activated VDCCs (HVA) or low-threshold activated VDCCs (LVA). At the molecular level, VDCCs are complex proteins composed of five subunits (α1, β, α2δ and γ) encoded by multiple genes (Fig 17). The principal subunit Ca_v (or α1) contains the pore, the selectivity filter, the voltage sensor and interaction sites for auxiliary subunits such as G proteins, RYR and synaptic proteins. Moreover, Ca_v subunits contain binding sites for agonists/antagonists and they are therefore responsible for the unique biophysical and pharmacological properties of VDCCs. Auxiliary subunits such as β, α2δ and γ however, are required for the functioning and trafficking of VDCCs (Fig 17).

1.2.1 The main subunits: α1 subunits or Ca_v.

In mammals, 10 distinct genes encode for 10 different isoforms of Ca_v subunits. These isoforms are grouped in three families: the Ca_v1 family ($Ca_v1.1$-1.4) corresponds to L-type VDCCs, the Ca_v2 family ($Ca_v2.1$, 2.2 and 2.3) corresponds to the P/Q, N and R-type VDCCs and the Ca_v3 family ($Ca_v3.1$, 3.2 and 3.3) representing T-type VDCCs (Ertel et al., 2000; Catterall et al., 2005; Table 1). The Ca_v amino acid sequences are more than 70% identical

within a family and less than 40% among the three families. Ca_v1 and Ca_v2 families are high-HVA whereas Ca_v3 family is low-threshold activated LVA.

Channel	Current	Localization	specific antagonists	cellular function
Cav1.1	L	Skeletal muscle; transverse tubules	Dihydropyridines; phenylalkylamines; benzothiazepines	Excitation-contraction coupling
Cav1.2	L	Cardiac myocytes; smooth muscle myocytes; endocrine cells; neuronal cell bodies; proximal dendrites	Dihydropyridines; phenylalkylamines; benzothiazepines	Excitation-contraction coupling; hormone release; regulation of transcription; synaptic integration
Cav1.3	L	Endocrine cells; neuronal cell bodies and dendrites; cardiac atrial myocytes and pacemarker cells; cochlear hair cells	Dihydropyridines; phenylalkylamines; benzothiazepines	Hormone release; regulation of transcription; synaptic regulation; cardiac pacemaking; hearing; neurotransmitter release from sensory cells
Cav1.4	L	Retinal rod and bipolar cells; spinal cord; adrenal gland; mast cells	Dihydropyridines; phenylalkylamines; benzothiazepines	Neurotransmitter release from photoreceptors
Cav2.1	P/Q	Nerve terminals and dendrites; neuroendocrine cells	ω-Agatoxin IVA	Neurostransmitter release; dendritic Ca^{2+} transients; hormone release
Cav2.2	N	Nerve terminals and dendrites; neuroendocrine cells	ω-Conotoxin-GVIA	Neurostransmitter release; dendritic Ca^{2+} transients; hormone release
Cav2.3	R	Neuronal cell bodies and dendrites	SNX-482	Repetitive firing; dendritic calcium transients
Cav3.1	T	Neuronal cell bodies and dendrites; cardiac and smooth muscle myocytes	None	Pacemaking; repetitive firing
Cav3.2	T	Neuronal cell bodies and dendrites; cardiac and smooth muscle myocytes	None	Pacemaking; repetitive firing
Cav3.3	T	Neuronal cell bodies and dendrites	None	Pacemaking; repetitive firing

Table 1: Localization, antagonists and cellular functions of VDCCs.
(From Catterall 2005).

1.2.1.1 Structure.

The pore–forming Ca_v subunit is the largest subunit (190-250 kDa) of the complex. In absence of crystal structure, sequence analyses predict that Ca_v subunit is composed by four homologous distinct domains (I-IV) containing six transmembrane segments (S1-S6) (Tanabe et al., 1987; Fig 17). The S4 segment contains five to six positively charged amino acids

(lysine and arginine) and serves as voltage sensor. The pore structure is formed by extracellular and partially transmembrane loops between S5-S6 segments (pore loops) in each domain. The pore loops contain negatively charged amino acids (glutamic acids) involved in calcium selectivity. The cytoplasmic loops connect the four domains and are involved in channel regulation (Zamponi, 2003).

A

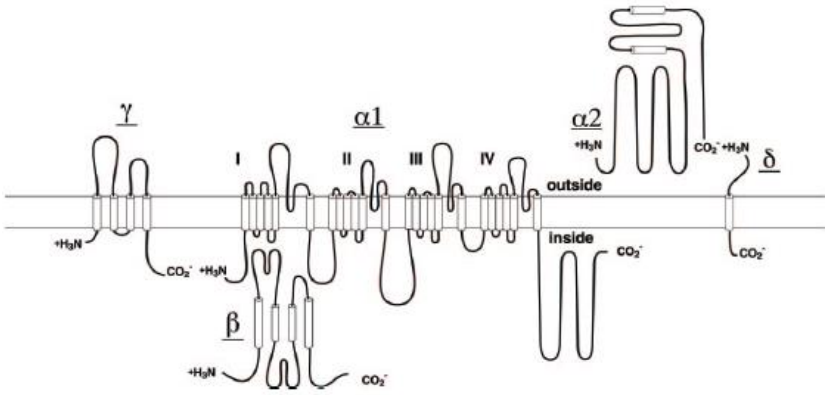

B

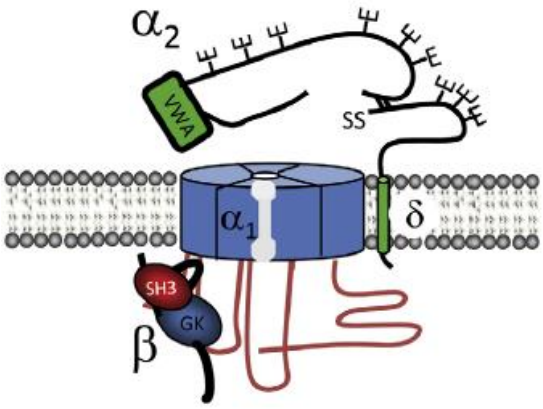

Fig 17: VDCC heteromeric complex.
A) Subunit structure of VDCCs (adapted from Catterall et al., 2005)
B) Representation of VDCC heteromeric complex (from Dolphin, 2009)

1.2.1.2 Biophysical and pharmacological properties.

HVA VDCCs

HVA VDCCs share common characteristics: they are activated by a strong depolarization and are blocked by Cd^{2+} (Catterall et al., 2005). Additionnally, HVA VDCCs familly members, P/Q, N, L and R-type have different biophysical and pharmacological properties (Table 1 for pharmacology).

L-type VDCCs open in response to depolarization and mediate long-lasting calcium current due to their slow inactivation kinetic and are characterized by their large single-channel conductance (Bean, 1985; Nowycky et al., 1985; Zhang et al., 1993). Table 2 summarizes all biophysical characteristics of $Ca_v1.2$ and $Ca_v1.3$ subunits.

$Ca_v1.2$	
Conductance	Ba^{2+} (25 pS) > Sr^{2+} = Ca^{2+} (9 pS)
Ion selectivity	Ca^{2+} > Sr^{2+} > Ba^{2+} >> Mg^{2+} from permeability ratios
Activation	V_a = -17 mV (in 2 mM Ca^{2+}; HEK cells); -4 mV (in 15 mM Ba^{2+}; HEK cells) to -18.8 mV (in 5 mM Ba^{2+}; HEK cells and *Xenopus* oocytes); τ_a = 1 ms at + 10 mV
Inactivation	V_h = -50 to -60 mV (in 2 mM Ca^{2+}; HEK cells), -18 to -42 mV (in 5-15 mM Ba^{2+}; HEK cells, τ_{fast} = 150 ms, τ_{slow} = 1100 ms; 61% inactivation after 250 ms in HEK cells (at V_{max} in 15 mM Ba^{2+}); ~ 70% inactivation after 1s (at V_{max} in 2 mM Ca^{2+}); inactivation is accelarated with Ca^{2+} as charge carrier (Calcium-dependent inactivation: 86% inactivated after 250 ms)
$Ca_v1.3$	
Conductance	Not established
Ion selectivity	Not established
Activation	V_a = -15 to -20 mV (mouse cochlear hair cells; 10 mM Ba^{2+}); -18 mV (in 15 mM Ba^{2+}; HEK cells) to -37 mV (5 mM Ba^{2+}; 2 mM Ca^{2+} HEK cells or *Xenopus* oocytes); τ_a < 1 ms at + 10 mV
Inactivation	V_h = -36 to -43 mV; τ_{fast} = 190 ms, τ_{slow} = 1700 ms (at V_{max} in HEK cells); calcium-induced inactivation is observed after expression in HEK cells and in cochlear outer hair cells but not in inner hair cells

Table 2: Biophysical properties of $Ca_v1.2$ and $Ca_v1.3$ subunits
(From Catterall et al., 2005)

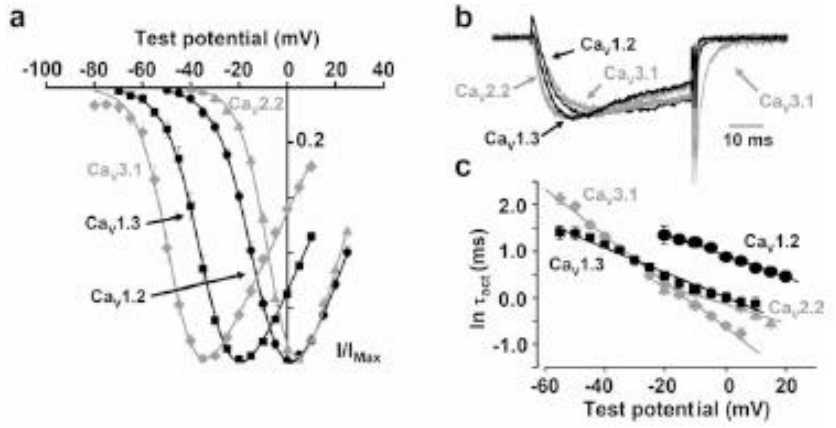

Fig 18: Biophysiological description of VDCC currents activated by step depolarization in tsA201 cells.
TsA201 cells express $Ca_v1.2$, $Ca_v1.3$ (grey), $Ca_v2.2$ or $Ca_v3.1$ (black) subunits with auxiliary subunits.
a) Average I-V curve relationships
b) Normalized current activated by a step depolarization
c) Averaged activation time constants at different test potentials calculated from exponential fits
(From Helton et al., 2005).

When recorded at physiological temperature, the average L-type current presents a half-maximal voltage activation of -20 mV (Liu et al., 2003) although some L-type channel complexes can be activated at lower voltage. L-type currents display fast activation kinetic similar to N-type currents and they are more resistant to steady-state inactivation than P/Q and N-type currents (Fig 18; Liu et al., 2003; Catterall et al., 2005; Helton et al., 2005). Current mediated by $Ca_v1.2$ and $Ca_v1.3$ subunits ($Ca_v1.2$ currents or $Ca_v1.3$ currents) activate in response to different voltage waveforms such as action potentials or step depolarization (Liu et al., 2003; Helton et al., 2005). Moreover, the activation threshold of $Ca_v1.3$ is significantly lower than this of $Ca_v1.2$ and (-45.7 mV *versus* -31.5 mV) accompanied by a faster overall and a slower inactivation during the depolarizing pulse (Fig 18, Koschak et al., 2001; Xu & Lipscombe 2001; Helton et al., 2005).

L-type VDCCs are sensitive to three groups of blockers: one selective: 1,4-dihydropyridine (DHP) and two imperfectly selective: phenylakylamines (verapamil) and benzothiazepines (diltiazem) (Cai et al., 1997 and for review see Catterall & Striessnig, 1992). L-type channels blockers are well characterized and are used therapeutically for treatment of hypertension (Triggle, 1992).

DHPs were first synthesized by Arthur Hantzch in 1882 and form now a large family (nimodipine, nifedipine, isradipine….) among which L-type channel agonist and antagonist can be distinguished. DHP antagonists typically block L-type VDCCs in a state and time-dependent manner and they preferentially bind to the channels in their active conformation (Bean, 1984; Holz et al., 1988). $Ca_v1.3$ and $Ca_v1.2$ subunits are not equally sensitive to DHP antagonists: $Ca_v1.3$ currents obtained in response to a step depolarization are incompletely blocked by DHPs. Interestingly this fact is overemphasized for one DHP antagonist: isradipine. Isradipine sensitivity is 8.5 fold lower for $Ca_v1.3$ than for $Ca_v1.2$ subunits (Koschak et al., 2001). Interestingly, it has to be noted that DHP antagonists fail to block L-type VDCCs currents opened by action potentials (Helton et al., 2005).

Besides, Schramm et al. (1983) showed that small modifications to nifedipine result in a new DHP with agonist effect on VDCCs: the BayK 8644 i) induces cardiac and skeletal muscle contraction; ii) increases the mean open time and the conductance of the channel (Schramm et al., 1983; Nowycky et al., 1985) iii) shifts the current-voltage (I-V) relationship towards hyperpolarizing potentials and iv) slows current activation and deactivation. DHP antagonists and agonists bind with high affinity on the same specific binding sites to Ca_v1 subunits. The DHP binding domains involve amino acid residues localized on the domain III of S5-S6 and on the domain IV on S6 on the Ca_v1 subunit (Striessnig et al., 1998).

Like BayK 8466, FPL 64176 a nonDHP agonist enhances Ca^{2+} current, slows activation and inactivation kinetics of $Ca_v1.2$ current and shifts the IV relationship curve to negative voltage (Rampe & Lacerda, 1991; Kunze & Rampe, 1992).

In contrast to DHP, phenylalkylamines block the L-type current in a state and use-dependent manner from the intracellular side of membrane. They bind the Ca_v subunit on the domain III and IV of S6 and the pore region (Hescheler et al., 1982; Cai et al., 1997). Furthermore, benzothiazepines block L-type current in a use and state-dependent manner binding extracellularly on the domain IV of S5 and S6 (Watanabe et al., 1993; Cai et al., 1997). Very recently, Kang and co-workers developed a new potent and highly selective $Ca_v1.3$ subunit antagonist bearing an IC_{50} as low as 1.7 µM for $Ca_v1.3$ *versus*1162 µM for $Ca_v1.2$, the (1-(3-chlorophenethyl)-3-cyclopenylpyrimidine-2,4,6-(1*H*,3*H*,5*H*)-thione called compound 8 in my thesis; Kang et al., 2012).

For many years P- and Q- type VDCCs were considered as two different VDCCs due to their different biophysical and pharmacological properties: P-type current was observed in Purkinje cells (Llińas et al., 1989) whereas Q-type current was seen in granule cells (Randall & Tsien, 1995). A later study showed that $Ca_v2.1$ knockout (KO) mice neither displayed P-type current in Purkinje cells nor Q-type current in granule cells (Jun et al., 1999). Finally, the results presented by Bourinet et al. (1999) indicated that alternative splicing of the gene encoding $Ca_v2.1$ generates P-type and Q-type channels as well as multiple phenotypic variants. As a consequence, P- and Q- type VDCCs are now grouped as P/Q-type VDCCs. N-type VDCCs (for "neuronal") were exclusively cloned from brain (Catterall et al., 2005). Interestingly, like P/Q-type VDCCs, they are mostly localized in neuron terminals. Table 3 summarizes all biophysical characteristics of $Ca_v2.1$ and $Ca_v2.2$ subunits.

$Ca_v2.1$	
Conductance	9, 14, 19 pS (P-type, cerebellar Purkinje neurones); 16-17 pS (for $\alpha_{1A}/\alpha_2\delta/\beta$ in *Xenopus* oocytes)
Ion selectivity	$Ba^{2+} > Ca^{2+}$
Activation	V_a = -5 mV for native P-type, V_a = -11 mV for native Q-type (with 5 mM Ba^{2+} charge barrier) V_a = -4.1 mV for rat $\alpha_{1A\text{-}a}/\alpha_2\delta/\beta_4$ V_a = +2.1 mV for rat $\alpha_{1A\text{-}b}/\alpha_2\delta/\beta_4$ (with 5 mM Ba^{2+} charge carrier) V_a = +9.5 mV; τ_a = 2.2 ms at +10 mV for human $\alpha_{1A\text{-}1}/\alpha_2\delta/\beta_{1b}$ in HEK293 cells (with 15 mM Ba^{2+} charge carrier)
Inactivation	V_h = -17.2 mV for $\alpha_{1A\text{-}a}/\alpha_2\delta/\beta_4$; V_h = -1.6 mV for $\alpha_{1A\text{-}b}/\alpha_2\delta/\beta_4$ (with 5 mM Ba^{2+} charge carrier); V_h = -17 mV, τ_h = 690 ms at +10 mV human $\alpha_{1A\text{-}1}/\alpha_2\delta/\beta_{1b}$ in HEK293 cells (with 15 mM Ba^{2+} charge carrier), τ_h > 1 s at 0 mV native P-type (with 5 mM Ba^{2+} charge carrier)
$Ca_v2.2$	
Conductance	20 pS (bullfrog sympathetic neurones); 14.3 pS (rabbit BIII cDNA in skeletal muscle myotubes)
Ion selectivity	$Ba^{2+} > Ca^{2+}$
Activation	V_a = +7.8 mV, τ_a = 3 ms at +10 mV (human $\alpha_{1B}/\alpha_2\delta/\beta_{1\text{-}3}$ in HEK293 cells, 15 mM Ba^{2+} charge carrier); V_a = + 9.7 mV, τ_a = 2.8 ms at +20 mV (rat $\alpha_{1B\text{-}II}/\beta_{1b}$, in *Xenopus* oocytes, 40 mM Ba^{2+} charge carrier)
Inactivation	V_h = -61 mV, τ_h ~200 ms at +10 mV (human $\alpha_{1B}/\alpha_2\delta/\beta_{1\text{-}3}$ in HEK293 cells, 15 mM Ba^{2+} charge carrier); V_h = -67.5 mV; τ_h = 112 ms at +20 mV (rat $\alpha_{1B\text{-}II}/\beta_{1b}$ in *Xenopus* oocytes, 40 mM Ba^{2+})

Table 3: Biophysical properties of $Ca_v2.1$ and $Ca_v2.2$ subunits.
(From Catterall et al., 2005).

P/Q type VDCCs currents are blocked by two neurotoxins: ω-agatoxin VIA isolated from *Agelenopsis aperta* spider venom and ω-conotoxin MVIIC purified from the venom of *Conus magnus*, a marine snail. Both toxins bind to an extracellular site on $Ca_v2.1$ subunits but they

act according two different mechanisms. ω-agatoxin VIA stabilize the channels closed state (McDonough et al., 1997) whereas ω-conotoxin MVIIC is a pore blocker (McDonough et al., 2002).

N-type VDCCs are blocked by ω-conotoxine MVIIC and also by a specific blocker: the ω-conotoxin GVIA (peptide isolated from *Conus geographus* marine snail vemon, see Catterall et al., 2005 for review).

R-type (for "residual") currents flow throw channels based up on the $Ca_v2.3$ subunit and are resistant to DHP, ω-agatoxin GVIA, ω-conotoxin GVIA and ω-conotoxine MVIIC (Randall & Tsien, 1995; Randall & Tsien, 1997). Note that biophysical characteristics of $Ca_v2.3$ subunits are summarized in Table 4.

	$Ca_v2.3$
Conductance	Not established
Ion selectivity	$Ba^{2+} \sim Ca^{2+}$ (rat); $Ba^{2+} > Ca^{2+}$ (human)
Activation	V_a = +3.5 mV , τ_a = 1.3 ms at 0 mV (human $\alpha_{1E}/\alpha_2\delta/\beta_{1-3}$, 15 mM Ba^{2+} charge carrier in HEK293 cells) V_a = -29.1 mV , τ_a = 2.1 ms at -10 mV (rat $\alpha_{1E}/\alpha_2\delta/\beta_{1b}$, 4 mM Ba^{2+} chage carrier in *Xenopus* oocytes)
Inactivation	V_h = -71 mV, τ_h = 74 ms at 0 mV (human $\alpha_{1E}/\alpha_2\delta/\beta_{1-5}$, 15 mM Ba^{2+} charge carrier in HEK293 cells); V_h = -78.1 mV, τ_h = 100 ms at - 10 mV (rat $\alpha_{1E}/\alpha_2\delta/\beta_{1b}$, 4 mM Ba^{2+} charge carrier in *Xenopus* oocytes)

Table 4: Biophysical properties of $Ca_v2.3$ subunit.
(From Catterall et al., 2005)

They are inhibited by two non-specific blockers such as nickel ion (IC_{50} = 27 µM) and mibefradil (IC_{50} = 0.4 µM) (Jiménez et al., 2000) as well by a selective partial antagonist: SNX482 (IC_{50} = 15-30 nM), a toxin isolated from an African tarantula, *Hysterocrates gigas* (Newcomb et al., 1998).

LVA VDCCs: T-type VDCCs

Compared to HVA, T-type VDCCs currents display a low threshold (between -70 to -50 mV, peak around -30 mV) and fast activation kinetics (See Table 5 and Fig 18, Catterall et al., 2005; Helton et al., 2005). $Ca_v3.1$, $Ca_v3.2$ and $Ca_v3.3$ currents are blocked by nickel ion (respectively IC_{50} = 250, 12 and 216 µM), by mibefradil (Lee et al., 1999, Martin et al., 2000) and by amiloride (Todorovic & Lingle 1998; Monteil et al., 2000). Pharmacology of T-type VDCCs is summarized in Lory & Chemin (2007). Recently, a specific and reversible T-type VDCCs antagonist (3,5-dichloro-*N*-[1-(2,2-dimethyl-tetrahydro-pyran-4-ylmethyl)-4-fluoro-piperidin-4-ylmethyl]-benzamide, called TTA-P2) was created by Shipe et al., (2008) and is nowadays acknowledged as the most specific T-type current blocker (Boehme et al., 2011; Choe et al., 2011; Dreyfus et al., 2010; Eckle et al., 2012; Evans et al., 2013).

$Ca_v3.1$	
Conductance	7.5 pS
Ion selectivity	$Sr^{2+} > Ba^{2+} = Ca^{2+}$
Activation	V_a = -46 mV , τ_a = 1 ms at -10 mV
Inactivation	V_h = -73 mV, τ_h = 11 ms at -10 mV
$Ca_v3.2$	
Conductance	9 pS
Ion selectivity	$Ba^{2+} = Ca^{2+}$
Activation	V_a = -46 mV , τ_a = 2 ms at -10 mV
Inactivation	V_h = -72 mV, τ_h = 16 ms at -10 mV
$Ca_v3.3$	
Conductance	11 pS
Ion selectivity	$Ba^{2+} = Ca^{2+}$
Activation	V_a = -44 mV , τ_a = 7 ms at -10 mV
Inactivation	V_h = -72 mV, τ_h = 69 ms at -10 mV

Table 5: Biophysical properties of $Ca_v3.1$, $Ca_v3.2$ and Cav3.3 subunits.
(From Catterall et al., 2005).

1.2.2 Auxilliary subunits.

In the case of HVA VDCCs, the Ca_v subunit is generally associated with a cytoplasmic β subunit, a membrane-anchored extracellular α2δ subunit and a γ subunit (Fig 17). The auxiliary subunit composition of LVA is not yet completely understood.

Amongst calcium channel auxiliary subunits, the β subunit is the most intensively studied. In mammals, four β subunit isoforms have been identified (β1, β2, β3 and β4) and are encoded by four different genes (see Birnbaumer et al., 1994 for review). All β subunits have several splice variants such as the β1a, β1b and β1c splice variants for β1 (See Dolphin, 2003a for review). All 4 beta subunits are known to be expressed in the CNS (Williams et al., 1992; Collin et al., 1993; Ludwig et al., 1997, Vendel et al., 2006). The β subunits is a cytosolic protein that contains an *src* homology 3 (SH3)/guanylate kinase (GK) domain (Fig 17B). They bind with high affinity to a conserved region of 18 residues on the intracellular I-II loop of Ca_v subunit via their GK domain as well as to the C or N termini of Ca_v subunit with lower affinity. In association with Ca_v1 and Ca_v2 subunits, all β subunit isoforms, increase calcium current amplitude, shift the voltage-dependence towards more negative values and modify channel inactivation and activation properties (see review Buraei & Yang, 2010). The β subunit has been shown to increase the number of P/Q-type VDCCs at membrane surface by masking ER retention signal on Ca_v subunit (Bichet et al., 2000). The I-II loop of the β subunit was suggested to be an ER export signal motif and accordingly the β subunit increases surface density of channels by binding I-II loop of $Ca_v1.2$ subunit for instance (Fang & Colecraft, 2011). In the cerebellum β subunits seem to play a role in the developmental regulation of VDCCs and bear different subcellular localizations. Indeed, β1, β3 and β4 subunits expression increase in mice from birth to adulthood. Whereas β1 and β3 are predominantly located in Purkinje cell dendrites, β4 is usually detected in dendrites and axons (Ferrándiz-Huertas et al., 2012).

HVA VDCCs also contain the auxiliary $\alpha_2\delta$ subunit (Chang & Hosey, 1988; Witcher et al., 1993; Liu et al., 1996, see Dolphin 2013 for review). Four $\alpha_2\delta$ genes have been cloned to date and they encode four different $\alpha_2\delta$ subunit isoforms namely $\alpha_2\delta$-1, $\alpha_2\delta$-2, $\alpha_2\delta$-3 and $\alpha_2\delta$-3. $\alpha_2\delta$-1 has an ubiquitous distribution, $\alpha_2\delta$-2 and $\alpha_2\delta$-3 are more selectively expressed in neurons ($\alpha_2\delta$2 is abundant in the cerebellum) and $\alpha_2\delta$-4 is mainly found in non-neuronal tissues except retina neurons (Klugbauer et al., 1999; Barclay et al., 2001; Qin et al., 2002; Wycisk et al., 2006). The $\alpha_2\delta$ subunit is encoded by a single messager RNA then linked by disulfide-bonded and finally subjected to proteolytic cleavage (De Jongh et al., 1990). The C-terminal of $\alpha_2\delta$ is hydrophobic and constitutes a potential transmembrane domain important for membrane anchoring using glycosyl-phosphatidylinositol (GPI)-anchored (Davies et al., 2010). As β subunit, the $\alpha_2\delta$ subunit isoforms promote channel trafficking and expression at plasma membrane (Shistik et al., 1995; Jones et al., 1998; Klugbauer et al., 2003) and modify biophysical properties of the calcium currents: effects on voltage-dependence of activation and inactivation as well as on steady-state inactivation have been reported (Shistick et al., 1995; Felix et al., 1997; Wakamori et al., 1999; Hobom et al., 2000). In addition, it has recently been shown that over-expression of $\alpha_2\delta$ in cultured hippocampal neurons induces accumulation of presynaptic $\alpha_2\delta$ and $Ca_v2.1$ subunit and, promotes exocytosis with a decrease of Ca^{2+} influx. This result suggests that the number of VDCCs increases at the active zone and hence Ca^{2+} entry is more efficient to trigger neurotransmitter release (Hoppa et al., 2012).

Eight γ genes have been identified and encode eight different γ subunit isoforms: γ1-8. The γ1 subunit was solely detected in skeletal muscle and γ2, γ3, γ4 and γ7 expression is detected in MLIs (Klugbauer et al., 2000, Fukaya et al., 2005; Bats et al., 2013 for review). γ2 and γ3 interact with $Ca_v2.1$ and $Ca_v2.2$ subunits as demonstrated with *in vivo* experiments (Kang et al., 2001). Contrary to β and $\alpha_2\delta$ subunits, γ subunit seems to negatively modulate biophysical properties of Ca_v subunits. γ2 subunit decelerates activation kinetic and decreases

the calcium current amplitude (Kang et al., 2001). In the other hand, γ subunits have been identified to play a critical role in AMPA receptors trafficking, expression at the cell surface and clustering at the synapse and they also modify biophysical properties of AMPA receptors (Tomita et al., 2003; Nicoll et al., 2006; Soto et al., 2007; Milstein & Nicoll, 2009). Interestingly, in *stargazer* mice (homozygous mice with spontaneous mutation of γ2), Ca^{2+} permeable AMPA receptor expression is increased in stellate cell (Bats et al., 2012).

1.2.3 Localization and role of VDCCs.

Ca_v isoforms bear different cellular and subcellular localizations as well as different functions (summarized in Table 1 and Fig 19). The involvement of VDCCs in neurotransmitter release will be detailed later on in this manuscript (part 1.3).

$Ca_v1.1$ and $Ca_v1.4$ subunit are respectively expressed in skeletal muscle and retina. More precisely, the $Ca_v1.1$ subunit mediates muscular contraction and is physically coupled to RyR (see 1.2.4) whereas $Ca_v1.4$ is localized in presynaptic termini at the ribbon sensory synapse and mediates glutamate release (Morgans, 2001). $Ca_v1.2$ and 1.3 subunits have been found in cardiac and smooth muscle as well as in endocrine cells (Catterall et al., 2005). Both isoforms are also found in brain (Calin-Jageman & Lee, 2008) and $Ca_v1.3$ is expressed in sensory cells such as in inner ear (Catterall et al., 2005). L-type VDCCs are involved in electrical coupling contraction in skeletal and cardiac muscle (see 1.2.4) and in hormone release (Sinnegger-Brauns et al., 2004, Marcatoni et al., 2007). In addition, $Ca_v1.3$ subunit is mainly involved in neurotransmitter release in the inner hear, $Ca_v1.3$ knockout mice being therefore completely deaf (Platzer et al., 2000). In central neurons, the $Ca_v1.2$ and $Ca_v1.3$ subunits are usually concentrated in the somato-dendritic compartment as well as in dendritic spines (Westenbroeck et al., 1990; Hell et al., 1993; Tippens et al., 2008). In the postsynaptic

compartment, they are known to regulate gene transcription (Dolmetsh et al., 2001). Moreover, $Ca_v1.3$ has been reported to mediate spontaneous firing in dopaminergic neurons in substantia nigra (Chan et al., 2007; Puopolo et al., 2007). L-type VDCCs are also found in presynaptic terminis at central synapses and involved in neurotransmitter release and in presynaptic plasticity (see part 1.3 for detailled explanations).

$Ca_v2.1$ and $Ca_v2.3$ subunit are expressed in neurons, heart and pancreas while $Ca_v2.2$ is restricted in neuron (Catterall et al., 2005). All these isoforms are mainly localized in presynaptic termini and are involved in neurotransmitter release (see part 1.3 and Catterall et al., 2005).

Finally, all members of the Ca_v3 family are expressed in neurons especially in dendrites (Williams and Stuart, 2000; McKay et al., 2006; Diana et al., 2007) and also in axons. T-type VDCCs mediate subthreshold oscillation, pacemaker activity and neurotransmitter release (see part 1.3 and Lambert et al., 2013 for review).

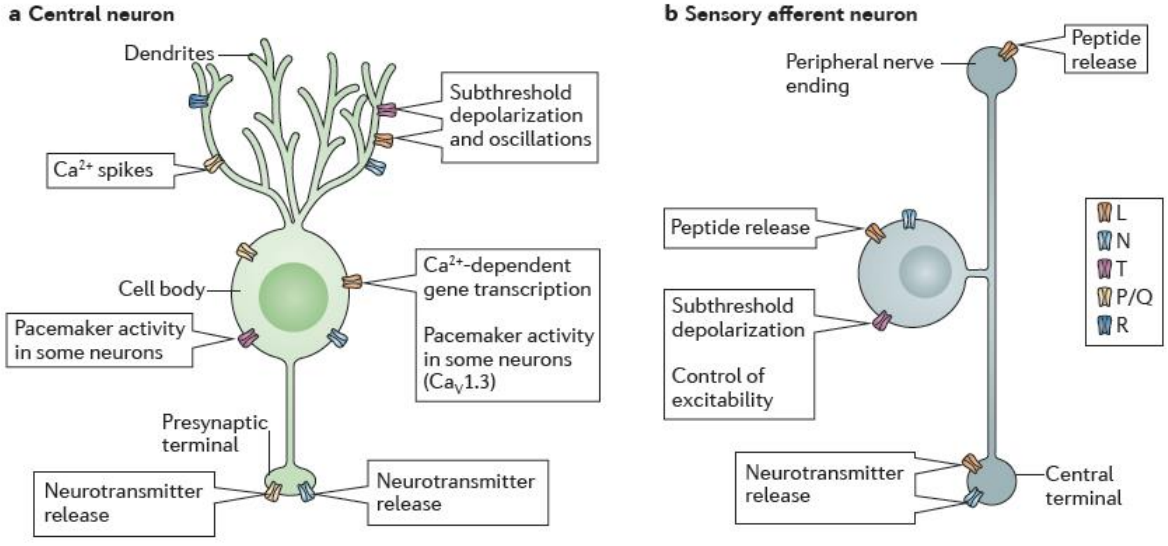

Fig 19: Localization and role of VDCCs in central and sensory neurons.
(From Dolphin 2012).

1.2.4 Interaction with other proteins.

VDCCs can interact with several intracellular proteins including calmodulin, Ca^{2+}-binding proteins, Ca^{2+} -dependent protein kinase II, RyR, PDZ domain containing proteins and synaptic proteins (Spafford & Zamponi, 2003; Calin-Jageman & Lee, 2008). These interactions are likely to mediate processes such as muscular contraction, gene regulation and neurotransmitter release. In the context of this thesis, I focused on the interactions with RyRs and synaptic proteins and therefore I will not detail the others.

1.2.4.1Physical coupling with RyR.

Coupling between $Ca_v1.1$ and ER is well characterized in skeletal muscle. In fact, in skeletal muscle, electrical contraction coupling requires direct coupling between $Ca_v1.1$ and RyR1 resulting in a calcium-release from the sarcoplasmic reticulum independently of Ca^{2+} influx (for review see Catterall, 1991). As in skeletal muscle, a few studies showed physical interaction between $Ca_v1.x$ and RyR in brain and spinal cord (Chavis et al., 1996; Mouton et al., 2001; Ouardouz et al., 2003; Kim et al., 2007). Of interest, Mouton and co-workers showed that $Ca_v1.3$ and $Ca_v1.2$ subunits co-immonuprecipitate with RyR1 (Mouton et al., 2001). In the spinal cord, $Ca_v1.2$ - RyR1 and Cav1.3 – RyR2 functional complexes are found in axons and induce a depolarization-mediated Ca^{2+} release independently of Ca^{2+} influx (Ouardouz et al., 2003). In a similar way, $Ca_v1.3$ and RyR2 form a functional and direct physical complex which the activation induces RyR2 mRNA level up-regulation (Kim et al., 2007).

1.2.4.2 Interaction with synaptic proteins.

Interaction between VDCCs with synaptic proteins is well characterized for Ca_v2 subunits and will be more detailed in part 1.3. In addition, some studies have suggested interactions with members of Ca_v1 family (Calin-Jagemam & Lee, 2008).

1.2.5 Regulation of VDCCs by G proteins.

VDCCs are modulated by activation of heterometrimeric G proteins (αβγ) coupled receptors (see for review Dolphin, 2003b) in response to several neurotransmitters or hormones. Activation of G protein produces two signaling molecules namely Gα-GTP and G βγ dimer. The Gα-GTP pathway requires a second messager such as a protein kinase that will phosphorylate Ca_v subunits and consequently induce a potentiation of the current (Osterrieder et al., 1982; Kameyama et al., 1985). The G βγ dimer is a direct pathway that does not require second messenger and usually results in an inhibition of the channels (Ikeda, 1996; Herlitze et al., 1996).

1.2.5.1 PKA.

The PKA-evoked regulation of VDCCs has mainly been studied in the muscular context and especially for L-type channel. Activation of β-adrenergic receptors coupled to heterotrimeric $G\alpha_s$ proteins induces phosphorylation of serine residues on $Ca_v1.1$ and $Ca_v1.2$ subunit C-terminal domain by cyclic AMP-dependent PKA (Bean et al., 1984; Curtis & Catterall, 1985; De Jongh et al., 1996; Gao et al., 1997; Naguro et al., 2001). The PKA phosphorylation of the channel results in an enhancement of Ca_v1 current through an increase in the channel open probability and a shift of the I-V curve towards negative voltages (Naguro et al., 2001). In the same way, in hippocampal neurons, calcium signals evoked by L-type VDCCs activation in dendrite and in dendritic spines are modulated by β-adrenergic agonists (Hoogland & Saggau 2004). In various different tissues L-type VDCC current amplitude and open probability in inside-out and whole cell patch-clamp recording decrease progressively (Armstrong & Eckert, 1987; Belles et al., 1988; Kepplinger et al., 2000). This phenomenon referred to as “run-down” can be reversed by addition of PKA in the bath in inside-out patch

clamp experiments (Ono & Fozzard, 1992). This “run-down” process is likely to result from the dialysis of cytoplasm during the whole cell recording.

PKA can also phosphoryle $Ca_v2.2$, $Ca_v2.3$ and β2 subunits but its involvements on biophysical properties of calcium channels is still unknown (Hell et al., 1995; Gao et al., 1997; Gerhardstein et al., 1999).

1.2.5.2 PKC.

In neurons, activation of heterotrimeric $G\alpha_q$ induces activation of PKC. A PKC phosphorylation is known to enhance P/Q, N, R and L-type currents by increasing the channel opening probability (Swartz, 1993; Swartz et al., 1993; Yang & Tsien, 1993; Stea et al., 1995). In hippocampal neurons, L-type current amplitude enhancement through $GABA_B$ receptor activation involves PLC-dependent PKC pathway (Bray & Mynlieff, 2011).

1.2.5.3 G βγ dimer.

G protein βγ dimer binding on Ca_v2 subunits results in an inhibition of the calcium current (Herlitze et al., 1996; Ikeda, 1996; Tedford & Zamponi, 2006). G protein βγ dimer binds directly with high affinity a short sequence QXXER in the intracellular loop on domain I and II (Herlitze et al., 1997; DeWaard et al., 1997; Furukawa et al., 1998). Interestingly, this sequence is not present in Ca_v1 family (Herlitze et al., 1997; DeWaard et al., 1997). A strong depolarization is required to unbind G βγ from the channel and then obtain a disinhibition of the channel (Elmslie et al., 1990). It has been suggested that G protein βγ dimer regulation may have an important role for synapse physiology (Brody et al., 1997; Williams et al., 1997). At the molecular level, the β subunit is involved for voltage–dependent G protein βγ dimer dissociation (Zhang et al., 2008).

1.3 VDCCs and neurotransmitter release.

At chemical synapses, it is classically accepted that neurotransmitter release is initiated by a Ca^{2+} influx through VDCCs opened by the arrival of an action potential at the presynaptic termini (Del Castillo & Stark, 1952; Katz & Miledi, 1970; summarized in Barret & Tsien, 2004). The local rise of intracellular Ca^{2+} concentration at the vicinity of VDCCs is necessary to trigger the exocytosis of neurotransmitter containing vesicles. At molecular level, vesicle docking and fusion of membrane bilayers are mediated by a complex composed of at least three proteins called SNARE proteins (SNARE for *synaptic α-soluble NSF attachment protein receptors*) and by SM proteins (SM for Sec1/Munc18-like proteins; for review see Südhof, 2004 and Barclay et al., 2005). Two SNARE proteins are located on the plasma membrane (t-SNARE): syntaxin and SNAP-25 (for *synaptosomal associated protein of 25 kDa*), and one on synaptic vesicles (v-SNARE): synaptobrevin/VAMP (for *vesicle associated membrane protein*). SNARE complex proteins do not have calcium sensitivity, and then to trigger Ca^{2+} dependent exocytosis a supplementary actor is required: the synaptotagmin. Synaptotagmin, the Ca^{2+} sensor of membrane fusion, is a conserved vesicular protein composed by two cytoplasmic Ca^{2+} binding C_2 domains (Davletov & Südhof, 1993; Li et al., 1995a; Li et al., 1995b). Interestingly, complexin (a small protein of 130 amino acids) stabilizes the SNARE complex to avoid spontaneous membrane fusion (Maximov et al., 2009). The current model proposes that the Ca^{2+} activated synaptotagmin triggers membrane fusion by displacing complexin action on the SNARE complex (Maximov et al., 2009; summarized in Südhof 2013).

Katz and Mideli (1965 a) observed a delay between the terminal axon spike and the appearance of the postsynaptic end-plate current at nerve-muscle junction (the synaptic delay). The same authors later showed that the synaptic delay is due to the release of neurotransmitter and has a minimal value of 0.4-0.5 ms (Katz & Mideli, 1965 b). More recently,

electrophysiological studies have demonstrated that Ca^{2+} ions induce vesicle fusion with plasma membrane in less than 100 µs (Sabatini & Regehr, 1996). This short synaptic delay requires a tight coupling between VDCCs and exocytoxic machinery.

1.3.1 Ca^{2+} dependence of neurotransmitter release.

1.3.1.1 Tight coupling between VDCCs and exocytotic machinery.

The Ca^{2+} dependence of neurotransmitter release following an action potential was initially observed by Del Castillo and Stark in 1952. Later on, Katz and Miledi (1970) proposed a mechanism for the squid giant synapse and proposed that an increase in intracellular Ca^{2+} is a prerequisite to excitation-exocytosis coupling, vesicles docking and fusion of the vesicles and the plasma membrane. Shahrezaei and co-workers (2006) demonstrated that Ca^{2+} influx through one or two VDCCs is sufficient to trigger synaptic vesicle fusion. Electron tomography experiments performed at the frog neuromuscular junction showed that the distance between VDCCs and synaptic vesicles is only 20 nm (Harlow et al., 2001). These studies have emphasized the idea that the distance between presynaptic VDCCs and the Ca^{2+} sensors responsible for vesicles exocytosis has a major impact on the properties of the synapses. The physical distance between VDCCs and Ca^{2+} sensors can be deduced from experiments based on the intracellular application of exogenous Ca^{2+} chelators bearing different binding rates, but relatively similar affinities. Briefly, if VDCCs and Ca^{2+} sensors are tightly coupled (distance shorter than ~100 nm), only BAPTA will be able to block the synaptic transmission by intercepting Ca^{2+} ions on their way from the pore of the VDCC to the sensor. For such a coupling, EGTA will be ineffective. If the distance is longer however, EGTA and BAPTA will definitely interrupt the synaptic transmission. The

limit between nanodomain and microdomain has been set at a distance of 100 nm (see Eggermann et al., 2012 for review), a value that is exactly in the middle of the radius of a synaptic vesicle (20 nm) and the radius of an active zone (~150 nm). This paradigm has been applied at the output synapses of inhibitory cells in the cerebellum. At the MLI/MLI synapse, the presence of 1 mM EGTA in the intracellular compartment did not affect the proportion of synaptic failures (Caillard et al., 2000). Moreover, at basket cell synapses, extracellular application of EGTA-AM (20 μM) did not significantly alter the GABA release evoked by a single presynaptic action potential (Christie et al., 2011). Taken together, these results suggest a tight coupling between VDCCs and Ca^{2+} sensors. It seems therefore likely that evoked transmitter release at fast cerebellar GABAergic synapses is controled by Ca^{2+} nanodomains. As a result of many studies (summarized in Eggermann et al., 2012) it appears that certain synapses such as fast GABAergic synapses of hippocampal or cerebellar basket cells rely on nanodomain coupling, whereas others such as glutamatergic synapses between layer 5 pyramidal neurons use microdomain coupling. Interestingly, the synapses that use nanodomain coupling were often characterized by their nearly exclusive usage of $Ca_v2.1$ for transmitter release (Forti et al., 2000; Stephens et al., 2001; Hefft and Jonas, 2005 and Bucurenciu et al., 2010). On the other hand, a longer distance between VDCCs and Ca^{2+} sensors is retrieved in synapses mainly relying on $Ca_v2.2$ and $Ca_v2.3$ for neurotransmitter release. Finally, $Ca_v1.3$ is known to be tightly coupled to the Ca^{2+} sensors in auditory hair cells (Brandt et al., 2005). The high efficacy of activation of $Ca_v2.1$ and $Ca_v2.2$ by action potentials (Li et al., 2007) suggests that the synapse may be functional with only a small number of VDCCs present at each active zone. By contrast, a high number of channels with a lower efficacy of activation (such as $Ca_v1.3$) would be required to obtain a working synapse (summarized in Eggermann et al., 2012).

1.3.1.2 Miniature currents.

Spontaneous miniature release discovered by Fatt and Katz (1952) at the neuromuscular junction is generated by presynaptic Ca^{2+} fluctuations in the absence of an action potential. They can be mediated by stochastic opening of presynaptic VDCCs and by Ca^{2+} release from ER (see Glitsch, 2008 for review). Postsynaptic currents in response to the spontaneous miniature release are referred to as miniature postsynaptic currents named mIPSC for inhibitory or mEPSC for excitatory. Miniature currents can be recorded in presence of TTX in the bath and may play various roles in the CNS. For instance, glutamatergic miniature currents in hippocampus are involved in the maintaining of dendrite spines and mRNA translation in dendrites (McKinney et al., 1999; Sutton et al., 2004). Furthermore, inhibitory miniature current can strongly modify MLIs firing in the cerebellar cortex (Carter & Regehr, 2002).

1.3.1.3 Analog signaling.

In mammalian brain, a somatic subthreshold depolarization can propagate along the axon to the presynaptic termini due to membrane cable properties and consequently modulate the shape of action potentials possibly leading to enhanced neurotransmitter release (Alle & Geiger, 2006; Shu et al., 2006). This process is referred to as “analog signaling”. The initial finding was that a somatic subthreshold depolarization of a MLI could enhance the mIPSC frequency recorded in a Purkinje cell (Glitsch & Marty, 1999). Recently, Christie and co-workers demonstrated that such a subthreshold depolarization of a MLI strengthens action potential-evoked GABA release, enhances axonal Ca^{2+} entry and evokes asynchronous release (Christie et al., 2011). Slightly controversial results were proposed by Bouhours et al. (2011) in the same preparation. These latter authors demonstrate that the autoreceptor GABAergic current recorded in MLIs is enhanced by subthreshold depolarization and that a presynatic Ca^{2+} elevation can be elicited by the same stimulation. However, they do not retrieve the

enhancement of the action potential-evoked Ca^{2+} transients proposed by Christie et al. (2011). Both studies argue in favor of an involvement of VDCCs in the analog signaling (Bouhours et al., 2011 propose presynaptic P/Q-type VDCCs and PKC activation as molecular mechanism) but they report conflicting effects of EGTA suggesting either micro- or nanodomain coupling.

1.3.2 P/Q and N-type VDCCs: the main actors of neurotransmission in the CNS.

P/Q- and N-type VDCCs are usually presented as crucial for the depolarization-induced neurotransmitter release process and they are classically detected in presynaptic termini (Takahashi & Momiyama, 1993, Dunlap et al., 1995; Mintz et al., 1995; Catterall et al., 2005). Moreover, direct interactions between Ca_v2 subunit and proteins of the exocytotic machinery are known to facilitate the coupling between a local rise of presynaptic Ca^{2+} ions and neurotransmitter release (Evans & Zamponi, 2006). Due to limited time and space, I mainly focused on the cerebellum and therefore I will not details this topic in the others parts of CNS.

Several immunolocalization studies have shown $Ca_v2.1$ expression in synaptic termini in the cerebellar molecular layer and the mossy fiber in the CA3 region of the hippocampus (Llinas et al., 1992; Westenbroek et al., 1995; Stephens et al., 2001). Moreover, autoradiography studies using the $Ca_v2.2$-specific ^{125}I-labeled ω-conotoxin GIVA showed high expression of $Ca_v2.2$ in presynaptic structures in striatum, hippocampus, cortex and cerebellum (Albensi et al., 1993; Kerr et al., 1988; Takemura et al., 1988; Azimi-Zonooz et al., 2001). Similar observations were reported in several immunochemistry studies: a strong $Ca_v2.2$ immunoreactivity was nearly always found in presynaptic termini of rat brain (Westenbroek et al., 1992; Hanson & Smith, 2002).

There is evidence for synaptic proteins such as syntaxin and SNAP-25 interacting

directly with $Ca_v2.1$ and $Ca_v2.2$ subunits via the intracellular loop between domain II and III called "synprit' site (Sheng et al., 1994; Rettig et al., 1996; Sheng et al., 1997; Sheng et al., 1998, Seager et al., 1999). Injection of a peptide containing the synprit site in the presynaptic neurons induces a reduction of the Ca^{2+} influx efficiency to trigger neurotransmitter release (Mochida et al., 1996), suggesting the destruction of an interaction.

In the cerebellar cortex, the pharmacological properties of presynaptic VDCCs have been examined at both excitatory and inhibitory synapses on Purkinje cells (Doroshenko et al., 1997; Forti et al., 2000; Stephens et al., 2001). Spontaneous EPSCs recorded Purkinje cell synapses are sensitive to ω-agatoxin IVA and ω-contoxin MVIIC. Unlike spontaneous EPSCs, spontaneous IPSCs are insensitive to ω-agatoxin IVA, ω-contoxin MVIIC and nimodipine but they are inhibited by Ni^{2+} ions and amiloride, suggesting a role of T-type VDCCs in GABA release in MLIs (Doroshenko et al., 1997). Forti et al. (2000) detected a partial reduction of action potential-evoked presynaptic Ca^{2+} transient in MLIs following the application of ω-agatoxin IVA and ω-contoxin MVIIC and a total block in presence of Cd^{2+}. In this study, nimodipine failed to affect axonal Ca^{2+} transient in MLIs and it was suggested that toxin-resistant VDCCs (such as R-type) could mediate the Ca^{2+} entry. Stephens and co-workers (2001) showed that spontaneous IPSCs recorded in Purkinje cells are blocked in a same proportion by ω-agatoxin IVA and by Cd^{2+}, arguing for a unique participation of presynaptic P/Q-type VDCCs in the onset of spontaneous IPSCs. Immunochemical experiments presented in the very same report plead in favor of a presynaptic localization of $Ca_v2.1$ subunits in MLIs.

1.3.3 Other VDCCs.

1.3.3.1 R-type VDCCs.

$Ca_v2.3$ subunits have been identified in different presynaptic locations in the CNS such

as mossy fiber termini in hippocampus (Day et al., 1996) and in globus pallidus neurons (Hanson & Smith, 2002). $Ca_v2.3$ and synaptotagmin immunoreactivity colocalize in the Calyx of Held and a fraction of $Ca_v2.3$ labeling appears distant from the active zone (Wu et al., 1999). Although the $Ca_v2.3$ subunit does not have a synprint site, it has been shown to be likely to interact with synaptic proteins such as syntaxin and synaptotagmin but the putative site of interaction remains unknown (Bergsman & Tsien, 2000; Wiser et al., 2002; Cohen et al., 2003; Cohen & Atlas, 2004).

In cerebellum, Stephens and co-workers (2001) have suggested a putative involvement of R-type VDCCs in action potential-evoked axonal Ca^{2+} transient in MLIs. R-type VDCCs have been shown to be located in granule cell presynaptic terminis (Brown et al., 2004) and they were also recently proposed to participate in the induction of presynaptic parallel fiber long term potentiation (LTP, Myoga & Regehr, 2011).

1.3.3.2 L-type VDCCs.

It is generally believed that presynaptic L-type VDCCs have a minor role in spontaneous neurotransmitter release triggered by an action potential except at sensory synapses. In cochlear inner hair cells for instance, exocytosis is triggered by a Ca^{2+} influx through presynaptic $Ca_v1.3$ channels (Platzer et al., 2000, Brandt et al, 2003). Furthermore, these channels are clustered at the active zone and few channels may controls exocytosis by a nanodomain coupling with the exocytotic apparatus (Brandt et al., 2005).

Only a few studies have reported the expression of L-type VDCCs in presynaptic termini in central neuron using electron microscopy experiments (Tippens et al., 2008; Leitch et al., 2009; Subramanian; 2013). In pancreatic β-cells however, syntaxin and SNAP-25 do interact with $Ca_v1.2$ subunit via the intracellular loop between domain II and III (Wiser et al., 1999) and this presynaptic L-type VDCCs play a role in presynaptic plasticity and learning

(see below).

Presynaptic plasticity at different synapses in hippocampus

L-type VDCCs have been reported to be involved in short-term plasticity at GABAergic synapses in the hippocampus. Using dual whole cell patch-clamp recordings on cultured hippocampal neurons, Jensen et al. (1999a) have found that the tetanization of the presynaptic neuron at frequencies neighboring 40 Hz results in a posttetanic potentiation (PTP) of the IPSCs recorded in the postsynaptic neuron. This minute lasting increase of evoked IPSC was meant to result from accumulation of Ca^{2+} in the presynaptic termini. Later on, the same authors have shown that this PTP process was dramatically reduced in the presence of nifedipine indicating an involvement of L-type VDCCs (Jensen et al., 1999b). More precisely, nifedipine and isradipine reduced the potentiation of IPSC evoked by a tetanic stimulation (40 Hz for 2 s) although they had no effect on single IPSC evoked at low frequency (0.2 Hz). It is of interest to note that BayK8644 had no effect on the induction of PTP with a high frequency stimulation, a lack of effect that was attributed to a saturating effect of Ca^{2+} ions. Such a result has been retrieved in slices with paired recordings from hippocampal basket cells and granule cells: a short-term plasticity of GABA release is controled by L-type VDCCs in the ϒ-frequency range (Jensen and Mody, 2001). Using the technique of styryl dye-destaining, Brager et al. (2003) studied GABA exocytosis in organotypic slice cultures, at single boutons in the CA1 stratum pyramidale region. They found that with 2 and 5 Hz stimulation, the release from most boutons declined similarly whether induced by Ca^{2+} ions flowing through N- or P/Q-type VDCCs. A 10 Hz stimulation however, caused a short-term facilitation of exocytosis in the presence of ω-agatoxin IVA in cells that would not express $Ca_v2.2$. These authors noted that although Cav1.x related Ca^{2+} influx does not participate in GABA release at low-stimulus frequencies (Jensen et al., 1999b), the facilitation of GABAergic exocytosis was inhibited by nifedipine suggesting an involvement of L-type VDCCs at high stimulation

frequencies.

Holmgaard and co-workers (2008) have visualized the Ca^{2+} entry through presynaptic L-type VDCCs on GABAergic termini after a posttetanic stimulation using intracellular Fluo-3 in hippocampal cultures. Besides, Murakami et al. (2002) have shown that the evoked IPSCs recorded in response to a focal stimulation of GABAergic termini on dissociated CA1 pyramidal neurons are sensitive to nivaldipine and BayK8644. In the context of a focal stimulation, L-type VDCCs are likely to contribute to Ca^{2+} action potentials further activating P/Q- and N-type VDCCs located closely to the active zone. Nivaldipine prevents the potentiation of IPSCs evoked by high frequency stimulation of Schaffer collateral but has no effect on IPSCs evoked at low stimulation frequency.

L-type VDCCs seem to be also involved in glutamatergic synapses plasticity. In rat hippocampal slice, stimulation of mossy fibers induces an NMDA-receptor-independent LTP that is fully blocked by simulated application of LY382884 (kainate receptors blocker) and nifedipine (Lauri et al., 2003).

Presynaptic L-type VDCCs and fear conditioning

Fear conditioning is associated with presynaptic LTP dependent of NMDA receptors at cortical afferents onto lateral amydala (Milner et al.,1998; Humeau et al., 2003). Interestingly, two *in vivo* studies suggest a role of presynaptic L-type VDCCs in fear conditioning induction. In fact, fear conditioning is impaired by injection of verapamil or nimodipine in lateral amydala (Bauer et al., 2002; Shinnick-Gallagher et al., 2003). Furthermore, this presynaptic LTP can be induced by application of the adenylyl cyclase activator forskolin, which activates the cAMP-PKA pathway and then enhance neurotransmitter release at cortico-lateral amydala synapse (Fourcaudot et al., 2008). VDCCs subtype contribution was confirmed by the pharmacological study of Fourcaudot and co-workers (2009) on acute brain slice. Spontaneous EPSC amplitude is strongly reduced by ω-agatoxin IVA and ω-conotoxin GIVA

whereas the induction of presynaptic LTP is prevented by verapamil and nimodipine. Finally, these authors show that application of BayK8644 strongly increases the EPSC amplitude and decreases the PPR.

Regulation of presynaptic L-type VDCCs

Subramanian and collaborators (2011, 2013) have recently investigated putative molecule that could regulate presynaptic L-type VDCCs in primary cortical neurons. Firstly, inhibition of Erk1/2 induces an increase in presynaptic Ca^{2+} influx and hence exocytosis. This process, unaffected by a mixture of ω-agatoxin IVA, ω-contoxin GVIA and Ni^{2+} ions, is not detected in the presence of nitrendipine. Moreover, they postulate that Erk1/2 inhibition induces the recruitment of new L-type VDCCs located at presynaptic cell surface (Subramanian & Morozov, 2011). Finally, they identified Erk1/2 as the downstream effector of small GTPase Rap1signaling (Subramanian et al., 2013).

Miniature synaptic currents and L-type VDCCs

Some studies have demonstrated an effect of DHP antagonists and agonists on miniature release in different part of the CNS. For example, BayK8644 administration into the caudate putamen significantly increased the extracellular dopamine level in presence of TTX, generating locomotor activity and rearing behavior (Okita et al., 2000). Furthermore, in dissociated rat substantia innominata, mIPSCs are sensitive to BayK8644, nicardipine and nimodipine (Watanabe et al., 2002). A pharmacological study performed on hippocampal granule cell showed that 50% of mIPSC were Ca^{2+} dependent and involved N- and L-type VDCCs (Goswani et al., 2012). Recently, Williams and co-workers (2012) showed that Ca^{2+} dependent mIPSC are resistant to application of toxins, suggesting a putative involvement of R- and L-type in mIPSC recorded in primary neocortical cell culture.

To conclude, L-type VDCCs which are often neglected for spontaneous release, seem to have an important role in presynaptic plasticity and in miniature release in different part of the CNS.

1.3.3.3 T-type VDCCs.

Immunogold labeling experiments have shown $Ca_v3.2$ subunit localization in the glutamatergic presynaptic termini on entorhinal cortical layer III pyramidal neurons (Huang et al., 2011). Some pharmacological studies have proposed an involvement of T-type VDCCs in neurotransmitter release at central and sensory synapses. In isolated axon-terminal preparation from bipolar cells, capacitance increased by step depolarization at -30 mV is insensitive to nimodipine and is abolished by application of mibefradil (Pan et al., 2001). In the olfactory bulb, amplitude of evoked IPSCs recorded in mitral cells was reduced by application of mibefradil (Egger et al., 2003). More recently, a study showed that presynaptic hyperpolarization-activated cyclic nucleotide-gated channels inhibit glutamate release on entorhinal cortical layer III pyramidal neurons by reduction of $Ca_v3.2$ VDCCs activity (Huang et al., 2011). In hippocampus, acetylcholine evoked asynchronous GABA release is sensitive to TTA-P2 (Tang et al., 2011). To reinforce the role of T-type VDCCs in neurotransmitter release, a recent study revealed that $Ca_v3.2$ subunit interacts with syntaxin in rat brain (Weiss et al., 2012).

Chapter 2

Materials and methods

Materials and methods used for my thesis are developed in the Results section (Chapter 3). In this part, I focused on some important points that are not detailed either in the "results" or in the "materials and methods" sections.

2.1 Electrophysiological experiments.

2.1.1 Liquid junction potential.

Liquid junction potentials are generated by the different motilities of ions at the interfaces between two solutions. Before sealing during an electrophysiological experiment, a net movement of charge is prevented by the negative offset potential applied in the patch pipette. In whole cell recording, liquid junction potential disappears, but the offset potential remains. It gives rise to an offset error in the recorded membrane potential. Generally junction potentials are comprised between 2 to 12 mV. Use of KCl solution minimizes the problem of the liquid junction potential because K^+ and Cl^- have nearly equal ionic motilities. We calculated the liquid junction potential created by our two internal solutions at a temperature of 22°C, using "Liquid Junction Potential" calculator under Igro Pro environment. We found a liquid junction potential of 3.7 mV for our KCl solution and of 9.5 mV for our CsGluconate solution. Liquid junction potentials were corrected off-line.

2.1.2 Bayk concentration – response on mIPSC frequency.

mIPSCs were recorded in MLIs as previously described in the article (Chapter 3). To perform the BayK8644 dose-response on mIPSC frequency, different concentrations of BayK8644 were added in the bath: 0.1, 0.3, 1 and 3 μM. For analysis, average increase of mIPSC frequency elicited by application of BayK8644 was plotted as a function of the log of BayK8644 concentration.

2.1.3 Preparation of acute brain slices for older rats.

For older rats (P17-P26), the solution slicing and incubation solutions used were (in mM): 87 NaCl, 2.5 KCl, 0.5 $CaCl_2$, 7 $MgCl_2$, 1.25 NaH_2PO_4, 25 $NaHCO_3$, 10 glucose and 75 sucrose (saturated with 95% O_2 – 5% CO_2, pH 7.3).

2.1.4 L-type current recordings.

For Ca^{2+} current recordings, a Cs^{+}-based intracellular solution was used and contained (in mM): 125 Cs-Gluconate, 20 KCl, 10 HEPES, 4 ATP-Mg, 10 Na-phosphocreatine, 0.5 EGTA and 0.3 GTP-Na, pH 7.3 with CsOH. To minimize the consumption of the VDCCs inhibitory toxins, an HEPES-buffered solution (HBS) was used and the flow was temporarily stopped. This solution containted (in mM): 135 NaCl, 4 KCl, 2 $NaHCO_3$, 25 glucose, 6 $CaCl_2$, 0.1 $MgCl_2$ and 10 HEPES, pH 7.4 with NaOH. We activated Ca^{2+} currents by a pulse of 50 ms from the holding potential to the test potential. Currents were filtered at 13.3 kHz and sampled at a rate of 25 μs per point. To record only L-type Ca^{2+} currents, ω-conotoxin MVIIC (200 nM) and TTX (200 nm) were added to the superfusate. Analysis of Ca^{2+} current was performed using Igor Pro (WaveMetrics, USA).

2.1.5 Others drugs for supplementary data.

Noradrenaline (30 µM) and forskolin (30 µM) were also added to the superfusate.

2.2 Immunochemistry experiments.

2.2.1 Specificity of anti-Ca_v1 antibodies.

For immunochemistry experiments, we used two rabbit polyclonal antibodies to recognize $Ca_v1.2$ and $Ca_v1.3$ subunits (Alomone, Jesuralem, Israel). Anti-$Ca_v1.2$ and Anti-$Ca_v1.3$ antibody were generated with the peptide (C)TTKINMDDLQPSENEDKS corresponding to amino acid residues 848-865 of the intracellular loop between domain II and III of rat $Ca_v1.2$ subunit and with the peptide (C)DNKVTIDDYQEEAEDKD, corresponding to amino acid residues 859-875 of intracellular loop between domains II and III of rat $Ca_v1.3$ subunit.

The specificity of anti-$Ca_v1.2$ and $Ca_v1.3$ subunit antibodies was tested by immunoreactivity inhibition experiments using respective antigenic peptides (data not shown). Moreover, two studies confirmed the specificity of rabbit anti-$Ca_v1.3$ antibody from Alomone using immunochemistry experiments on homozygous $Ca_v1.3^{-/-}$ KO mice. Pérez-Alvarez et al., (2011) failed to detect $Ca_v1.3$ in chromaffin cells from $Ca_v1.3^{-/-}$ KO mice. $Ca_v1.2$ labeling was similar in wild type mice and in $Ca_v1.3^{-/-}$ KO mice (Fig 20). Similar results were obtained by Vandael and co-workers (2010, Fig 20). Unfortunately, homozygous $Ca_v1.2^{-/-}$ KO mice are not viable and then immunoreactivity experiments in $Ca_v1.2^{-/-}$ KO mice are not possible.

2.2.2 Others antibodies for supplementary data.

We also used two non-commercial antibodies against RyR1 (Mitchell et al., 2003) and RyR2 (Tunwell et al., 1996), which were generously provided by F. Anthony Lai. Anti-RyR1

and anti-RyR2 antibodies were both used at 1/100. Furthermore, we performed pre-embedding immunogold labeling using an anti-$Ca_v2.1$ subunit antibody (1/500, Synaptic System). The specificity the anti-$Ca_v2.1$ subunit antibody was tested on Purkinje cell lacking P/Q-type VDCCs mice model (Mark et al., 2011, Fig 21).

I

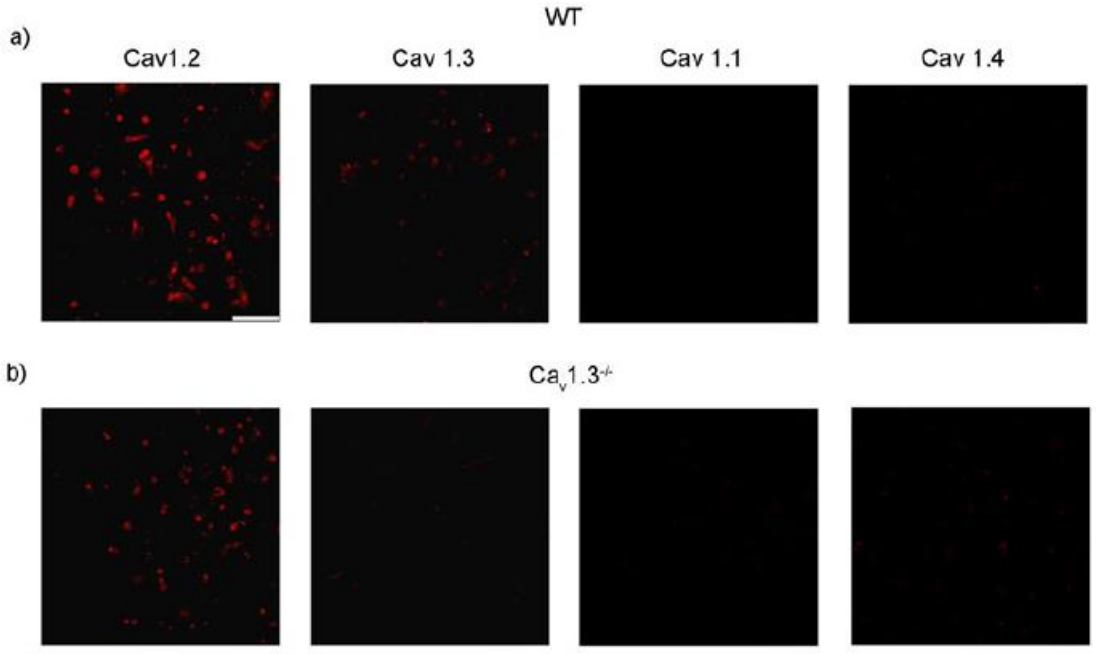

II

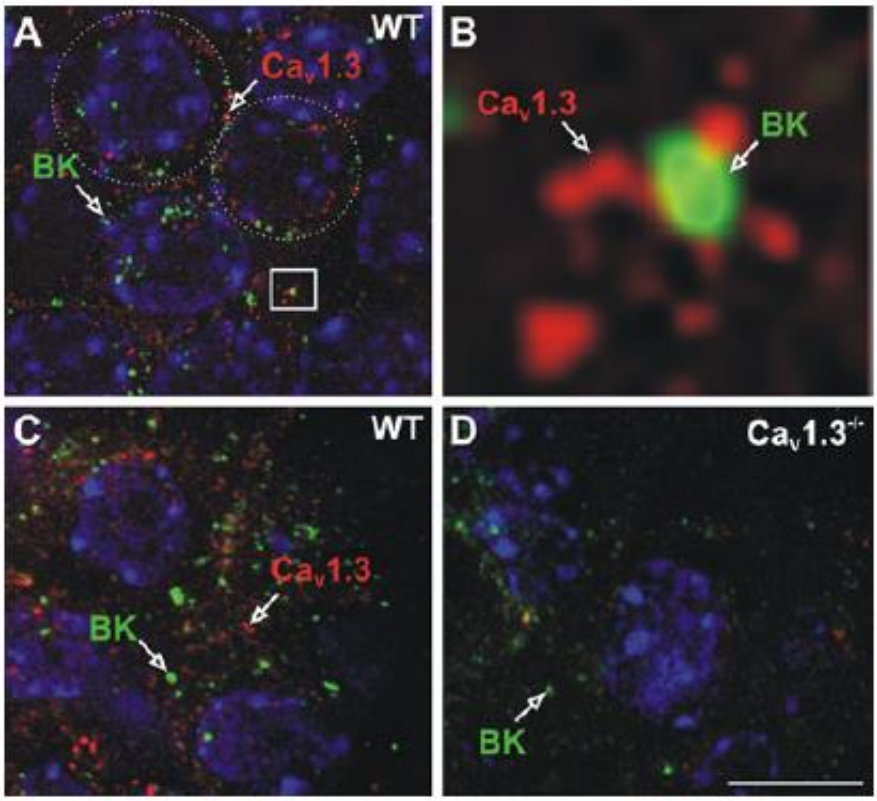

Fig 20: Alomone anti-$Ca_v1.3$ antibody tested on $Ca_v1.3^{-/-}$ KO mice.

I) Figure from Pérez-Alvarez et al. (2011) shows immunoreactivity of anti-$Ca_v1.3$ antibody (Alomone) on adrenal gland chromaffin cells from wild type (WT) and $Ca_v1.3^{-/-}$ KO mice. As shown in b, no immunoreactivity is observed in $Ca_v1.3^{-/-}$ KO mice in comparison to control wild type mice.

II) The same observation is described by Vandael et al. (2010). Positive immunostainning in wild type mice (WT, A, B and C) is completely absent in $Cav1.3^{-/-}$KO mice (D).

(Adapted from Pérez-Alvarez et al., 2011 and Vandael et al., 2010).

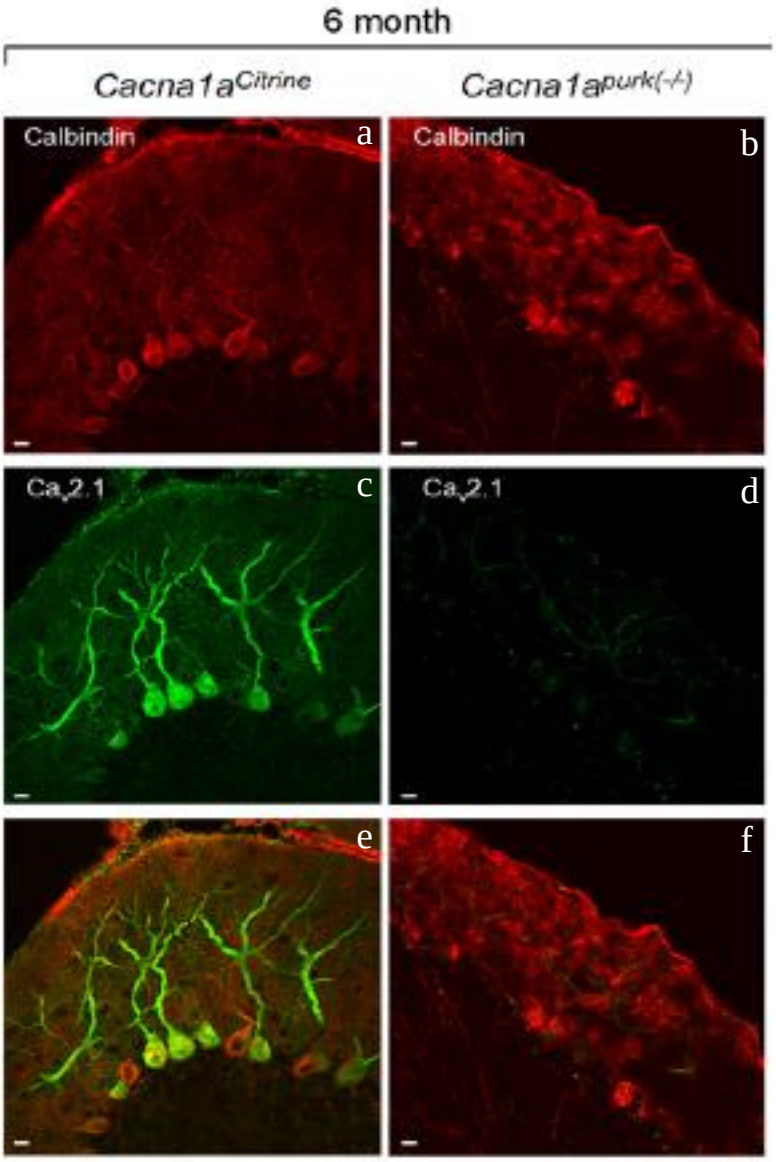

Fig 21: Anti-Ca_v2.1 antibody from Synaptic System tested on Cacna1a $^{purky\ (-/-)}$ mice.
In Cacna1a $^{purky(-/-)}$ mice from Mark et al. (2011) which do not express Ca_v2.1 in Purkinje cells, immunoreactivity of anti-Ca_v2.1 antibody from Synaptic System is negative (d) in comparison to the control Cacna1a^{citrine} mice (c).
(Adapted from Mark et al., 2011).

Chapter 3

Results

3.1 Article in preparation.

3.1.1 Introduction.

It is well-established that neurotransmitter release is triggered by Ca^{2+} occurring within the presynaptic termini. P/Q and N -type VDCCs are considered as the main actors of the fast neurotransmitter release and are classically localized in the presynaptic membrane.

The pharmacological properties of presynaptic VDCCs in the cerebellar cortex have been investigated at the GABAergic synapses between MLIs and from MLIs to Purkinje cells. More precisely, spontaneous IPSCs were shown to be sensitive to nickel ions and amiloride but not to ω-agatoxin IVA, ω-contoxin MVIIC and nimodipine (Doroshenko et al., 1997). These results suggest an involvement of T-type VDCCs in the spontaneous GABA release by MLIs. By contrast, action potential-evoked presynaptic Ca^{2+} transients in MLIs are sensitive to ω-agatoxin IVA, ω-conotoxin GVIA and ω-contoxin MVIIC but are resistant to nimodipine (Forti et al., 2000). In this latter study, although Cd^{2+} completely blocked the transients, ω-contoxin MVIIC inhibited only 50% of signal, suggesting a participation of R-type VDCCs. T-type VDCCs do not seem to be involved in the Ca^{2+} entry process since this latter is completely inhibited by Cd^{2+}. Stephens and co-workers (2001) reported that spontaneous IPSC recorded onto Purkinje cells are reduced in same proportion in terms of amplitude and frequency in the presence of Cd^{2+} or ω-agatoxin IVA. These results plead in favor of the sole involvement of P/Q-type VDCCs in the release of GABA by MLIs. The slight discrepancies

observed among these studies may result from species or age differences (Doroshenko et al., 1997: P8-21 Spague-Dawley rats, Forti et al., 2000: P12-16 Wistar rats; Stephens et al., 2001: adult mice). It has to be noted however that presynaptic L-type VDCCs role in neurotransmitter release might have been underestimated due to the relative ineffectiveness of DHP to block L-type current activated by a train of action potential (Helton et al., 2005). On the other hand, the presence of L-type VDCCs in MLIs is documented (Chavas et al., 2004; Collin et al., 2009). Indeed, DHP antagonists block L-type VDCCs in a state-dependent manner, preferentially in their active conformations (Bean, 1984; Holz et al., 1988) which may result in blockade failures when the opening time is too short as in the case in the time scale of an action potential. Using different paradigms, it has been proposed that presynaptic L-type VDCCs are involved in the short-term plasticity at GABAergic synapses in hippocampus (Jensen et al., 1999a,b; Jensen and Mody, 2001; Murakami et al., 2002; Holmgaard et al., 2008), in LTP at glutamatergic synapses in hippocampus (Lauri et al., 2003) and in presynaptic LTP associated with fear conditioning at cortical afferent onto lateral amydala (Fourcaudot et al., 2008; Fourcaudot et al., 2009). Other studies propose an involvement of presynaptic L-type VDCCs in GABAergic miniature release in the substantia innominata, hippocampus and the neocortex (Watanabe et al., 2002; Goswani et al., 2012; Williams et al., 2012).

A series of single cell RT-PCR experiments performed by Gilliane Maton clearly acknowledged the presence of $Ca_v1.2$ and $Ca_v1.3$ α1 subunits in MLIs. The other striking results were that all Ca_v3s were present but also that $Ca_v2.3$ (R-type) was not found in any of the MLI tested. Therefore, the question of the nature of the VDCCs supporting the action potential-evoked presynaptic Ca^{2+} entry reappeared. Application of nickel ions neither affected mIPSC recorded in MLIs nor action-potential evoked axonal Ca^{2+} transients. The same results were obtained with SNX482 and TTA-P2 and taken together; these data excluded

an involvement of T- and R-type VDCCs in axonal Ca^{2+} signaling. By contrast, a positive allosteric modulation of L-type VDCCs by BayK 8644 slowed action potential evoked axonal Ca^{2+} transient decay time and induced an increase of the mIPSC frequency recorded either in MLIs or in Purkinje cells, suggesting the presence of L-type VDCCs in MLIs presynaptic termini. This idea is now confirmed by immunochemistry experiments using confocal and electron microscopy. $Ca_v1.2$ and $Ca_v1.3$ subunit immunogold labeling is higher at less than 100 nm from the active zone. Moreover, we show that presynaptic L-type VDCCs can activate RyR through a putative physical coupling and/or CICR and that the enhancement in mIPSC frequency following an application of noradrenaline or forskolin (Llano & Gerschenfeld, 1993) is mediated by positive modulation of presynaptic L-type VDCCs. Our data argue that presynaptic L-type VDCC have a crucial importance in presynaptic Ca^{2+} influx and in GABA release properties of MLIs.

3.1.2 Article

Physiological involvement of presynaptic L-type voltage dependent calcium channels in GABA release of cerebellar molecular layer interneurons

Stéphanie Rey[1], Abdelali Jalil[1], Gilliane Maton[1], Alain Schimtt[2], Shin'Ichiro Satake[3] and Thibault Collin[1]

[1] Laboratoire de Physiologie Cérébrale, CNRS-UMR 8118 Université Paris Descartes, Université Paris Diderot, 45 rue des Saints Pères 75006 Paris, France

[2] Université Paris Descartes, Sorbonne Paris Cité, 75015 Paris, France

[3] National Institute for Physiological Sciences (NIPS), Departement of Information Physiology 5 – 1 Higashiyama, Myodaiji-cho, Okazaki 444-8787, Japan

- Correspondance should be addressed to TC thibault.collin@parisdescartes.fr

- Classification: Biological Sciences, Neuroscience

- keywords: calcium channels, synapse, calcium imaging, cerebellum

GM's present address: Institut Jacques Monod, Université Paris Diderot / CNRS, 15 rue Hélène Brillon 75205 Paris Cédex 13.

Introduction

Neurotransmitter release is known to be triggered by the opening of voltage-dependent Ca^{2+} channels (VDCCs). The entry of Ca^{2+} ions and their binding to the secretion apparatus ends up with the docking and discharge of a vesicle. High threshold VDCC subtypes involved in neurotransmitter release classically belong to the N and P/Q (Ca_v2) family with $Ca_v2.1$ and $Ca_v2.2$ α1 subunits being mostly located in axons (For review see Catterall and Few, 2008). Three isoforms of the L-type VDCCs (LTCCs) α1 subunit ($Ca_v1.2$, 1.3 and 1.4) are known to be expressed in the CNS and bear various subcellular distributions (Lipscombe et al., 2004) but the lack of effect of dihydropyridine (DHP) antagonists on transmitter release has suggested that they do not play any role in presynaptic Ca^{2+} entry (Dunlap et al., 1995; Elliott et al., 1995; Stephens et al., 2001). In the cerebellar cortex, the pharmacological properties of presynaptic VDCCs have been examined at the three kinds of synapses innervating Purkinje cells i.e. the excitatory parallel fibers and climbing fibers, and the inhibitory synapses from molecular layer interneurons (MLIs). Although excitatory synapses were relying on different VDCCs subtypes compared to their inhibitory counterpart, no effect of DHP antagonists was ever detected on synaptic transmission (Doroshenko et al., 1997). In MLIs loaded with a fluorescent Ca^{2+} indicator, AP (action potential) -evoked Ca^{2+} transients were abolished in the presence of the broad range high-threshold VDCC antagonist Cd^{2+} and significantly reduced after bath perfusion of ω-AgaIVA, ω-CgTxGVIA and ω-CgTxMVIIC (Forti et al., 2000). Although it made no doubts that Ca_v2s represent the main actors in the Ca^{2+} entry process, the absence of effect of nimodipine tended to exclude a role for LTCCs in the GABA release from MLIs, a result that had been confirmed by a later study based up on the recording of spontaneous inhibitory postsynaptic currents (IPSCs, Stephens et al., 2001). Nonetheless DHP are known to be weakly effective against AP-dependent Ca^{2+}

entry in both post- and presynaptic compartments (Helton et al., 2005) and consequently, they are not worth using to establish the contribution of LTCCs to various neuronal processes. Surprisingly, administration of the LTCC positive allosteric modulator BayK8644 (BayK) into the caudate-putamen induced a large increase of motor activity and dopamine release in hyperactive rats (Okita et al., 2000). Furthermore, the frequency of GABAergic miniature IPSCs (mIPSCs) was significantly increased in acutely dissociated rat substantia innominata neurons by BayK (Watanabe et al., 2002).

In the present report, we show that BayK dramatically increases mIPSCs frequency in MLIs and Purkinje cells indicating that LTCCs could be present in presynaptic sites. This effect is dependent on ryanodine receptor since dantrolene reduces the potentiation elicited by BayK. The expression of $Ca_v1.2$ and 1.3 α1 subunit in MLIs is confirmed by single-cell RT-PCR and immunocytochemistry. Pharmacological experiments exclude the involvement of both $Ca_v2.3$ (R-type) and Ca_v3s (T-types) in the release of GABA by MLIs. Furthermore, electron microscopy experiments demonstrate the presence of both $Ca_v1.2$ and 1.3 α1 subunit at presynaptic locations in MLIs. Ca^{2+} imaging experiment allowed us to elucidate the role of LTCCs in shaping the presynaptic AP evoked Ca^{2+} transient. Altogether, our data demonstrate that LTCCs, although often neglected at presynaptic sites, are of crucial importance in the GABA release process of MLIs.

Results:

LTCCs positive modulation increases GABA release from MLIs

$GABA_A$ receptors-mediated synaptic transmission was analyzed in MLIs or Purkinje cells from P11-16 rat cerebellar slices using whole-cell recording at a holding potential of – 60 mV. The DHP agonist BayK prolongs channel time opening, increases the open state probability and induces a leftward shift in the current to voltage relationship of

the channel (Hess et al., 1984). Therefore, in its presence (10 µM, final concentration) and at the resting potential, LTCCs tend to be more frequently open than in control conditions. In MLIs, interestingly, mIPSCs frequency was significantly enhanced in the presence of BayK compared to control conditions (2.5 ± 0.4 Hz vs. 0.7 ± 0.2 Hz; n = 14, Fig. 1Aa,b,c) although the amplitude of mIPSCs however was not altered (108 ± 10 vs. 114 ± 12 pA; n = 14, Fig. 1Aa,b,d). As depicted on Fig. 1Ab and d, the mIPSCs amplitude distribution was similar in control than in the presence of BayK. The same experiments were performed in Purkinje cells with NBQX (5 µM) being added to the bath to block AMPA receptors. The presence of BayK led the mIPSCs frequency to reach 19.7 ± 2.7 Hz vs. 6.5 ± 1.5 Hz in control conditions (n=11 cells, Fig. 1Ba,b,c). As observed in MLIs, the amplitude of the mIPSCs was not significantly affected (157 ± 25 pA vs. 116 ± 14 pA; n = 11, Fig. 1Ba,b,d). Finally, mIPSCs amplitude distribution remained unchanged (Fig 1Bb,d). Our experiments show that LTCCs activation by BayK induces an increase of the mIPSC frequency recorded in MLIs and Purkinje cells. These results suggest that LTCCs are potentially localized in MLI presynaptic terminal and involved in GABA release.

MLIs terminals express Cav1.2 and Cav1.3 α subunits

Our electrophysiological data suggest the presynaptic expression of LTCCs. To confirm this hypothesis, we performed multiple immunolabeling experiments using antibodies against $Ca_v1.2$ or $Ca_v1.3$ α subunits, Vgat (vesicular GABA transporter used as GABAergic presynaptic marker) and calbindin that was used as a Purkinje cell marker. $Ca_v1.2$ and $Ca_v1.3$ were found in Purkinje cells as previously reported (Hell et al., 1993; Stephens et al., 2001) and also in MLIs (Fig 2Aa). To emphasize the labeling on MLIs, a mask performed on the calbindin channel (Calb; Fig 2Ab) was subtracted from Ca_v1s channels. The colocalization with the Vgat channel (Vgat; Fig 2Ac) was next used to

quantify the presynaptic MLI terminals expressing $Ca_v1.2$ and $Ca_v1.3$ (Fig 2Ad). High magnification of the merged images (Fig 3Ae, inset) revealed an overlap between Vgat and both LTCC α subunits as illustrated in the intensity profiles (Fig 2Af). Altogether, 72.89 ± 9.67 % (n = 2857 terminals; N = 3 rats) of Vgat terminals were $Ca_v1.2$-positive, and 80.46 ± 2.69 % (n = 4802 terminals; N = 3 rats) were $Ca_v1.3$-positive (n = 4802 terminals; N = 3 rats). These data strongly support the localization of LTCCs in Vgat terminals. To further study this particular location, electron microscopy experiments were carried out. Using pre-embedding immunogold labeling to visualization of cell ultrastucture characteristic, $Ca_v1.2$ and $Ca_v1.3$ were detected at the presynaptic terminals between MLIs and Purkinje cell somata (Fig 2B). The density of $Ca_v1.2$ was higher in the vicinity of the membrane (100 nm wide segments) than in the remainder of the presynaptic area (90 ± 8 vs. 48 ± 6 nanogold particles / μm^2; n = 39 synapses). The same result was retrieved regarding $Ca_v1.3$ (108 ± 18 vs. 78 ± 20 nanogold particles / μm^2, n = 32 synapses). The post-embedding immunogold labeling technique, which allows double labeling, was next used to confirm the previous results. Presynaptic terminals were labeled by anti-Vgat antibody revealed by 10 nm gold particles and LTCCs α subunits were revealed by 5 nm gold particles. As shown in Fig 2C, $Ca_v1.2$ or $Ca_v1.3$ α subunits and Vgat are localized to the same area. We also calculated the distance between Vgat and Ca_v1 labelings, we found 29 ± 4 nm for Vgat/$Ca_v1.2$ (n = 22 distances on 11 synapses) and 32 ± 6 nm for Vgat/$Ca_v1.3$ (n = 22 distances on 6 synapses). Taken together, our results demonstrate the expression of $Ca_v1.2$ and $Ca_v1.3$ in the presynaptic terminals of MLIs.

VDCCs and presynaptic Ca^{2+} transients:

If LTCCs are expressed presynaptically, they are likely to affect the AP-evoked axonal Ca^{2+} transient. Previous studies indicated that $Ca_v2.1$ (P/Q -type) Ca^{2+} channel plays the

major role in mediating axonal Ca^{2+} entry in MLIs (Forti et al., 2000; Stephens et al. 2001). At the MLI-PC synapse, no evidence was found for involvement of Ca_v1s, Ca_v3s, $Ca_v2.2$ or $Ca_v2.3$ VDCCs in GABA release (Stephens et al. 2001). As reported by Forti et al. (2000), nimodipine neither affects the amplitude nor the kinetics of AP-evoked presynaptic Ca^{2+} transients that were reduced by 50 % in the presence of ωCgTxMVIIC and by 100 % in the presence of Cd^{2+} (100 µM). These results indicated that LTCCs are not involved in the presynaptic Ca^{2+} entry process (Forti et al., 2000) and suggested that R-type VDCCs could be responsible for the ωCgTxMVIIC resistant axonal Ca^{2+} entry. Besides, the expression of Ca_v3s (T-type channels) has been demonstrated in MLIs (Molineux et al., 2005) and their involvement was solely suggested in AP-elicited dendritic Ca^{2+} transients (Myoga et al., 2009). With the aim to clarify the situation, we performed Ca^{2+} imaging experiments in the presence of Ni^{2+}, a common blocker of R-type (Zamponi et al., 1996) and $Ca_v3.2$ T -type Ca^{2+} channels (Lee et al., 1999). Blocking a Ca^{2+} channel involved in presynaptic Ca^{2+} entry would certainly result in a reduction of the amplitude of AP-induced Ca^{2+} transients as reported (Forti et al., 2000). However, application of Ni^{2+} (100 µM) did not affect the amplitude of the axonal transients (90 ± 10 vs. 98 ± 7 %, n = 5; Fig. 3B,C). These results tend to exclude any involvement of $Ca_v2.3$ and $Ca_v3.2$ in the presynaptic Ca^{2+} dynamics. Since the expression of the corresponding α1 subunits had not been challenged in MLIs, we performed single-cell RT-PCR experiments with specific primers for $Ca_v1.2$, 1.3, 2.1, 2.2, 2.3, 3.1, 3.2 and 3.3 α1 subunits. The results of these experiments, summarized on the baregraph in Fig. 3D, indicate that $Ca_v2.3$ is simply not expressed in MLIs, as suggested by electron microscopy experiments (Parajuli et al., 2012). This result was further confirmed by the lack of effects of SNX 482 (200 nM), a R-type VDCC specific toxin of the amplitude of AP-evoked axonal Ca^{2+} transients (87.1 ± 5.6 vs. 94.1 ± 2.2 %, n = 3; Fig. 3E). Furthermore, $Ca_v3.2$ was only expressed in 1 cell over 19 whereas

$Ca_v3.1$ seems to be robustly expressed. To check for a putative involvement of Cav3.1, we performed the same experiments in the presence of TTA-P2, a specific Ca_v3s blockers (Dreyfus et al., 2010). As previously, presynaptic Ca^{2+} transients were not specifically affected by the antagonist (96 ± 8 vs. 97 ± 9 %, n = 5; Fig. 3E). Finally, the presence of Ni^{2+} affected neither the frequency (0.17 ± 0.11 vs. 0.21 ± 0.15 Hz, n = 3; Fig. 3Fa,b) nor the amplitude (85 ± 22 vs. 92 ± 20 pA, n = 3; Fig. 3Fa,b) of mIPSCs recorded in MLIs. Altogether, these experiments strongly suggest that the ωCgTxMVIIc-resistent component of presynaptic Ca^{2+} current relies on $Ca_v1.2$ and $Ca_v1.3$ α1 subunits which are largely expressed in MLIs as depicted on Fig. 3D (detected in 14 over 19 cells). Nonetheless, since our data indicate that BayK triggers an increase in the mIPSCs frequency, we challenged it on a Ca^{2+} transient-inducing paradigm. Fig. 3Gb depicts the time course of a typical Ca^{2+} transient elicited by 4 propagated APs in control conditions (red trace) and in the presence of BayK for 6 min (black trace). Fitting Ca^{2+} transients with single exponential yielded average taus that were significantly higher when BayK was added to the superfusate (1.60 ± 0.28 vs. 1.03 ± 0.13 s in control conditions; n = 19, Fig. 3Gc). By contrast, the amplitude of the transients was not significantly affected by the treatment (91 ± 10 vs. 100 ± 10 %; n = 19, Fig. 3Gc). Taken together, these data confirm that LTCCs are present at the presynaptic level and that they are likely to play a role in GABA release through the regulation of the Ca^{2+} transients kinetics. We finally questionned the effects of nimodipine on the very same experimental paradigm and ended up with the same results as Forti et al. (2000) i.e. neither the amplitude (69 ± 8 vs. 75 ± 10 %, n = 8, not illustrated) nor the tau values (1.33 ± 0.19 vs. 1.14 ± 0.19 s, n = 8, not illustrated) were significantly different than in control conditions.

Activation of axonal LTCCs under somatic voltage clamp conditions

The fact that mIPSC frequency is largely increased in the presence of BayK strongly suggest that presynaptic LTCCs open and lead to local Ca^{2+} increases even in the absence of depolarization. We therefore examined local axonal Ca^{2+} signalling following bath application of BayK by performing 2-photon imaging of axon stretches in voltage clamped MLIs. In each experiment the identification of the recorded neurite as the axon was confirmed by analysis of action potential induced Ca^{2+} transients, which are markedly larger in the axon than in dendrites (Llano et al., 1997). Following this identification, TTX (0.2 µM) was added to the bath solution. In 6 over 7 tested MLIs, bath application of 10 µM BayK a net increase in the axonal Ca^{2+}-related fluorescence sometimes accompanied by rapid spontaneous transients that were not observed before the application of the drug (Fig. 4B). As depicted in Fig. 4C, the fluorescence changes were analysed in terms of standard deviation (SD) vs. time for each experiment. In this context, the SD significantly increased from 2.90 ± 0.70 to 10.04 ± 2.37 (n = 18 varicosities on 7 cells) when BayK was applied. Altogether, these data demonstrate that LTCCs are capable of inducing strong presynaptic Ca signals that are likely to trigger GABA release from MLIs. This tacitely implicates that LTCCs open at very low voltage especially in the presence of BayK.

Link between LTCCs and Ca^{2+} stores in MLI axon.

The data presented above indicate that opening of LTCCs triggers an elevation of the Ca^{2+} concentration withing the presynaptic compartment. However, whether this augmentation is solely due to Ca^{2+} entry through the channels or is the result of synergistic process leading to Ca^{2+} store emptying remains unknown. Of interest, ryanodine receptors (RyRs) located in MLI axons have been proposed to play a crucial role in the control of the frequency and of the amplitude of mIPSCs recorded in either Purkinje cells or MLIs (Llano

et al., 2000; Conti et al., 2004 and Rossi et al., 2008). In line with this latter idea, addition of dantrolene (10 µM), a muscle relaxing agent inhibiting ryanodine receptors, significantly reduced the potentiating effect of BayK on mIPSC frequency (ratio over control : 2.6 ± 0.4 vs. 4.9 ± 0.5 fold control, n = 8; m = 14; Fig. 1D and Fig.5a,b,e). These data indicate that presynaptic LTCCs are likely to recruit RyRs to fully amplify the GABA release process although a significant part of the emphasis seems to rely on Ca^{2+} influx through the channels. Whether the coupling between LTCCs and RyRs is conformational or Ca^{2+} releated remains to be elucidated. Nevertheles, a physical coupling between those two protagonists has been reported in the brain (Chavis et al., 1996; Mouton et al., 2000; Ouardouz et al., 2003). To test the hypothesis of a physical coupling, we applied BayK in the presence of Cd^{2+} to inhibit the Ca^{2+} influx. Under these conditions, we noted a frequency increase over control of 2.5 ± 0.4 fold (n=7, Fig. 5c,d,e) which is significantly different from the value obtained when BayK was applied in the sole presence of TTX (4.9 ± 0.7 fold, n = 14, Fig 1). Taken together, these results tend to indicate that presynaptic LTCCs can trigger a significant part of GABA release through physical coupling to RyRs.

Discussion

The present study confirms that VDCCs are not directly involved in the onset of miniature release since mIPSCs recorded in MLIs are not altered in the presence of Cd^{2+} or Ni^{2+}. The lack of effect of Ni^{2+} on mIPSC frequency suggests either a weak participation of both $Ca_v2.3$ and $Ca_v3.2$ or the absence of expressions of these α1 subunits in MLIs. Single-cell RT-PCR experiments confirmed the latter hypothesis regarding $Ca_v2.3$: the mRNA encoding this α1 subunit could not be detected in any of the MLI tested. Regarding $Ca_v3.2$, our RT-PCR experiments clearly show that this isoform (as well as the other Ca_v3s) is expressed in MLIs. One of the most striking finding of the present work is that BayK, the

positive allosteric modulator of L-type VDCCs, is able to trigger a massive increase in the frequency of mIPSC recorded in MLIs and Purkinje cells. A similar result has been reported in cultured substantia innominata neurons (Watanabe et al., 2002) and a weak increase in mIPSC frequency has been recently reported in hippocampal granule cells (Goswami et al., 2012). L-type VDCCs have been functionally identified in MLIs and involved in somato-dendritic signaling mechanism such as GABA-induced regulatory volume decrease (Chavas et al., 2004) and mGluR1-dependent Ca^{2+} oscillations (Collin et al., 2009) but their putative presynaptic functions had not been looked after. The role of VDCCs in miniature release remains unclear and the question arises as to whether stochastic opening of Ca^{2+} channels can lead to neurotransmitter release. Their blockade with non-specific blockers such as Cd^{2+} and specific blockers such as toxins gives controversial results. In the cerebellar cortex, mIPSCs recorded in Purkinje cells or MLIs are not affected by either Cd^{2+} or Ni^{2+} suggesting that VDCCs are not involved in miniature release (Llano & Gerschenfeld, 1993; Glitsch, 2006). However, modifying the extracellular Ca^{2+} concentration for a long time has been shown to alter miniature neurotransmitter release in a way that is independent of VDCCs (Llano et al., 2000). The interpretation of this latter results was that the loading of the Ca^{2+} stores is crucial in maintaining mIPSCs frequency. In hippocampal granule cells, spontaneous release appears to rely on both L- and N-type VDCCs under their stochastic opening (Goswami et al., 2012). In cultured neocortical neurons, Williams et al. (2012) propose that several types of VDCCs synergistically contribute to spontaneous release of GABA. The single-cell RT-PCR experiments presented hereby demonstrate the presence of two distinct isoforms of LTCCs namely $Ca_v1.2$ and $Ca_v1.3$, bearing distinct voltage dependency properties. Due to its low voltage activation, $Ca_v1.3$ appears a good candidate for stochastic opening leading to GABA release from MLIs.

The nature of voltage-dependent Ca^{2+} channels involved in producing action potential-stimulated axonal Ca^{2+} rises has been investigated in MLIs by combining imaging experiments and pharmacological manipulations using several VDCCs blockers. Using ω-CgTxMVIIC at a very high concentration (5 to 6 µM), which potently blocks native N- and P/Q-type Ca^{2+} currents as well as some R-type current components, Forti et al., (2000) noted a maximal inhibition of 50 % of the action potential-evoked Ca^{2+} rises. The lack of reversibility of the blockade argued against a large contribution of N-type channels and the use of CgTxGVIA allowed these latter authors to conclude that voltage dependent Ca^{2+} entry in MLIs is mainly attributable to P/Q channels. These results were in agreement with the low efficacy of opening upon an AP that is usually reported regarding LTCCs, N- and P/Q-type channels being known to be more efficiently opened through an AP. We refined the pharmacology of the presynaptic VDCCs using the very same paradigm and we noted that BayK superfusion is able to slow down the inactivation kinetics of AP evoked Ca^{2+} transients whereas these latter were not altered in the presence of nimodipine. Moreover, AP-evoked presynaptic Ca^{2+} transient are not sensitive to Ni^{2+}, SNX482 and TTA-P2. These data are in agreement with those we obtained with mIPSCs and confirm i) the absence of $Ca_v2.3$ in MLIs and ii) the independence of presynaptic Ca^{2+} signals towards T-type channels. Taken together, our Ca^{2+} imaging data support the fact that LTCCs are present in the presynaptic compartment of MLIs and that they might regulate the duration of internal Ca^{2+} elevations triggered by APs.

The actual distance between presynaptic VDCCs and Ca^{2+} sensors of exocytosis is of crucial importance for efficacy and speed of synaptic transmission (Neher & Sakaba, 2008; Eggermann et al., 2012). The tightness of the coupling is known to have major implications for spontaneous release (Eggermann et al., 2012). The huge effect of BayK we observed on mIPSC frequency pleades in favor of a tight coupling between LTCCs and the release

machinery. However, immunochemistry experiments performed in adult animal have indicated that LTCCs are mostly located in the somatodendritic compartment (Hell et al., 1993; Stephens et al., 2001; Tippens et al., 2008). At the resolution of immunofluorescence, we show that $Ca_v1.2$ and $Ca_v1.3$ stainings co-localize with Vgat labeling (used to label GABAergic axon) in the molecular layer of P11-16 rats. Obermair et al. (2004) have reported that $Ca_v1.2$ clusters were transiently found in the axon of cultured hippocampal neurons during development and were then excluded from the distal part of axon in mature neuron. Our results tend to indicate that the Ca_v1s can be transiently expressed in the presynaptic compartment of young animals (i.e. up to 20 days old) and tend to be mostly redistributed in somata and dendrites as reported (Stephens et al., 2001). Our electrophysiological data suggest that this developmental redistribution in cerebellum appears after the 4^{th} postnatal week since BayK enhances in a similar manner mIPSC frequency in P11-16 and in P17-24 rats (data not shown). A few electron microscopy studies have revealed the expression of LTCCs in presynaptic termini in adult rat hippocampus and in cortical cell culture from E16 embryonic mice (Tippens et al., 2008; Leitch et al., 2009; Subramanian et al., 2013). Nevertheless, these studies did not provide a quantification of the spatial distribution of LTCCs in axon termini. A quantitative analysis of our pre-embedding immunogold experiment reveals that $Ca_v1.2$ and $Ca_v1.3$ subunits are located in axonal termini with higher density close to the active zone (at less than 100 nm) and bear a distribution similar to the $Ca_v2.1$ subunit (Kulik et al., 2004). These results confirm our electrophysiological experiments in a sense that a positive modulation of Ca_v1s is able to massively increase the release of GABA by MLIs. Whether Ca_v1s are directly coupled to the release machinery remains to be elucidated. Finally, using pre-embedding and post-embedding double (anti-Ca_v1 and anti-Vgat antibodies) immunogold labeling, we find that $Ca_v1.2$ and $Ca_v1.3$ are in the nanodomain. This latter technique

allowed to evaluate the distance between $Ca_v1.2$/ $Ca_v1.3$ and Vgat labeling: the value of 30 nm that we found confirms the nanodomain coupling.

Altogether, the data presented hereby demonstrate the actual presence of $Ca_v1.2$ and $Ca_v1.3$ in the presynaptic compartment of developing MLIs. Their very localization in the active zone of the synapses confer to them a key role in controling GABA release. To our knowledge however, LTCCs are rather unlikely to be coupled with the release machinery in neurons and therefore, they might mostly serve as a link between Ca^{2+} entry and Ca^{2+} stores. Such an hypothesis is strongly supported by: i) the partial inhibition of the BayK8644 effect on mIPSCs obtained by the ryanodine receptor antagonist dantrolene; ii) the huge presynaptic Ca^{2+} elevations observed in response to BayK superfusion on streches of axons and iii) the reported coupling between LTCCs and RyR in neurons. Moreover, as indicated in our immunocytochemistry experiments, the presynaptic expression of LTCCs seems to be transient (Stephens et al., 2001; our data). Such a developmentally regulated expression had been noted in cultured hippocampal neurons and was correlated with axonal growth (Obermair et al., 2004). Indeed, the presence of LTCCs in the presynaptic compartment of developing MLIs could clearly reflect the growth of their axons and the establishment of their synapses.

Materials and methods

Animals: Sprague–Dawley rats were purchased at the Elevage Janvier (Saint Berthevin, France) and not selected for their sex. Animals were kept at the animal house of the Centre Universitaire des Saints Pères which has been approved by the ‘Préfecture de Police’ following inspection by Veterinary Services and the French Ministry of Research and the Ministry for Health (European Directive 86/609/EEC / approval number A-750607). Postnatal day 12–16 rats were anaesthetized by inhalation of isoflurane and killed by

decapitation prior to cerebellum dissection.

Electrophysiology: Vermis parasagital slices (200 µm) were cut from 11-16 postnatal day old (P11-16) Sprague Dawley rats using a vibroslicer in ice-cold slicing solution (VT 1200S, Leica Microsystems, Germany). Bicarbonate buffered saline (BBS) solution was used as slicing and incubation solutions and contained (in mM): 152 NaCl, 2.5 KCl, 2 $CaCl_2$, 1 $MgCl_2$, 1.25 NaH_2PO_4, 26.2 $NaHCO_3$ and 10 glucose (saturated with 95% O_2 – 5% CO_2), pH 7.3 with NaOH. Slices were incubated at 34°C for 45 minutes in BBS solution and stored at room temperature. In the recording chamber, slices were perfused with BBS at 2.5 ml/min at room temperature. MLIs and Purkinje cells were identified using an Axio Examiner A1 upright microscope (Zeiss, Germany) with a Nomarski differential interference contrast (DIC) optics and water immersion 60X objectif (0.90 numerical aperture). MLIs and Purkinje cells were voltage clamped in the whole-cell configuration of the patch clamp using an EPC-9 amplifier (HEKA Electronik, Germany). Gigaseals were obtained using borosilicate pipettes of 4-6 MΩ resistance for MLIs and 2-3 MΩ for Purkinje cells. Series resistance was comprised between 15 to 25 MΩ for MLIs and 5 to 10 MΩ for Purkinje cells and compensated for by 60 to 80 %. For IPSCs recording, pipettes were filled with a KCl-based intracellular solution which contained (in mM): 150 KCl, 4.6 $MgCl_2$, 0.1 $CaCl_2$, 10 HEPES, 1 EGTA-K, 0.4 Na-GTP and 4 Na-ATP, pH 7.3 with KOH. Miniature IPSCs (mIPSCs) were recorded in the presence of 200 nM TTX. Currents were filtered at 1.3 kHz and sampled at a rate of 250 µs per point. For MLIs, IPSCs and EPSCs could be distinguished accorting to their decay kinetics (Llano & Gerschenfeld, 1993). In the case of Purkinje cells, NBQX (5 µM) was added to the bath to block AMPA receptors. Analysis of IPSCs was performed off-line with personal routines under the Igor Pro programming environment (WaveMetrics, USA).

Calcium imaging. Two different setups were used for Ca^{2+} imaging experiments, either a

custom two-photon laser-scanning microscopy (2PLSM) system (Collin et al., 2005 and references therein) or a single-photon system. The 2PLSM setup was used to assess the axonal Ca^{2+} rise induced by bath application of BayK. Other experiments were performed on a single photon setup from TILL Photonics (Germany) based on a Polychrome 2 monochromator and a Peltier-cooled CCD camera (IMAGO QE; 1376 X 1040 pixels; pixel size: 244 nm after 53X magnification and 2 X 2 binning). Excitation was at 480 nm and images were acquired with emission at 510-550 nm. To induce axonal $[Ca^{2+}]i$ rises, trains of 4 action potentials (20 ms intervals) were produced by depolarizing the cell for 3 ms to 0 mV from a holding value of -70 mV thus inducing a propagated action potential.

Drugs: Extracellular solutions were eventually supplemented with tetrodotoxin (TTX, 200 or 500 nM, Ascent, UK), BayK8644 (10 µM, Tocris, UK), Nimodipine (50 µM), Dantrolene (10 µM), Cadmium (Cd^{2+}, 200 µM), Nickel (Ni^{2+}, 100 µM), SNX482 (200 nM). Chemicals were purchased at Sigma-Aldrich (USA) unless otherwise stated.). We also used TTA-P2 (3 µM) which was generously provided from Régis Lambert.

Single-cell RT-PCR: the expression patterns of 8 genes encoding α1 VDCC subunits was determined by single-cell reverse transcription (RT)-multiplex PCR using specific primers as previously described (Diana et al., 2007).

Antibodies and Reagents: Rabbit anti- $Ca_v1.2$ and $Ca_v1.3$ polyclonal antibodies and respective antigenic peptides were purchased from Alomone (Israel); guinea pig anti-calbindin polyclonal antibody and mouse anti-Vgat monoclonal antibody from Synaptic Systems (Germany); mouse anti-parvalbumin monoclonal from SWANT (Switzerland); goat anti-rabbit IgG conjugated to Alexa546, goat anti-mouse IgG conjugated to Alexa488 and goat anti-guinea pig IgG conjugated to Alexa647 from invitrogen (Molecular Probes, Europe); 1.4 nm nanogold conjugated goat anti-rabbit antibody and HQ silver enhancement kit from Nanoprobes (Yaphank, USA). Paraformaldehyde (PFA),

glutaraldehyde and Durcupan acm resin were from Sigma-Aldrich (USA).

Immunofluorescence and confocal microscopy analysis: P14-15 Sprague Dawley rats were anesthetized by intra-peritoneal injection of 0.1 ml sodium pentobarbital (Ceva, France) and exsanguinated by transcardial perfusion of 10 ml cold phosphate buffered saline (PBS) followed by 10 ml of 4 % PFA in PBS. The cerebellum was immediately immersed in 4 % PFA for overnight treatment. Vermis parasagittal 50 µm slices were prepared using a vibrating slicer (VT1000S, Leica, Germany) and kept in PBS until use. Free floating slices were incubated in cold methanol at -20°C for 10 minutes, then washed with PBS and incubated in PBS supplemented with 10 % foetal bovine serum. For multiple labeling, slices were incubated overnight at 4°C with either anti-$Ca_v1.2$ (1/100) or anti-$Ca_v1.3$ (1/100) associated with anti-Vgat (1/500) and anti-calbindin (1/500) all diluted in PBS containing 1 mg/ml of bovine serum albumin (PBS/BSA buffer). Slices were then washed 3 times in PBS and incubated in PBS/BSA buffer for 3 hours with a mix of goat serum anti-mouse IgG, anti-rabbit IgG and anti-guinea pig IgG conjugated respectively to Alexa 488, Alexa 546 and Alexa 647 all diluted to 1/500. After a wash with PBS, slices were mounted with Fluoromont G (Southern Biotech, USA). Images stacks were collected using a LSM 510 laser scanning microscope (Zeiss, Oberkochen, Germany) with a 63x /1.4 Plan-Apochromat objective. Excitation wavelengths were 488, 543 and 633 nm and images were acquired using appropriate emission filters. Image analysis and quantification of GABAergic presynaptic terminals expressing $Ca_v1.2$ or $Ca_v1.3$ on MLIs was performed using ImageJ. A mask was set up on Purkinje cells using calbindin channel and was subtracted from the Vgat, $Ca_v1.2$ and $Ca_v1.3$ channels using “Image calculator” under ImageJ. Presynaptic $Ca_v1.2$ and $Ca_v1.3$ aggregates were quantified by their precise colocalization with Vgat using the “colocalization” plugin (by Bourdoncle P.; http://rsbweb.nih.gov/ij/plugins/colocalization.html) and 3D object counter (by Cordelières F. and

Jackson J.; http://rsbweb.nih.gov/ij/plugins/track/objects.html) under ImageJ environment. The ratio of colocalized aggregates and Vgat clusters was considered proportional to presynaptic terminals expressing $Ca_v1.2$ or $Ca_v1.3$.

Immunogold labelling and electron microscopy analysis: For pre-embedding electron microscopy experiments, fixed slices were prepared as above except that PFA 4 % in PBS was substituted by phosphate buffer 0.1 M (PB) containing 2 % PFA and 0.2 % glutaraldehyde. Slices were first immersed in a 25 % sucrose solution in PB for 20 min then briefly in cold isopentane (-80°C). They were washed with PBS and incubated for 30 min in PBS containing 4 % FBS. Slices were then incubated overnight at 4°C with anti-$Ca_v1.2$ (1/100) or anti-$Ca_v1.3$ (1/100) in PBS/BSA buffer. After 3 washes with PBS, the slices were kept for 3 hours with 1.4 nm nanogold conjugated goat anti-rabbit IgG diluted to 1/100 in PBS/BSA buffer containing 0.1 % cold fish gelatine. The slices were post-fixed 10 min with 1 % glutaraldehyde in PBS and submitted to the HQ silver enhancement kit according to manufacturer's guidelines (Nanoprobe, USA). After spending 10 min in 1 % osmium tetroxide (Euromedex, France) for post-fixation, the slices were successively dehydrated for 10 min in 50 %, 70 %, 90 % and finally twice in 100% ethanol. These steps were followed by a final dehydratation in propylene oxide for 10 min. Slices were embedded in Durcupan resin for 48 h at 60°C and 90 nm ultra-thin sections were cut using an ultra-microtome (Reichert Ultracut S, Germany).

For the pre-embedding experiments, fixed slices of 500 µm were prepared after intra-cardiac perfusion with PB containing 2 % PFA and 0.2 % glutaraldyde. Slices were fixed in PB supplemented with 1% glutaraldehyde (pH 7.4) then embedded in sucrose and frozen under liquid nitrogen. Cryosections were made with the ultra-microtome and the sections were mounted on Formvar-coated nickel grids. Briefly, sections were incubated for 15 min with PBS 15 % glycine, for 5 min with PBS 15% glycine 0.1% BSA and for 20 min with

PBS 15 % glycine, 0.1 % BSA, 10 % normal goat serum followed by 1 hour incubation with anti-$Ca_v1.2$ (1/100) or anti-$Ca_v1.3$ (1/100) with anti-V-gat antibodies (1/50) in PBS 15 % glycine, 0.1 % BSA, 4 % normal goat serum. After extensive rinsing in PBS 15 % glycine, 0.1 % BSA, sections were incubated for 1 hour with gold-labeled secondary goat anti-rabbit antibody with a gold particle size of 5 nm and with goat anti-mouse with a particle size of 10 nm (British Biocell, Cardiff, UK). Sections were then washed for 30 min with PBS 15% glycine, stained with 4% uranyl acetate in 2% methyl-cellulose for 10 min and air dried. Observations were performed on the JOEL 1011 electron microscope (JOEL Ltd, Japan). Electron micrographs were analysed using ImageJ. For pre-emmbedding experiments, the density of intensified nanogold particles was quantified in both the presynaptic area (100 nm from the membrane contact) and remaining area of the axon terminal of MLI-MLI or MLI-Purkinje cell soma synapses. The synapses were morphologically identified according to the description of Palay and Chan-Palay (1974). For post-embedding experiments, the distance between Vgat and Ca_v1 labelings was measured.

Statistical analysis: Data were considered significantly different when $P < 0.05$ and indicate by a star (*) on the figures. Mean values are given with S.E.M.

References

Catterall WA, Few AP. (2008). Calcium channel regulation and presynaptic plasticity. Neuron. 59(6):882-901.

Chavas J, Forero ME, Collin T, Llano I, Marty A. (2004). Osmotic tension as a possible link between GABA(A) receptor activation and intracellular calcium elevation. Neuron. 44(4):701-713.

Chavis P, Fagni L, Lansman JB, Bockaert J. (1996). Functional coupling between ryanodine receptors and L-type calcium channels in neurons. Nature. 382(6593):719-722.

Christophe E, Doerflinger N, Lavery DJ, Molnár Z, Charpak S, Audinat E. (2005) Two populations of layer v pyramidal cells of the mouse neocortex: development and sensitivity to anesthetics. J Neurophysiol. 94:3357-67.

Collin T, Chat M, Lucas MG, Moreno H, Racay P, Schwaller B, Marty A, Llano I (2005) Developmental changes in parvalbumin regulate presynaptic Ca2+ signaling. J Neurosci 25:96-107.

Collin T, Franconville R, Ehrlich BE, Llano I. (2009). Activation of metabotropic glutamate receptors induces periodic burst firing and concomitant cytosolic Ca2+ oscillations in cerebellar interneurons. J Neurosci. 29(29):9281-9291.

Conti R, Tan YP, Llano I. (2004). Action pontial-evoked and ryandine-sensitive spontaneous Ca2+ transients at the presynaptic terminal of the developing CNS inhibitory synapse. J Neurosci. 24(31):6946-6957.

Diana MA, Otsu Y, Maton G, Collin T, Chat M, Dieudonné S. (2007) T-type and L-type Ca2+ conductances define and encode the bimodal firing pattern of vestibulocerebellar unipolar brush cells. J Neurosci. 27:3823-38.

Doroshenko PA, Woppmann A, Miljanich G, Augustine GJ. (1997) Pharmacologically

distinct presynaptic calcium channels in cerebellar excitatory and inhibitory synapses. Neuropharmacology. 36:865-72.

Dreyfus FM, Tscherter A, Errington AC, Renger JJ, Shin HS, Uebele VN, Crunelli V, Lambert RC, Leresche N. (2010) Selective T-type calcium channel block in thalamic neurons reveals channel redundancy and physiological impact of I(T)window. J Neurosci. 30:99-109.

Dunlap K, Luebke JI, Turner TJ. (1995). Exocytotic Ca2+ channels in mammalian central neurons. Trends Neurosci. 18(2):89-98.

Elliott EM, Malouf AT, Catterall WA. (1995). Role of calcium channel subtypes in calcium transients in hippocampal CA3 neurons.. J Neurosci. 15(10):6433-6444.

Forti L, Pouzat C, Llano I. (2000). Action potential-evoked Ca^{2+} signals and calcium channels in axons of developing rat cerebellar interneurones. J Physiol. 527(1):33-48.

Glitsch M. (2006). Selective inhibition of spontaneous but not Ca2+ -dependent release machinery by presynaptic group II mGluRs in rat cerebellar slices. J Neurophysiol. 96(1):86-96.

Goswami SP, Bucurenciu I, Jonas P. (2012). Miniature IPSCs in hippocampal granule cells are triggered by voltage-gated Ca2+ channels via microdomain coupling. J Neurosci. 32(41):14294-14304.

Hell JW, Westenbroek RE, Warner C, Ahlijanian MK, Prystay W, Gilbert MM, Snutch TP, Catterall WA. (1993). Identification and differential subcellular localization of the neuronal class C and class D L-type calcium channel alpha 1 subunits. J Cell Biol. 123(4): 949-962.

Helton TD, Xu W and Lipscombe D. (2005). Neuronal L-type calcium channels open quickly and are inhibited slowly. J Neurosci. 25(44):10247-10251.

Hess P, Lansman JB & Tsien RW (1984) Different modes of Ca channel gating behavior favoured by dihydropyridine Ca agonist and antagonists. Nature 311:538-544.

Ishibashi H, Murai Y, Akaike N.(1998) Effect of nilvadipine on the voltage-dependent Ca2+ channels in rat hippocampal CA1 pyramidal neurons.Brain Res. 813:121-7.

Kulik A, Nakadate K, Hagiwara A, Fukazawa Y, Luján R, Saito H, Suzuki N, Futatsugi A, Mikoshiba K, Frotscher M, Shigemoto R. (2004). Immunocytochemical localization of the alpha 1A subunit of the P/Q-type calcium channel in the rat cerebellum.Eur J Neurosci. 19(8):2169-2178.

Lee JH, Gomora JC, Cribbs LL, Perez-Reyes E. (1999). Nickel block of three cloned T-type calcium channels: low concentrations selectively block alpha1H. Biophys. 77(6):3034-3042.

Leitch B, Szostek A, Lin R, Shevtsova O. (2009). Subcellular distribution of L-type calcium channel subtypes in rat hippocampal neurons. Neuroscience. 164(2):641-657.

Llano I, González J, Caputo C, Lai F.A, Bayney M, Tan YP, Marty A. (2000). Presynaptic

calcium stores underlie large-amplitude miniatures IPSCs and spontaneous calcium transients. Nat Neurosci. 3(12):1256-65.

Llano I, Gerschenfeld HM. (1993). Inhibitor synaptic currents in stellate cells of rat cerebellar slices. J Physiol. 468:177-200.

Llano I, Tan YP, Caputo C (1997) Spatial heterogeneity of intracellular Ca2+ signals in axons of basket cells from rat cerebellar slices. J Physiol 502:509-519.

Lipscombe D, Helton TD, Xu W. (2004). L-type calcium channels: the low down. J Neurophysiol. 92(5):2633-2641.

Molineux ML, Fernandez FR, Mehaffey WH, Turner RW. (2005). A-type and T-type currents interact to produce a novel spike latency-voltage relationship in cerebellar stellate cells. J Neurosci. 25(47):10863-10873.

Mouton J, Marty I, Villaz M, Feltz A, Maulet Y. (2001). Molecular interaction of dihydropyridine receptors with type-1 ryanodine receptors in rat brain. Biochem J. 354:597-603.

Myoga MH, Regehr WG. (2011). Calcium microdomains near R-type calcium channels control the induction of presynaptic long-term potentiation at parallel fiber to purkinje cell synapses. J Neurosci. 31(14):5235-5243.

Obermair GJ, Szabo Z, Bourinet E, Flucher BE. (2004). Differential targeting of the L-type

Ca2+ channel alpha 1C (CaV1.2) to synaptic and extrasynaptic compartments in hippocampal neurons. Eur J Neurosci. 19(8): 2109-2122.

Okita M, Watanabe Y, Kobayashi H, Fujiwara M. (2000) Presynaptic L-type Ca2+ channel on dopamine excessive release from rat caudate putamen. Physiology and Behavior 68:641–9.

Ouardouz M, Nikolaeva MA, Coderre E, Zamponi GW, McRory JE, Trapp BD, Yin X, Wang W, Woulfe J, Stys PK. (2003). Depolarization-induced Ca2+ release in ischemic spinal cord white matter involves L-type Ca2+ channel activation of ryanodine receptors. Neuron. 40(1):53-63.

Parajuli LK, Nakajima C, Kulik A, Matsui K, Schneider T, Shigemoto R, Fukazawa Y. (2012) Quantitative regional and ultrastructural localization of the Ca(v)2.3 subunit of R-type calcium channel in mouse brain. J Neurosci. 32:13555-67.

Rossi B, Maton G, Collin T. (2008). Calcium-permeable presynaptic AMPA receptors in cerebellar molecular layer interneurones. J Physiol. 586:5129-5145.

Stephens GJ, Morris NP, Fyffe RE, Robertson B. (2001) The Cav2.1/alpha1A (P/Q-type) voltage-dependent calcium channel mediates inhibitory neurotransmission onto mouse cerebellar Purkinje cells. Eur J Neurosci 13:1902-12.

Subramanian J, Dye L, Morozov A. (2013). Rap1 signaling prevents L-type calcium channel-dependent neurotransmitter release. J Neurosci. 33(17):7245-7252.

Tan YP, Llano I (1999) Modulation by K+ channels of action potential-evoked intracellular Ca2+ concentration rises in rat cerebellar basket cell axons. J Physiol 520:65-78.

Tippens AL, Pare JF, Langwieser N, Moosmang S, Milner TA, Smith Y, Lee A. (2008). Ultrastructural evidence for pre- and postsynaptic localization of Cav1.2 L-type Ca2+ channels in the rat hippocampus. J Comp Neurol. 506(4):569-583.

Watanabe Y, Lawlor GF, Fujiwara M. Role of nerve terminal L-type Ca2+ channel in the brain. Life Sciences 1998;62:1671–5.

Williams C, Chen W, Lee CH, Yaeger D, Vyleta NP, Smith SM. (2012). Coactivation of multiple tightly coupled calcium channels triggers spontaneous release of GABA. Nat Neurosci. 15(9):1195-1197.

Zamponi GW, Bourinet E, Snutch TP (1996) Nickel block of a family of neuronal calcium channels: subtype- and subunit-dependent action at multiple sites. J Membr Biol 151:77–9

Figure legends

Figure 1. Bay-K 8644 increases mIPSCs frequency in MLIs and Purkinje cells.

mIPSCs were recorded in MLIs **(A)** or in Purkinje cells **(B)** in the presence of TTX (200 nM) before (TTX, **Aa**, **Ba**) and after (BayK, **Ab**, **Bb**) addition of BayK (10 µM) to the superfusate. In both cases, the frequency increases in the presence of the agonist (**Ac**, **Bc**; the mean ± sem is displayed by dark symbols) whereas the amplitude distribution remains unaffected (**Ad**, **Bd**; control: gray line; BayK: black line).

Figure 2. $Ca_v1.2$ and $Ca_v1.3$ immunoreactivity at MLIs presynaptic termini.

(A) Confocal microscopy images of a rat cerebellar slice immunolabeled with anti-$Ca_v1.2$ or anti-$Ca_v1.3$ (**a**), anti-calbindin (Purkinje cell marker, **b**) and anti-Vgat (GABAergic terminal marker, **c**) antibodies. The yellow dots in merged images (**d**) show the colocalization between Vgat and $Ca_v1.2$ or $Ca_v1.3$ (scale bars: 10µm). **(e)** high magnification images of insets from **d** (scale bars: 3 µm). **(f)** spatial fluorescence intensity profiles (FI) of $Ca_v1.2$ or $Ca_v1.3$ (red) and Vgat (green) of the region of interest (black lines in **e**). **(B)** Representative electron micrographs of pre-embedding immunogold labeling of rat cerebellar slice using anti-$Ca_v1.2$ or $Ca_v1.3$ antibodies. **(a)** $Ca_v1.2$ or $Ca_v1.3$ presynaptic expression at MLI GABAergic synaptic contact with neighboring MLI postsynaptic dendrite (scale bars: 0.1 µm). **(b)** synaptic contact between Purkinje cell soma and MLI axon (scale bars: 2 µm). **(c)** high magnification images of the regions of interest (black insets in **b**) showing the expression of $Ca_v1.2$ or $Ca_v1.3$ subunits in the presynaptic termini (scale bars: 0.1 µm). **(C)** Representative electron micrographs of double post-embedding immunogold staining of $Ca_v1.2$ or $Ca_v1.3$ (5 nm gold particles, white arrows) and Vgat (10 nm gold particles, black arrows). Both are detected in MLIs presynaptic terminals (scale bars: 30 nm; pre: presynaptic MLI, post: postsynaptic MLI, Pc: Purkinje

cell soma).

Figure 3. VDCCs and axonal calcium transients.

(A) MLI filled with 50 µM OGB1 (scale bar: 10 µm) The fluorescence image of the axon is shown in the lower panel **(B)** Ca transients in the two axonal varicosities indicated by the white squares and corresponding numbers in **(A)** were studied by propagating 4 somatically triggered action potentials in control conditions (black trace) and after 6 min in the presence of Ni^{2+} (Ni, 100 µM; red trace). **(C)** The amplitude of the transients were not altered by Ni superfusion (n = 6). **(D)** Baregraph summarizing single-cell RT-PCR experiments performed on 13 MLIs with regards to Ca_v α1 subunits. Note that all classes of a1 subunits could be detected except $Ca_v2.3$. **(E)** AP-evoked Ca transients were analyzed in the presence of SNX 482 (200 nM) and TTA-P2 (3 µM). No significant effects of the drugs were found (n = 3 for SNX 482 and n = 5 for TTA-P2). **(F)** mIPSCs were recorded in control conditions (**a**, upper trace) and in the presence of Ni (100 µM). Neither their frequency nor their amplitude were significantly affected (**b**. average trace in red; n = 6). **(G) a**. axonal segment (scale bar : 5 µm) in which AP evoked Ca^{2+} transients were recorded in control conditions (**b**. black trace) and after 10 min in the presence of BayK (10 µM; **b**. red trace). **c**. Summary of the results obtained in 26 cells. Upper panel: Ca^{2+} transients are fitted by a single exponential and the time constant is plotted in the baregraph vs. the time spent in the presence of BayK (10 µM); lower panel: Same as in **c** with regards to the amplitude of the transients.

Figure 4. 2-photon laser scanning Ca^{2+} imaging of a MLI during bath application of BayK.

The cell was voltage clamped at a holding potential of -60 mV in normal extracellular [Ca^{2+}] (2 mM). BayK (10 µM) was added to the bath perfusion during the time indicated

by bars (0.5 µM TTX throughout), while imaging the varicosities illustrated. (**A)** fluorescence image from 2-photon laser scanning Ca^{2+} imaging (**B)** time course of the fluorescence in the two varicosities indicated in A (1: blue; 2: orange) before (ctl) and during (BayK) application of BayK. **(C),** the SD of the Ca^{2+} related fluorescence signal is display vs. WCR time for the two varicosities displayed in A (1: blue; 2: orange). BayK application is figured by a blue rectangle on the graph.

Figure 5. L-type VDCCs can recrute RyRs for the GABA release process.

Sample of mIPSCs recording from MLIs in presence of dantrolene (Dantro, 10 µM,) or Cadmium (Cd, 200 µM) only (a,c) or in addition of BayK (10 µM) in the bath (b,d). e, Effect of dantrolene (n=8 cells) and Cd^{2+} (n=7 cells) on BayK induced increase of the mIPSCs frequency (control: Clt, n=14, see Fig.1). Each column represents the mean ± S.E.M. * on figure indicate statistical significant difference.

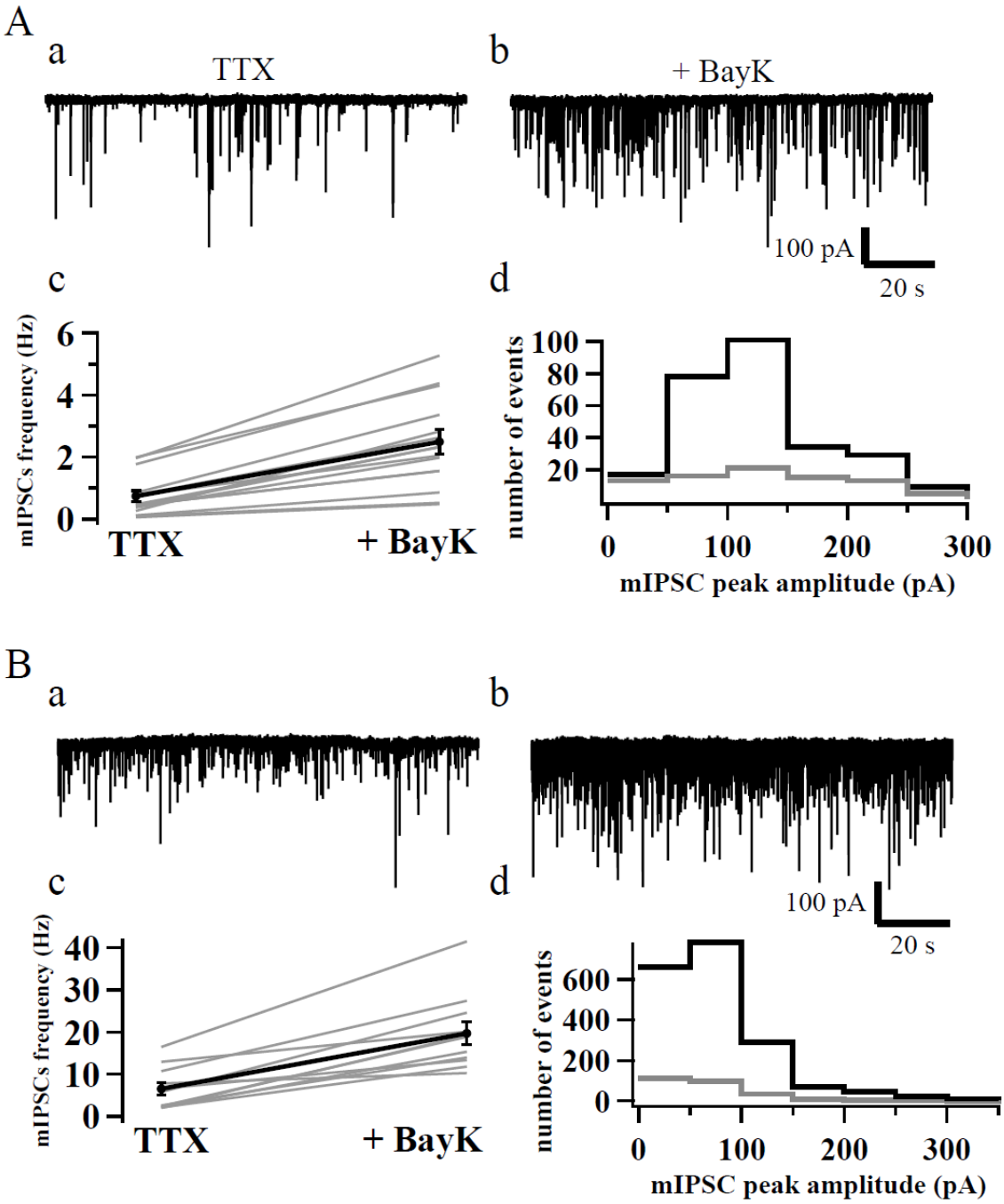
A
a
TTX
b
+ BayK
100 pA
20 s
c
d
mIPSCs frequency (Hz)
6
4
2
0
TTX
+ BayK
number of events
100
80
60
40
20
0
100
200
300
mIPSC peak amplitude (pA)
B
a
b
c
d
100 pA
20 s
mIPSCs frequency (Hz)
40
30
20
10
0
TTX
+ BayK
number of events
600
400
200
0
0
100
200
300
mIPSC peak amplitude (pA)

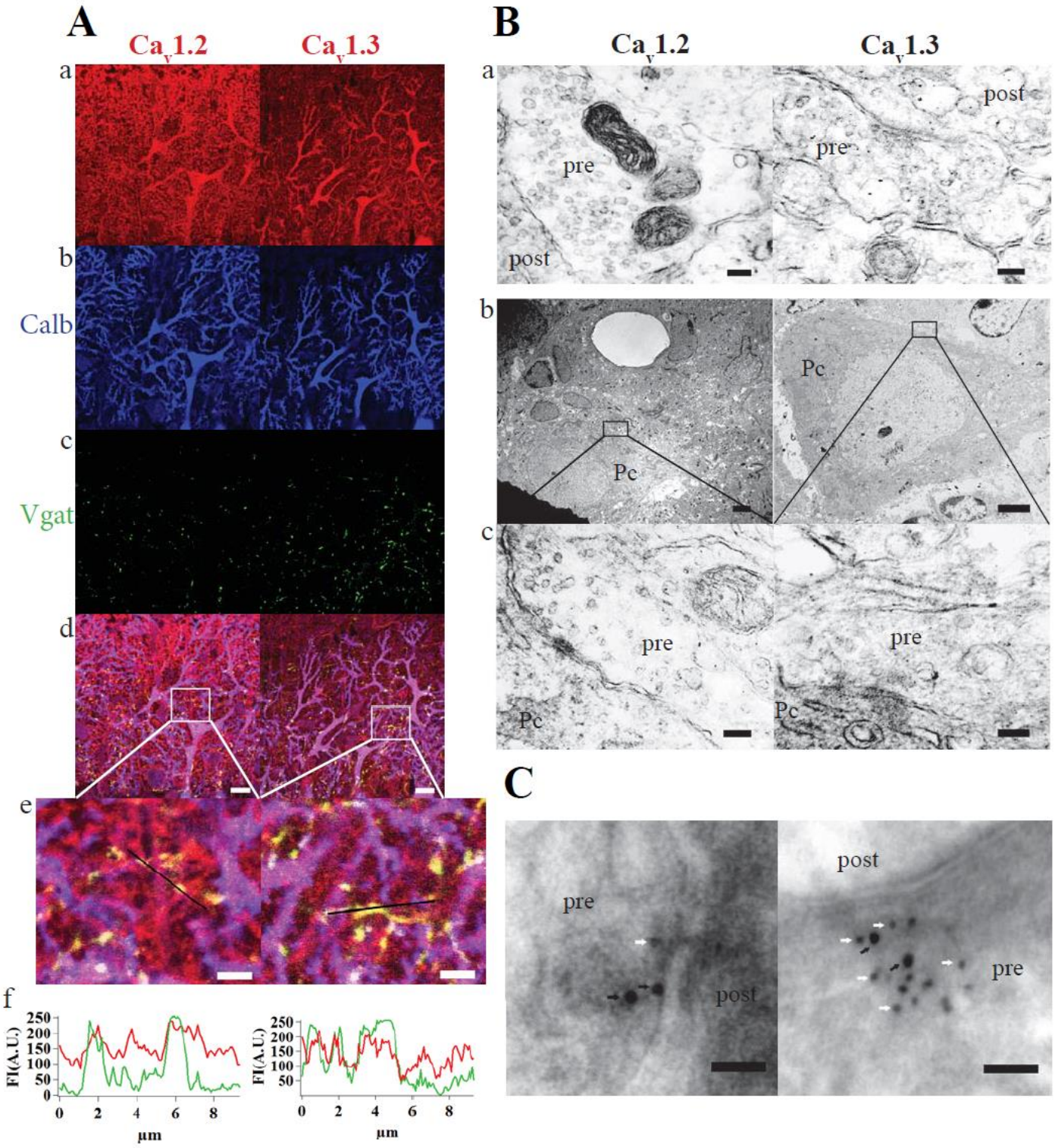
A
Cav1.2
Cav1.3
a
b
Calb
c
Vgat
d
e
f
FI(A.U.)
250
200
150
100
50
0
0
2
4
6
8
µm
B
Cav1.2
Cav1.3
a
pre
post
pre
post
b
Pc
Pc
c
pre
Pc
pre
Pc
C
pre
post
post
pre

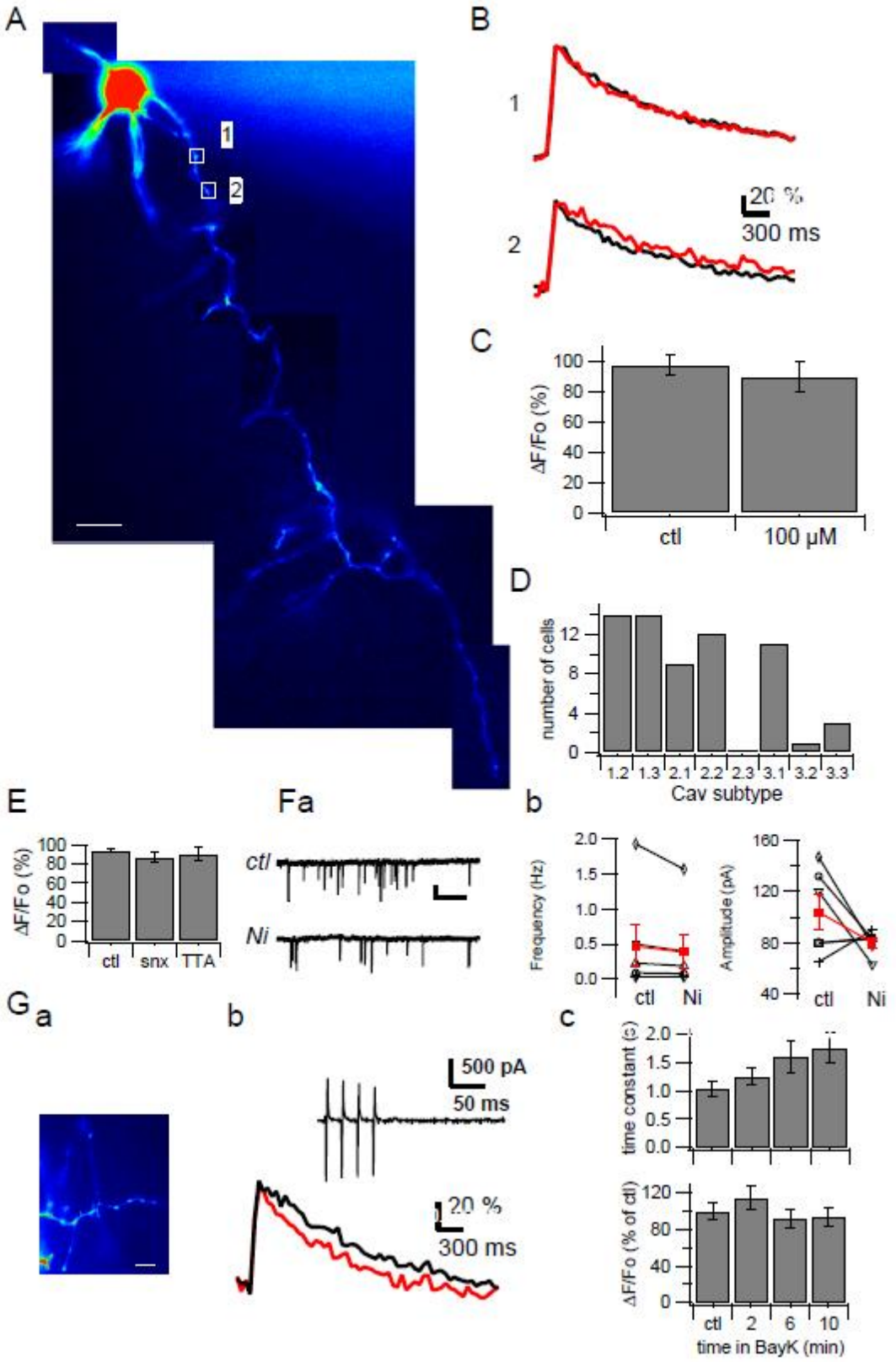
A
1
2
B
1
2
20 %
300 ms
C
ΔF/Fo (%)
100
80
60
40
20
0
ctl
100 µM
D
number of cells
12
8
4
0
1.2
1.3
2.1
2.2
2.3
3.1
3.2
3.3
Cav subtype
E
ΔF/Fo (%)
100
80
60
40
20
0
ctl
snx
TTA
Fa
ctl
Ni
b
Frequency (Hz)
2.0
1.5
1.0
0.5
0.0
ctl
Ni
Amplitude (pA)
160
120
80
40
ctl
Ni
G a
b
500 pA
50 ms
20 %
300 ms
c
time constant (s)
2.0
1.5
1.0
0.5
0.0
ΔF/Fo (% of ctl)
120
80
40
0
ctl
2
6
10
time in BayK (min)

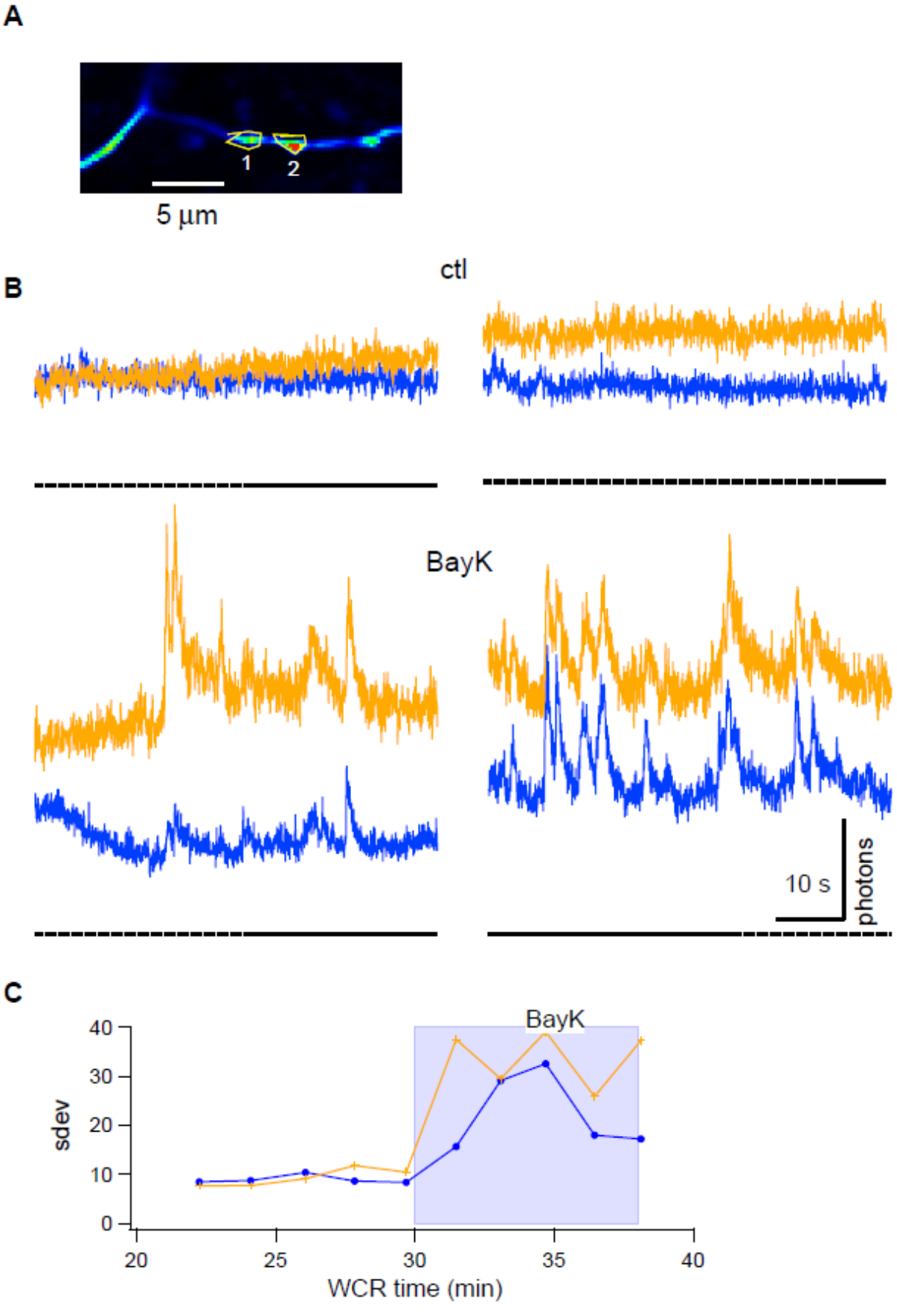
A
1
2
5 µm
B
ctl
BayK
10 s
photons
C
BayK
sdev
40
30
20
10
0
20
25
30
35
40
WCR time (min)

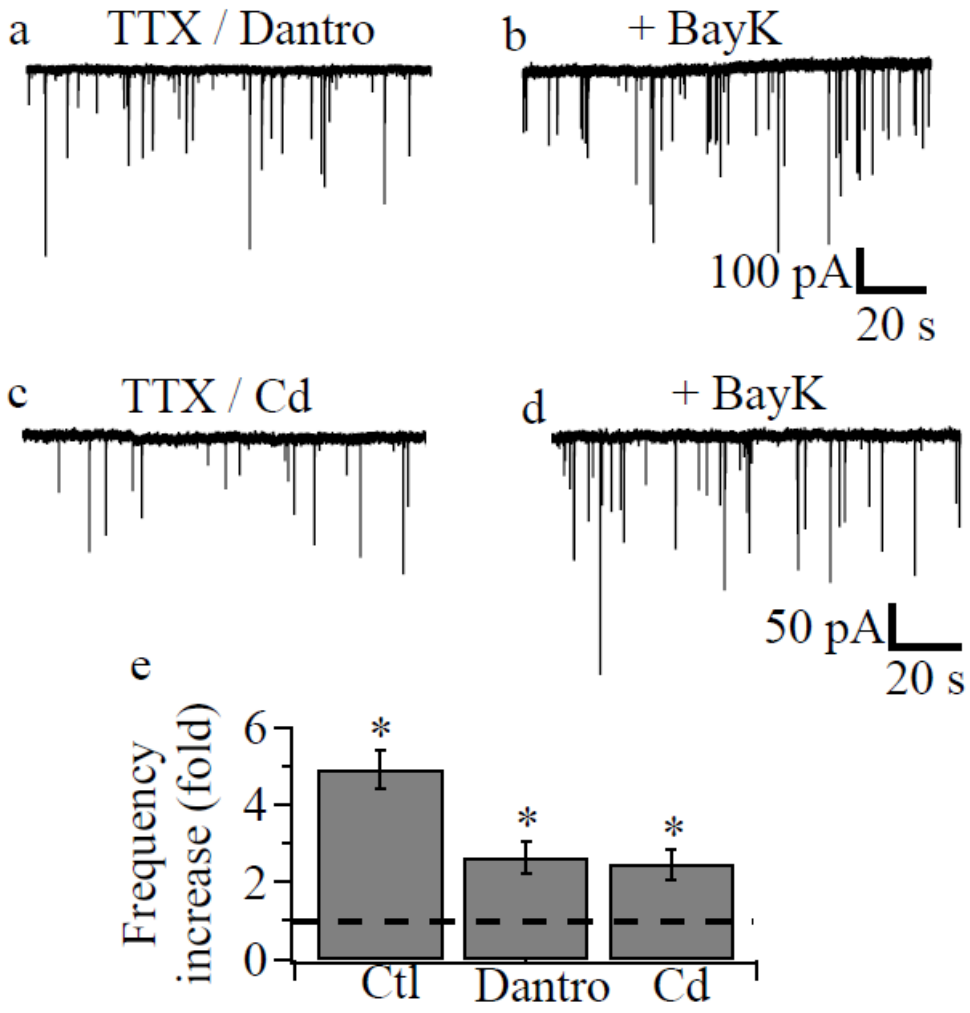
a
TTX / Dantro
b
+ BayK
100 pA
20 s
c
TTX / Cd
d
+ BayK
50 pA
20 s
e
Frequency increase (fold)
6
4
2
0
*
*
*
Ctl
Dantro
Cd

3.2 Supplementary results:

3.2.1 Dose response relationship of BayK 8644 on mIPSC frequency recorded in MLIs.

BayK8644 concentration dependence for mIPSC frequency recorded in MLIs was studied using BayK8644 concentration (logarithmic form)-response curve. No enhancement of mIPSC frequency was detected after addition of 0.1 and 0.3 µM of BayK8644 in the bath (n=6 cells respectively, Fig 22). The maximal enhancement was observed from 1 µM of BayK8644 (1 µM: n= 5, 3 µM: n=5, 10 µM: n=14, Fig 22). To conclude, pharmacological experiments were performed at a saturating concentration of BayK 8644.

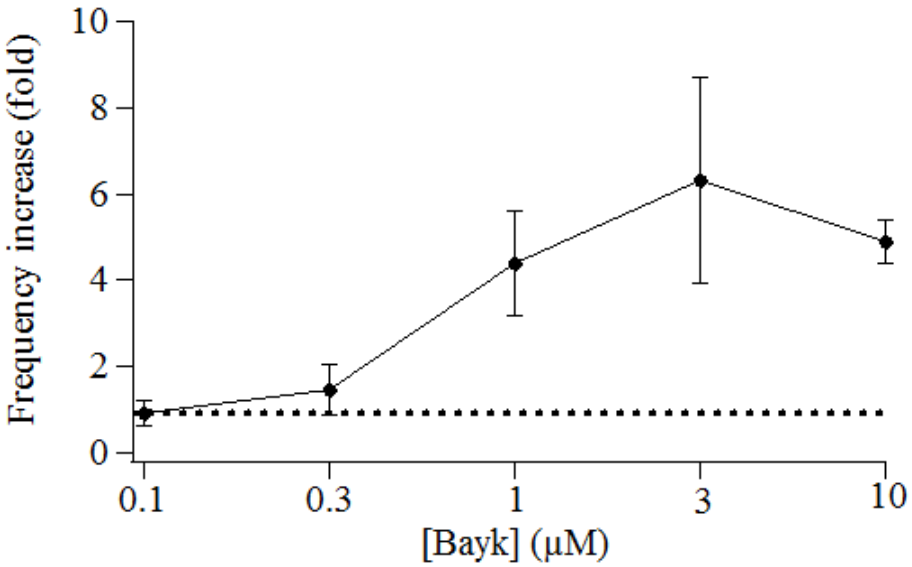

Fig 22: BayK8644 concentration effects on mIPSC frequency.
Change in the mIPSC frequency recorded in MLIs after addition in the bath of various doses of BayK8644.

3.2.2 BayK effect on mIPSC frequency in older rats.

To detect whether L-type VDCCs axonal expression decreases with age, we performed mIPSC recording in MLIs using BayK8644 (10 µM) in older rats (P17-24). In the presence of TTX (200 nM), IPSCs frequency was significantly enhanced with BayK8644 application (1.8

± 0.4 vs. 0.9 ± 0.3 Hz) although IPSC amplitude was not modified (100 ± 11 vs. 92 ± 12 pA, n=9, paired t test). No significant difference was detected on mIPSC frequency enhancement in the presence of BayK8644 between young (n=14) and old (n=9) animals (4.9 ± 0.5 vs. 3.7 ± 1.5 fold; unpaired t test). Our results show that activation L-type VDCCs have a similar effect in young and in older animals, suggesting a stable L-type VDCCs axonal expression in rat postnatal development.

3.2.3 Physiological modulation of L-VDCCs by Noradrenaline.

Cerebellum receives noradrenergic innervations form the locus coeruleus in the molecular layer (Olson & Fuxe, 1971, Pickel et al., 1974a,b). Activation of β-adrenergic receptors by noradrenaline induces an increase of mIPSC frequency recorded in MLIs and Purkinje cells (Llano & Gerschenfeld 1993; Kondo & Mary 1998). L-type VDCCs potentialization by β-adrenergic receptors via cAMP-dependent PKA has been well described (De Jongh et al. 1996; Gao et al. 1997). Moreover, in dentritic spines of CA1 pyramidal neurons, L-type VDCCs are positively modulate by β adrenergic receptors through PKA (Hoogland & Saggau, 2004). We tested whether mIPSCs frequency enhancement observed in presence of noradrenaline (30 µM) is mediated by VDCCs sensibilization. The mIPSCs frequency in presence of Cd^{2+} (200 µM) was not significantly increase in the presence of noradrenaline (0.3 ± 0.1 Hz vs. 0.4 ± 0.1 Hz; n= 9 cells, paired t test; Fig. 23Aa,b,c). The mIPSCs amplitude was also not modified (50 ± 4 pA vs. 49 ± 5 pA ; n=9 cells, Fig. 23Aa,b,c). L-type VDCCs current is known to rundown in whole cell recording. Several mechanisms have been suggested including dephosphorylation (Belles et al., 1988). We mimic β-adrenergic receptor activation using forskolin. Activation of adenylate cyclase by forskolin results in an increase of cAMP, which activates PKA. We showed that L-type VDCCs current amplitude in MLIs decreased to 20 ± 18 % of initial amplitude after 20 min of whole cell

recording (n=4, Fig 23Ba,b). In addition of forskolin in the bath, L-type VDCCs current amplitude was not modified (97 ± 3 % of initial amplitude, n= 5, Fig. 23Ba,c).

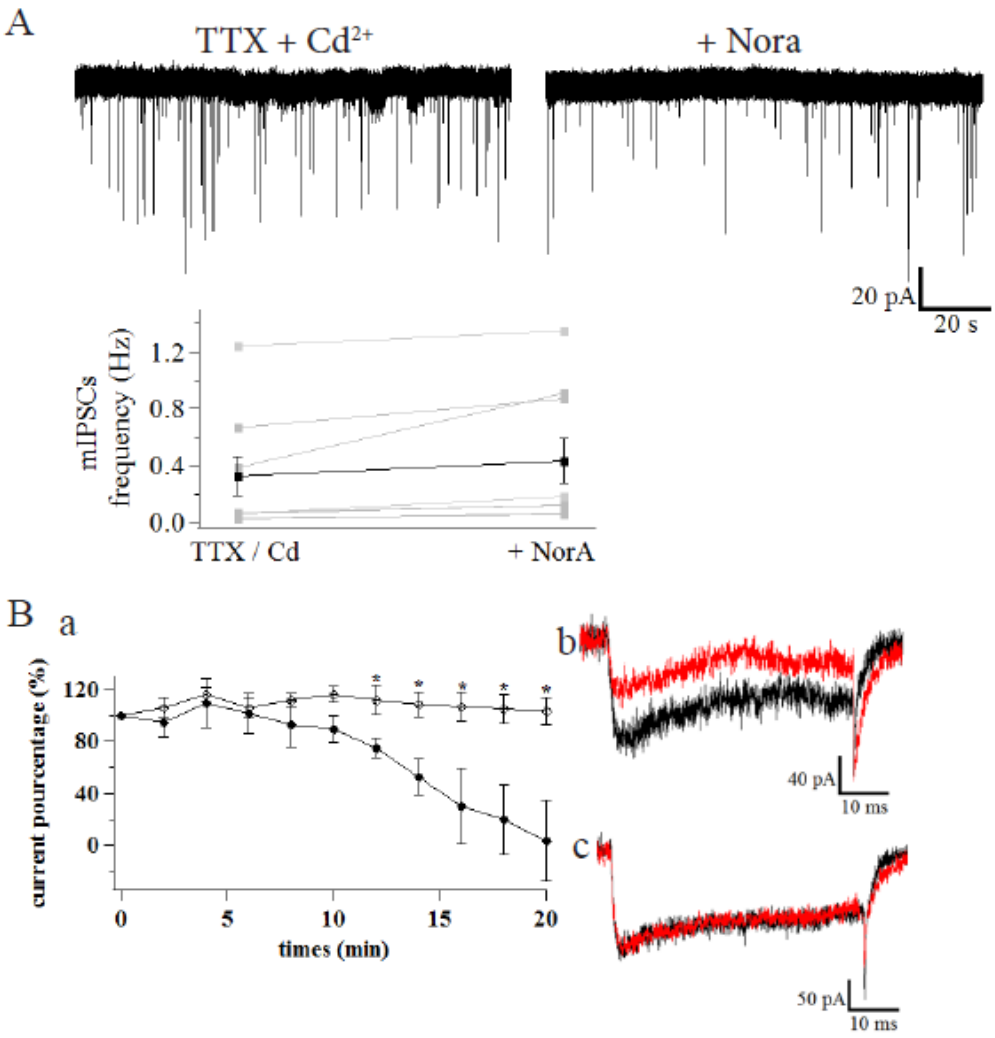

Fig 23: Noradrenaline fails to increase the mIPSCs frequency in presence of Cd^{2+} but forskolin prevents the L-type VDCCs current run-down.

A) mIPSCs were recorded in MLIs in presence of TTX (200 nM) and Cd^{2+} (200 µM) show that mIPSCs frequency does not increase following addition of noradrenaline (Nora, 30 µM) in MLIs (a, b,c). B) L-type VDCCs current were recorded in whole cell mode in presence of ω-conotoxin MVIIC (200 nM) for 20 min. The current amplitude (pulse at -10 mV) were measured each 2 min. Application of

forskolin (30 µM) in the bath prevents the L-type VDCCs current run-down (a, black circles: control, open circles: with forkolin). Example of current traces recorded in whole cell mode at 2 min (black traces) and after 20 min of whole cell recording (b, control; c, in presence of forskolin).

3.2.4 Different RyR isoforms are expressed in MLIs axon.

Our pharmacological experiments suggested that presynaptic L-type VDCCs in MLIs could recruit RyR by CICR or/and physical coupling. As mentioned in the introduction, three isoforms of RyR (RyR1, RyR2 and RyR3) are expressed in the cerebellum, but the isoforms present in MLIs are not identified. We performed immunochemistry experiments using confocal microscopy to examine RyR isoform expression in MLIs axon. As for Ca_v1 labeling, we stained Purkinje cells with calbindin to highlight on MLIs (Fig. 24b) and we used colocalization with Vgat to visualize the expression of RyR1 and RyR2 in MLI axons (Fig. 24a,b,c). High magnification of the inset in the merge images (Fig. 24d,e) showed an overlap between Vgat and RyR1 or RyR2 staining as is seen in the spatial fluorescence intensity profiles (Fig. 24f). Our results show expression of both RyR1 and RyR2 isoforms in MLI axon.

Fig 24: Expression of RyR1 and RyR2 in MLI axons.
Confocal images showing rat cerebellar slice immunostained by anti-RyR1 or anti-RyR2 (a, Red), anti-calbindin, (b, blue) and anti-Vgat (c, green) antibodies. Merge images (d) show overlap between Vgat and RyR1 or RyR2 (yellow dots, scale bars: 20 µm). (e) are high magnification of insets from d (white insets). (f) show spatial fluorescence intensity profiles (FI) of RyR1 or RyR2 (red) and Vgat (green) of the region of interest (white lines in e).

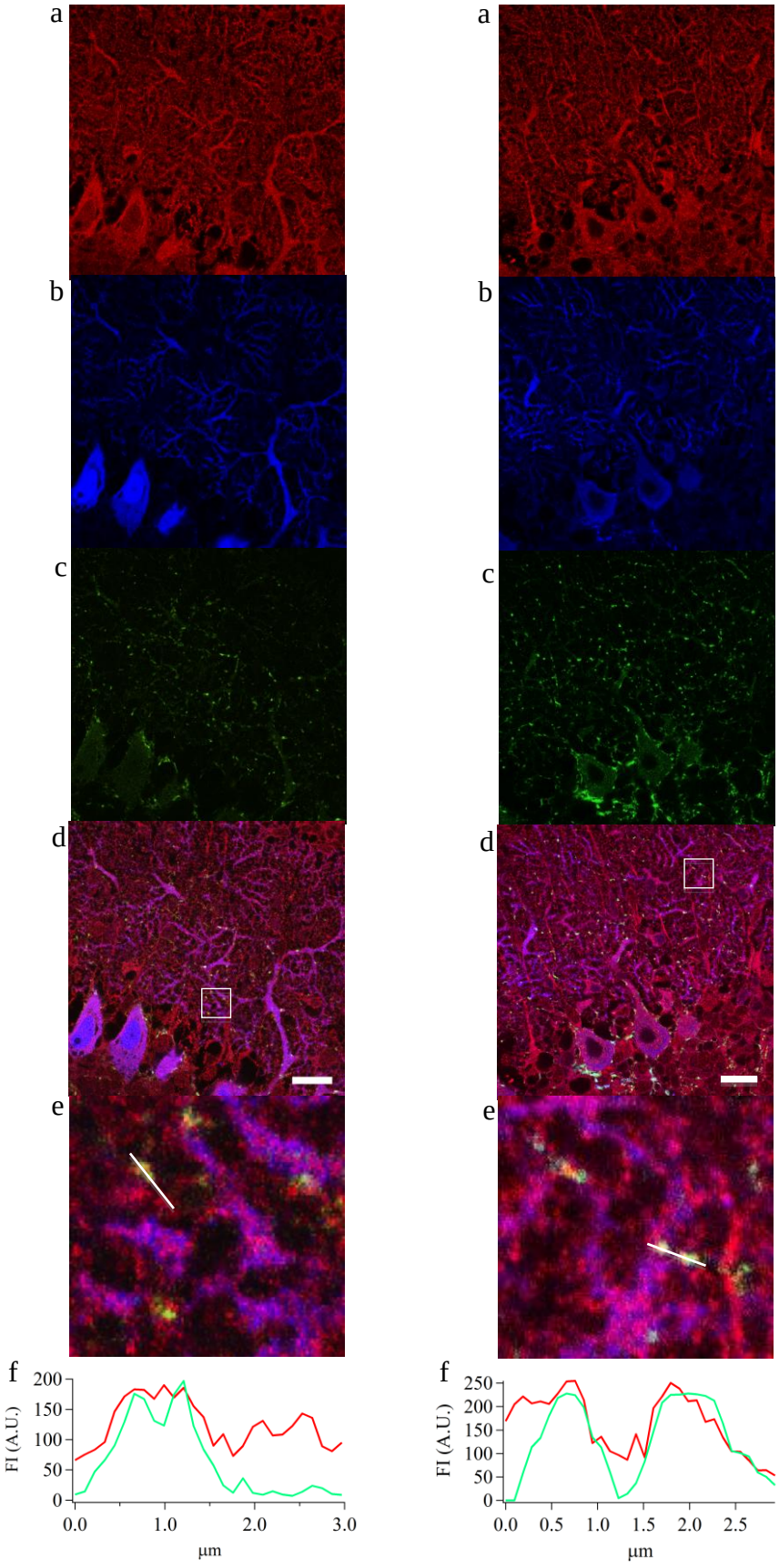
a
b
c
d
e
f
FI (A.U.)
200
150
100
50
0
0.0
1.0
2.0
3.0
µm
a
b
c
d
e
f
FI (A.U.)
250
200
150
100
50
0
0.0
0.5
1.0
1.5
2.0
2.5
µm

3.2.5 P/Q-type and L-type VDCCs display similar localization in MLI termini.

P/Q-type VDCCs are known to be mostly localized in the presynaptic termini and involved neurotransmitter release. To compare the localization and the distribution of $Ca_v2.1$ and Ca_v1, we performed $Ca_v2.1$ pre-embedding immunogold. GABAergic synapses were detected on the Purkinje cell somata or in the molecular layer using Palay and Chan-Palay characteristics. We showed that $Ca_v2.1$ presynaptic density was higher close to the active zone (100 nm wide segments) than in the remaining presynaptic area (123 ± 26 nanogold particles / μm^2 vs. 76 ± 19 nanogold particles / μm^2 , n=23 synapses). No significant difference was found between $Ca_v2.1$, $Ca_v1.2$ and $Ca_v1.3$ expression distribution in MLI presynaptic termini (unpaired t test).

3.2.6 L-type VDCCs are expressed in parallel fiber termini.

According to Palay and Chan-Palay (1974) morphological characteristics, we detected parallel fiber – Purkinje cell synapses in the molecular layer. As previously described, $Ca_v1.2$ and $Ca_v1.3$ subunits were revealed by pre-embedding immunogold labeling. Interestingly, we found that $Ca_v1.2$ and $Ca_v1.3$ subunits are also localized in parallel fiber termini and preferentially at less than 100 nm from the active zone (Fig 25).

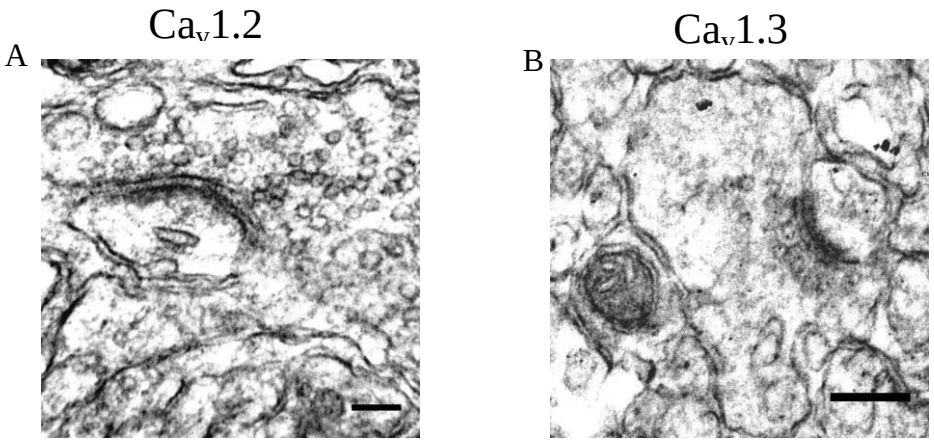

Fig 25: Presynaptic expression of $Ca_v1.2$ and $Ca_v1.3$ in parallel fiber termini.
Representative electron micrographs of pre-embedding immunogold labeling on rat cerebellum using an anti-$Ca_v1.2$ and $Ca_v1.3$ subunit primary antibodies. $Ca_v1.2$ (A) and $Ca_v1.3$ (B) subunit presynaptic expression at parallel fiber synapses with Purkinje cell thorns. (Scale bars = 0.1 μm for $Ca_v1.2$ and 0.2 μm for $Ca_v1.3$).

Chapter 4

Discussion

Action potential-evoked neurotransmitter vesicles exocytosis is known to require Ca^{2+} influx through VDCCs. The action potentials are supposed to depolarize the presynaptic termini to open VDCCs, the ensuing Ca^{2+} entry triggering the fusion of docked vesicles with the presynaptic membrane. However, neurotransmitter release can occur in the absence of action potentials: spontaneous vesicle fusion will happen supposedly without any stimulation.

The question arises whether this spontaneous fusion of vesicles is Ca^{2+} dependent or not, and several lines of evidence indicate that neurotransmitter release can be positively affected by elevating the intracellular Ca^{2+} concentration. At the experimental level, spontaneous release is observed when Na^{+} channels are blocked in the presence of TTX, the resulting postsynaptic currents being referred to as miniature currents. A significant fraction of miniature release has been shown to rely on Ca^{2+} release from presynaptic Ca^{2+} stores (Llano et al., 2000) and on Ca^{2+} entry through either presynaptic glutamatergic ionotropic receptors (Bureau & Mulle, 1998; Glitsch & Marty, 1999) or potentially through TRP channels (see Ramsey et al., 2006 for review). These data suggest that increases in intracellular Ca^{2+}, irrespective the way they appear, trigger a detectable amount of neurotransmitter release in a fashion that is somehow similar to the one elicited by action potentials, the only difference being the route followed by the Ca^{2+} ions (i.e. different channel or intracellular stores). This suggests that a significant fraction of miniature synaptic currents may be driven by rises in intracellular Ca^{2+} concentration that are similar to increases in intracellular Ca^{2+} concentration achieved following an action potential.

There is no doubt that VDCCs and release machinery proteins physically interact

(Jarvis & Zamponi, 2005) but such an interaction is not documented between IP3Rs or RyRs and docked vesicles. Similarly, Ca^{2+} entry through VDCCs produces nano/micro domains but such a concept is not yet extended to intracellular Ca^{2+} release channels. In this context, the role of VDCCs remains unclear and the question arises as to whether stochastic opening of Ca^{2+} channels could be involved in miniature release? Their blockade with non-specific blockers such as Cd^{2+} and specific blockers such as toxins gives controversial results. For instance, mIPSCs recorded in Purkinje cells or MLIs are not affected by either Cd^{2+} or Ni^{2+} suggesting that VDCCs are not involved in miniature release (Llano & Gerschenfeld, 1993a; Glitsch, 2006). However, modifying the extracellular Ca^{2+} concentration for a long time has been shown to alter miniature neurotransmitter release in a way that is independent of VDCCs (Llano et al., 2000). The interpretation of these results was that the loading of the Ca^{2+} stores was crucial in maintaining mIPSCs frequency. In hippocampal granule cell evoked release from parvalbumin (PV)-expressing interneurons is triggered by P/Q-type VDCCs, whereas release from cholecystokinin (CCK)-containing interneurons is under the control of N-type channels. Spontaneous release however appears to rely on both L- and N-type VDCCs under their stochastic opening (Goswami et al., 2012). In cultured neocortical neurons, Williams et al. (2012) propose that several types of VDCCs synergistically contribute to spontaneous release of GABA.

In the present study performed on the cerebellar cortex, we confirm that VDCCs are not directly involved in the onset of miniature release since mIPSCs recorded in MLIs are not altered in the presence of Cd^{2+} or Ni^{2+}. The lack of effect of Ni^{2+} on the same parameter suggested either a weak participation of both $Ca_v2.3$ and $Ca_v3.2$ or the absence of expressions of these α1 subunits in MLIs. Single-cell RT PCR experiments confirmed the latter hypothesis regarding $Ca_v2.3$: the mRNA encoding this α1 subunit could not be detected in any of the MLI tested. Regarding $Ca_v3.2$, our RT-PCR experiments clearly show that this isoform (as

well as the other Ca_v3s) is expressed in MLIs. However, TTA-P2, a new specific T-type channel blocker (Dreyfus et al., 2010; Boehme et al., 2011; Choe et al., 2011; Eckle et al., 2012; Evans et al., 2013) failed to alter mIPSC frequency when applied on MLIs excluding the involvement of T-type VDCCs in miniature release. One of the most striking finding of the present work is that BayK8644, the positive allosteric modulator of L-type VDCCs, is able to trigger a massive increase in the frequency of mIPSC recorded in MLIs and Purkinje cells. A similar result had been previously reported in cultured substantia innominata neurons (Watanabe et al., 2002). L-type VDCCs have been functionally identified in MLIs and involved in somato-dendritic signaling mechanism such as GABA-induced regulatory volume decrease (Chavas et al., 2004) and mGluR1-dependent Ca^{2+} oscillations (Collin et al., 2009) but their putative presynaptic functions had not been looked after.

The nature of voltage-dependent Ca^{2+} channels involved in producing action potential-stimulated axonal Ca^{2+} rises has been investigated in MLIs by combining imaging experiments and pharmacological manipulations using several VDCCs blockers. Using ω-conotoxin-MVIIC at a very high concentration (5 to 6 µM), which potently blocks native N- and P/Q-type Ca^{2+} currents (Hillyard et al.,1992; Randall & Tsien, 1995; McDonough et al., 1996), as well as some toxin-resistant, R-type current components (Wu & Saggau, 1995; McDonough et al., 1996), Forti et al., (2000) noted a maximal inhibition of 50 ± 17 % of the action potential-evoked Ca^{2+} rises. The lack of reversibility of the blockade argued against a large contribution of N-type channels (Grantham et al. 1994; McDonough et al. 1996). The use of ω-agatoxin IVA (500 nM: P/Q type channel blocker) allowed these latter authors to further distinguish between channel types. As expected, ω-agatoxin IVA inhibited the Ca^{2+} transients up to 39 %; and was irreversible. It was then concluded that voltage dependent Ca^{2+} entry in MLIs is mainly attributable to P/Q-type channels. These results were in agreement with the low efficacy of opening upon an action potentiel that is usually reported regarding L-

type VDCCs. N- and P/Q-type channels are known to be much more efficient. In the present study, we refined the pharmacology of the presynaptic VDCCs using the very same paradigm. In that respect, we noted that BayK8644 superfusison is able to slow down the inactivation kinetics of action potential evoked Ca^{2+} transients whereas these latter were not altered in the presence of nimodipine (see results). Moreover, in our hands, AP-evoked presynaptic Ca^{2+} transient are not sensitive to Ni^{2+}, SNX482 and TTA-P2. These data are in agreement with those we obtained with mIPSCs and confirm i) the absence of $Ca_v2.3$ in MLIs and ii) the independence of presynaptic Ca^{2+} signals towards T-type channels. Taken together, our Ca^{2+} imaging data support the fact that L-type VDCCs are present in the presynaptic compartment of MLIs and that they might regulate the duration of internal Ca^{2+} elevations triggered by action potentiels.

The actual distance between presynaptic VDCCs and Ca^{2+} sensors of exocytosis is of crucial importance for efficacy and speed of synaptic transmission (Neher & Sakaba, 2008; Eggermann et al., 2012). The tightness of the coupling is known to have major implications for spontaneous release (Eggermann et al., 2012). Indeed, stochastic openings of presynaptic VDCCs may trigger spontaneous release events, which are likely to appear as a high frequency of miniature (Ribrault et al., 2011). The huge effect of BayK8644 observed on mIPSC frequency pleades in favor of a tight coupling between L-type VDCCs and the release machinery. However, immunochemistry experiments performed in adult animal indicate that L-type VDCCs are mostly located in the somatodendritic compartment (Hell et al., 1993; Stephens et al., 2001; Tippens et al., 2008). At the fluorescence microscopy level, the $Ca_v2.1$ subunit was detected in basket cell axon onto Purkinje cell in adult rat although $Ca_v1.2$ and $Ca_v1.3$ were not. By contrast, the expression of the $Ca_v1.2$ subunit was found in Purkinje cells dendrites (Stephens et al., 2001). At the resolution of immunofluorescence, we show that $Ca_v1.2$ and $Ca_v1.3$ stainings co-localize with Vgat labeling (used to label GABAergic axon) in

the molecular layer of P11-16 rats. Obermair et al. (2004) have reported that $Ca_v1.2$ clusters were transiently found in the axon of cultured hippocampal neurons during development and were then excluded from the distal part of axon in mature neuron. Our results tend to indicate that the Ca_v1s can be transiently expressed in the presynaptic compartment of young animals (i.e. up to 20 days old) and tend to be mostly redistributed in somata and dendrites as reported (Stephens et al., 2001). Our electrophysiological data suggest that this developmental redistribution in cerebellum appears after the 4^{th} postnatal week since BayK8644 enhances in a similar manner mIPSC frequency in P11-16 and in P17-24 rats.

Using electron microscopy, a few studies have revealed the expression of L-type VDCCs in presynaptic termini in adult rat hippocampus and in cortical cell culture from E16 embryonic mice (Tippens et al., 2008; Leitch et al., 2009; Subramanian et al., 2013). Nevertheless, these studies did not provide a quantification of the spatial distribution of L-type VDCCs in axon termini. Using the pre-embedding immunogold technique, a quantification of $Ca_v2.1$ expression on adult rat indicated that 61% of gold particles are localized in the active zone whereas 39% are found in the rest of the synaptic plasma membrane the axons of MLI (Kulik et al., 2004). The present study confirms that $Ca_v2.1$ labeling is higher in the active zone (1.6 fold, at less than 100 nm) than in the remaining presynaptic area. Note that the proportion of the $Ca_v2.1$ labeling is relatively lower in the vicinity of the active zone in comparison to Kulik et al. (2004). This slight discrepancy may reflect a redistribution of $Ca_v2.1$ localization during axonal development.

A quantitative analysis of our pre-embedding immunogold experiment reveals that $Ca_v1.2$ and $Ca_v1.3$ subunits are located in axonal termini with higher density close to the active zone (at less than 100 nm) and bear a distribution similar to the $Ca_v2.1$ subunit. These results confirm our electrophysiological experiments in a sense that a positive modulation of Ca_v1s is able to massively increase the release of GABA by MLIs. Whether Ca_v1s are directly

coupled to the release machinery remains to be elucidated. Finally, using pre-embedding and post-embedding double (anti-Cav1 and anti-Vgat antibodies) immunogold labeling, we find that $Ca_v1.2$ and $Ca_v1.3$ are in the nanodomain. This latter technique allowed to evaluate the distance between $Ca_v1.2$/ $Ca_v1.3$ and Vgat labeling: the value of 30 nm that we found confirms the nanodomain coupling.

Altogether, the data presented hereby demonstrate the actual presence of $Ca_v1.2$ and $Ca_v1.3$ in the presynaptic compartment of developing cerebellar molecular interneurons. Their very localization in the active zone of the synapses confer to them a key role in controling GABA release. To our knowledge however, L-type VDCCs are rather unlikely to be coupled with the release machinery in neurons and therefore, they might mostly serve as a link between Ca^{2+} entry and Ca^{2+} stores. Such an hypothesis is strongly supported by: i) the partial inhibition of the BayK8644 effect on mIPSCs obtained by the ryanodine receptor antagonist dantrolene; ii) the huge presynaptic Ca^{2+} elevations observed in response to BayK8644 superfusion on streches of axons and iii) the reported coupling between L-type VDCCs and RyR in neurons. Moreover, as indicated in our immunocytochemistry experiments, the presynaptic expression of L-type VDCCs seems to be transient (Stephens et al., 2001; our data). Such a developmentally regulated expression had been noted in cultured hippocampal neurons and was correlated with axonal growth (Obermair et al., 2004). Indeed, the presence of L-type VDCCs in the presynaptic compartment of developing MLIs could clearly reflect the growth of their axons and the establishment of their synapses.

During the writing process of this manuscript, we obtained interesting but intriguing results with a specific $Ca_v1.3$ antagonist published by Kang et al. (2012). These results are currently under analysis and we hope to have them ready to show by the time of the PhD defense.

References

Albensi BC, Ryujin KT, McIntosh JM, Naisbitt SR, Olivera BM, Fillous F. (1993). Localization of [125I]omega-conotoxin GVIA binding in human hippocampus and cerebellum. Neuroreport. 4(12):1331-1334.

Alle H, Geiger JR. (2006). Combined analog and action potential coding in hippocampal mossy fibers. Science. 311(5765): 1290-1293.

Altman J. (1972a). Postnatal development of the cerebellar cortex in the rat. I. The external germinal layer and the transitional molecular layer. J Comp Neurol. 145(3):353-397.

Altman J. (1972b). Postnatal development of the cerebellar cortex in the rat. II. Phases in the maturation of Purkinje cells and of the molecular layer. J Comp Neurol. 145(4):399-463.

Armstrong D, Eckert R., (1987). Voltage-activated calcium channels that must be phosphorylated to respond to membrane depolarization. Proc Natl Acad Sci USA. 84(8):2518-2522.

Azimi-Zonooz A, Kawa CB, Dowell CD, Olivera BM. (2001). Autoradiographic localization of N-type VGCCs in gerbil hippocampus and failure of omega-conotoxin MVIIA to attenuate neuronal injury after transient cerebral ischemia. Brain Res. 907(1-2):61-70.

Barclay J, Balaguero N, Mione M, Ackerman SL, Letts VA, Brodbeck J, Canti C, Meir A, Page KM, Kusumi K, Perez-Reyes E, Lander ES, Frankel WN, Gardiner RM, Dolphin AC, Rees M. (2001). Ducky mouse phenotype of epilepsy and ataxia is associated with mutations in the Cacna2d2 gene and decreased calcium channel current in cerebellar Purkinje cells. J Neurosci. 21(16):6095-9104.

Barclay JW, Morgan A, Burgoyne RD. Calcium-dependent regulation of exocytosis. Cell Calcium. 38(3-4):343-353.

Barrett CF, Tsien RW. (2004). Brief history of calcium channel discovery. In: Voltage-gated Calcium Channels, ed. Zamponi GW. P1-21. Kluwer Academic/Plenum.

Bastianelli E. (2003). Distribution of calcium-binding proteins in the cerebellum. Cerebellum. 2:242-262.

Bats C, Farrant M, Cull-Candy SG. (2013). A role of TARPs in the expression and plasticity of calcium-permeable AMPARs: evidence from cerebellar neurons and glia. Neuropharmacology. 74:76-85.

Bats C, Soto D, Studniarczyk D, Farrant M, Cull-Candy SG. (2012). Channel properties reveal differential expression of TARPed and TARPless AMPARs in stargazer neurons. Nat Neurosci. 15(6):853-861.

Bauer EP, Schafe GE, LeDoux JE. (2002). NMDA receptors and L-type voltage-gated calcium channels contribute to long-term potentiation and different components of fear memory formation in the lateral amygdala. J Neurosci. 22(12):5239-5249.

Bean BP. (1984). Nitrendipine block of cardiac calcium channels: high-affinity binding to the inactivated state. Proc Natl Acad Sci USA. 81(20):6388-6392.

Bean BP. (1985). Two kinds of calcium channels in canine atrial cells. Differences in kinetics, selectivity, and pharmacology. J Gen Physiol. 86(1):1-30.

Bean BP, Nowycky MC, Tsien RW. (1984). Beta-adrenergic modulation of calcium channels in frog ventricular heart cells. Nature. 307(5949):371-375.

Belles B, Malécot CO, Hescheler J, Trautwein W. (1988). "Run-down" of the Ca current during long whole-cell recordings in guinea pig heart cells: role of phosphorylation and intracellular calcium. Pflugers Arch. 411(4):353-360.

Bergsman JB, Tsien RW. (2000). Syntaxin modulation of calcium channels in cortical synaptosomes as revealed by botulinum toxin C1. J Neurosci. 20(12):4368-4378.
Berridge M, Lipp P, Bootman M. (1999). Calcium signalling. Curr Biol. 9(5):157-159.

Bichet D, Cornet V, Geib S, Carlier E, Volsen S, Hoshi T, Mori Y , De Waard M. (2000). The I-II loop of the Ca2+ channel α1 subunit contains an endoplasmic reticulum retention signal antagonized by the β subunit. Neuron. 25:177-190.

Birnbaumer L, Campbell KP, Catterall WA, Harpold MM, Hofmann F, Horne WA, Mori Y, Schwartz A, Snutch TP, Tanabe T, Tsien WR. (1994). The naming of voltage-gated calcium channels. Neuron. 13(3):505-506.

Boehme R, Uebele VN, Renger JJ, Pedroarena C. (2011). Rebound excitation triggered by synaptic inhibition in cerebellar nuclear neurons is suppressed by selective T-type calcium channel block. J Neurophysiol. 106(5):2653-2661.

Bouhours B, Trigo FF, Marty A. (2011). Somatic depolarization enhances GABA release in cerebellar interneurons via a calcium/protein kinase C pathway. J Neurosci. 31(15):5804-5815.

Bourinet E, Soong TW, Sutton K, Slaymaker S, Mathews E, Monteil A, Zamponi GW, Nargeot J, Snutch TP. (1999). Splicing of alpha 1A subunit gene generates phenotypic variants of P- and Q-type calcium channels. Nat Neurosci. 2(5):407-415.

Brager DH, Luther PW, Erdélyi F, Szabó G, Alger BE. (2003). Regulation of exocytosis from single visualized GABAergic boutons in hippocampal slices. J Neurosci. 23(33):10475-10486.

Brandt A, Khimich D, Moser T. (2005). Few Cav1.3 channels regulate the exocytosis of a synaptic vesicle at the hair cell ribbon synapse. J Neurosci. 25(50):11577-11585.

Brandt A, Striessnig J, Moser T. (2003). Cav1.3 channels are essential for development and presynaptic activity of cochlear inner hair cells. J Neurosci. 23(34):10832-10840.

Bray JG, Mynlieff M.(2011). Involvement of protein kinase C and protein kinase A in the enhancement of L-type calcium current by GABAB receptor activation in neonatal hippocampus. Neuroscience. 179:62-72.

Brody DL, Patil PG, Mulle JG, Snutch TP, Yue DT. (1997). Bursts of action potential

waveforms relieve G-protein inhibition of recombinant P/Q-type Ca2+ channels in HEK 293 cells. J Physiol. 499:637-644.

Brown SP, Safo PK, Regehr WG. (2004). Endocannabinoids inhibit transmission at granule cell to Purkinje cell synapses by modulating three types of presynaptic calcium channels. J Neurosci. 24(24):5623-5631.

Bucurenciu I, Bischofberger J, Jonas P. (2010). A small number of open Ca2+ channels trigger transmitter release at a central GABAergic synapse. Nat Neurosci. 13(1): 19-21.

Buraei Z, Yang J. (2010). The β subunit of voltage gated Ca2+ channels. Physiol Rev. 90:1461-1506.

Bureau I, Mulle C. (1998). Potentiation of GABAergic synaptic transmission by AMPA receptors in mouse cerebellar stellate cells: changes during development. J Physiol. 509:817-831.

Cai D, Mulle JG, Yue DT. (1997). Inhibition of recombinant Ca2+ channels by benzothiazepines and phenylalkylamines: class-specific pharmacology and underlying molecular determinants. Mol Pharmacol. 51(5):872-881.

Caillard O, Moreno H, Schwaller B, Llano I, Celio MR, Marty A. (2000). Role of the calcium-binding protein parvalbumin in short-term synaptic plasticity. Proc Natl Acad Sci USA. 97(24): 13372-13377.

Calin-Jageman I, Lee A. (2008). Ca(v)1 L-type Ca2+ channel signaling complexes in neurons. J Neurochem. 105(3):573-83.

Carter AG, Regehr WG. (2002). Quantal events shape cerebellar interneuron firing. Nat Neurosci. 5(12):1309-1318.

Catterall WA. (1991). Excitation-contraction coupling in vertebrate skeletal muscle: a tale of two calcium channels. Cell. 64(5):871-874.

Catterall WA, Few AP. (2008). Calcium channel regulation and presynaptic plasticity. Neuron. 59(6):882-901.

Catterall WA, Perez-Reyes E, Snutch TP and Striessnig J. (2005). International union of pharmacology. XLVIII. Nomenclature and structure-function relationship of voltage-gated calcium channels. Pharmacol Rev. 57(4), 411-425.

Catterall WA, Striessnig J. (1992). Receptor sites for Ca2+ channel antagonists. Trends Pharmacol Sci. 13(6):256-262.

Chan CS, Guzman JN, Ilijic E, Mercer JN, Rick C, Tkatch T, Meredith GE, Surmeier DJ. (2007). 'Rejuvenation' protects neurons in mouse models of Parkinson's disease. Nature. 447(7148):1081-1086.

Chang FC, Hosey MM. (1988). Dihydropyridine and phenylalkylamine receptors associated with cardiac and skeletal muscle calcium channels are structurally different. J Biol Chem.

263(35):18929-18937.

Chan-Palay V, Palay SL. (1972). The form of velate astrocytes in the cerebellar cortex of monkey and rat: high voltage electron microscopy of rapid golgi preparation. Z. Anat. Entwickl. Gesch. 138: 1-19.

Chavas J, Forero ME, Collin T, Llano I, Marty A. (2004). Osmotic tension as a possible link between GABA(A) receptor activation and intracellular calcium elevation. Neuron. 44(4):701-713.

Chavis P, Fagni L, Lansman JB, Bockaert J. (1996). Functional coupling between ryanodine receptors and L-type calcium channels in neurons. Nature. 382(6593):719-722.

Choe W, Messinger RB, Leach E, Eckle VS, Obradovic A, Salajegheh R, Jevtovic-Todorovic V, Todorovic SM. (2011). TTA-P2 is a potent and selective blocker of T-type calcium channels in rat sensory neurons and a novel antinociceptive agent. Mol Pharmacol. 80(5):900-910.

Christie JM, Chiu DN, Jahr CE. (2011). Ca(2+)-dependent enhancement of release by subthreshold somatic depolarization. Nat Neurosci. 14(1):62-68.

Christophe E, Doerflinger N, Lavery DJ, Molnár Z, Charpak S, Audinat E. (2005). Two populations of layer v pyramidal cells of the mouse neocortex: development and sensitivity to anesthetics. J neurophysiol. 94(5):3357-3367.

Cohen R, Atlas D. (2004). R-type voltage-gated Ca(2+) channel interacts with synaptic proteins and recruits synaptotagmin to the plasma membrane of Xenopus oocytes. Neuroscience. 128(4):831-841.

Cohen R, Elferink LA, Atlas D. (2003). The C2A domain of synaptotagmin alters the kinetics of voltage-gated Ca2+ channels Ca(v)1.2 (Lc-type) and Ca(v)2.3 (R-type). J Biol Chem. 278(11):9258-9266.

Collin T, Chat M, Lucas MG, Moreno H, Racay P, Schwaller B, Marty A, Llano I. (2005). Developmental changes in parvalbumin regulate presynaptic Ca^{2+} signaling. J Neurosci. 25(1):96-107.

Collin T, Franconville R, Ehrlich BE, Llano I. (2009). Activation of metabotropic glutamate receptors induces periodic burst firing and concomitant cytosolic Ca2+ oscillations in cerebellar interneurons. J Neurosci. 29(29):9281-9291.

Collin T, Wang JJ, Nargeot J, Schwartz A. (1993). Molecular cloning of three isoforms of the L-type voltage-dependent calcium channel beta subunit from normal human heart. Circ Res. 72(6):1337-1344.

Conti R, Tan YP, Llano I. (2004). Action pontial-evoked and ryandine-sensitive spontaneous Ca2+ transients at the presynaptic terminal of the developing CNS inhibitory synapse. J Neurosci. 24(31):6946-6957.

Curtis BM, Catterall WA. (1985). Phosphorylation of the calcium antagonist receptor of the

voltage-sensitive calcium channel by cAMP-dependent protein kinase. Proc Natl Acad Sci USA. 82(8):2528-2532.

Davies A, Kadurin I, Alvarez-Laviada A, Douglas L, Nieto-Rostro M, Bauer CS, Pratt WS, Dolphin AC. (2010). The alpha2delta subunits of voltage-gated calcium channels form GPI-anchored proteins, a posttranslational modification essential for function. Proc Natl Acad Sci USA. 107(4):1654-1659.

Davletov BA, Südhof TC. (1993). A single C2 domain from synaptotagmin I is sufficient for high affinity Ca2+/phospholipid binding. J Biol Chem. 268(35):26386-26390.

Day NC, Shaw PJ, McCormack AL, Craig PJ, Smith W, Beattie R, Williams TL, Ellis SB, Ince PG, Harpold MM, Lodge D, Volsen SG. (1996). Distribution of alpha 1A, alpha 1B and alpha 1E voltage-dependent calcium channel subunits in the human hippocampus and parahippocampal gyrus. Neuroscience. 71(4):1013-1024.

De Jongh KS, Murphy BJ, Colvin AA, Hell JW, Takahashi M, Catterall WA. (1996). Specific phosphorylation of a site in the full-length form of the alpha 1 subunit of the cardiac L-type calcium channel by adenosine 3',5'-cyclic monophosphate-dependent protein kinase. Biochemistry. 35(32):10392-10402.

De Jongh KS, Warner C, Catterall WA. (1990). Subunits of purified calcium channels. Alpha 2 and delta are encoded by the same gene. J Biol Chem. 265(25):14738-14741.

Del Castillo J, Stark L. (1952). The effect of calcium ions on the motor end-plate potentials. J Physiol. 116(4): 507-515.

De Waard M, Liu H, Walker D, Scott VE, Gurnett CA, Campbell KP. (1997). Direct binding of G-protein betagamma complex to voltage-dependent calcium channels. Nature. 385(6615):446-450.

Diana MA, Otsu Y, Maton G, Collin T, Chat M, Dieudonné S. (2007). T-type and L-type Ca2+ conductances define and encode the bimodal firing pattern of vestibulocerebellar unipolar brush cells. J Neurosci. 27(14):3823-3838.

Dickman DK, Kurshan PT, Schwarz TL. (2008). Mutations in a Drosophila alpha2delta voltage-gated calcium channel subunit reveal a crucial synaptic function. J Neurosci. 28(1):31-38.

Dieudonné S, Dumoulin A. (2000). Serotonin-driven long-range inhibitory connections in the cerebellar cortex. J Neurosci. 20(5): 1837-1848.

Dolmetsch RE, Pajvani U, Fife K, Spotts JM, Greenberg ME. (2001). Signaling to the nucleus by an L-type calcium channel-calmodulin complex through the MAP kinase pathway. Science. 294(5541):333-339.

Dolphin AC. (2003a). Beta subunits of voltage-gated calcium channels. J Bioenerg Biomembr. 35(6):599-620.

Dolphin AC. (2003b). G protein modulation of voltage-gated calcium channels. Pharmacol

Rev. 55(4):607-627.

Dolphin AC. (2006). A short history of voltage-gated calcium channels. Br J Pharmacol. 147:56-62.

Dolphin AC. (2009). Calcium channel diversity: multiple roles of calcium channel subunits. Curr Opin Neurobiol. 19(3):237-244.

Dolphin AC. (2013). The α2δ subunits of voltage-gated calcium channels. Biochim Biophys Acta. 1828(7):1541-1549.

Doroshenko PA, Woppmann A, Miljanich G, Augustine GJ. (1997). Pharmacologically distinct presynaptic calcium channels in cerebellar excitatory and inhibitory synapses. Neuropharmacology. 36(6):865-872.

Dreyfus FM, Tscherter A, Errington AC, Renger JJ, Shin HS, Uebele VN, Crunelli V, Lambert RC, Leresche N. (2010). Selective T-type calcium channel block in thalamic neurons reveals channel redundancy and physiological impact of I(T)window. J Neurosci. 30(1):99-109.

Dunlap K, Luebke JI, Turner TJ. (1995). Exocytotic Ca2+ channels in mammalian central neurons. Trends Neurosci. 18(2):89-98.

Eckle VS, Digruccio MR, Uebele VN, Renger JJ, Todorovic SM. (2012). Inhibition of T-type calcium current in rat thalamocortical neurons by isoflurane. Neuropharmacology. 63(2):266-273.

Egger V, Svoboda K, Mainen ZF. (2003). Mechanisms of lateral inhibition in the olfactory bulb: efficiency and modulation of spike-evoked calcium influx into granule cells. J Neurosci. 23(20):7551-7558.

Eggermann E, Bucurenciu I, Goswami SP, Jonas P. (2012). Nanodomain coupling between Ca^{2+} channels and sensors of exocytosis at fast mammalian synapses. Nat Rev Neurosci. 13(1):7-21.

Elliott EM, Malouf AT, Catterall WA. (1995). Role of calcium channel subtypes in calcium transients in hippocampal CA3 neurons.. J Neurosci. 15(10):6433-6444.

Elmslie KS, Zhou W, Jones SW. (1990). LHRH and GTP-gamma-S modify calcium current activation in bullfrog sympathetic neurons. Neuron. 5(1):75-80.

Ertel EA, Campbell KP, Harpold MM, Hofmann F, Mori Y, Perez-Reyes E, Schwartz A, Snutch TP, Tanabe T, Birnbaumer L, Tsien RW and Catterall WA. (2000). Nomenclature of voltage-gated calcium channels. Neuron. 25(3):533-535.

Evans MD, Sammons RP, Lebron S, Dumitrescu AS, Watkins TB, Uebele VN, Renger JJ, Grubb MS. (2013). Calcineurin signaling mediates activity-dependent relocation of the axon initial segment. J Neurosci. 33(16):6950-6963.

Evans RM, Zamponi GW. (2006). Presynaptic Ca2+ channels--integration centers for neuronal signaling pathways. Trends Neurosci. 29(11):617-624.

Fang K, Colecraft HM. (2011). Mechanism of auxiliary β-subunit-mediated membrane targeting of L-type (Ca(v)1.2) channels. J Physiol. 589:4437-4455.

Fatemi SH, Aldinger KA, Ashwood P, Bauman ML, Blaha CD, Blatt GJ, Chauhan A, Chauhan V, Dager SR, Dickson PE, Estes AM, Goldowitz D, Heck DH, Kemper TL, King BH, Martin LA, Millen KJ, Mittleman G, Mosconi MW, Persico AM, Sweeney JA, Webb SJ, Welsh JP. (2012). Consensus paper: pathological role of the cerebellum in autism. Cerebellum. 11(3):777-807.

Fatt P, Katz B. (1952). Spontaneous subthreshold activity at motor nerve endings. J Physiol. 117:109-128.

Felix R, Gurnett CA, De Waard M, Campbell KP. (1997). Dissection of functional domains of the voltage-dependent Ca2+ channel alpha2delta subunit. J Neurosci. 17(18):6884-6891.

Ferrándiz-Huertas C, Gil-Mínguez M, Luján R. (2012). Regional expression and subcellular localization of the voltage-gated calcium channel β subunits in the developing mouse brain. J Neurochem. 122(6):1095-1107.

Flourens P. (1824) Recherches expérimentales sur les propriétés et les fonctions du système nerveux dans les animaux vertébrés. Crevot, Paris

Forti L, Pouzat C, Llano I. (2000). Action potential-evoked Ca2+ signals and calcium channels in axons of developing rat cerebellar interneurones. J Physiol. 527(1):33-48.

Fourcaudot E, Gambino F, Casassus G, Poulain B, Humeau Y, Lüthi A. (2009). L-type voltage-dependent Ca(2+) channels mediate expression of presynaptic LTP in amygdala. Nat Neurosci. 12(9):1093-1095.

Fourcaudot E, Gambino F, Humeau Y, Casassus G, Shaban H, Poulain B, Lüthi A. (2008). cAMP/PKA signaling and RIM1alpha mediate presynaptic LTP in the lateral amygdala. Proc Natl Acad Sci USA. 105(39):15130-15135.

Fremeau RT Jr, Troyer MD, Pahner I, Nygaard GO, Tran CH, Reimer RJ, Bellocchio EE, Fortin D, Storm-Mathisen J, Edwards RH. (2001). The expression of vesicular glutamate transporters defines two classes of excitatory synapse. Neuron. 31(2):247-260.

Fukaya M, Yamazaki M, Sakimura K, Watanabe M. (2005). Spatial diversity in gene expression for VDCC gamma subunit family in developing and adult mouse brains. Neurosci Res. 53(4):376-383.

Furukawa T, Miura R, Mori Y, Strobeck M, Suzuki K, Ogihara Y, Asano T, Morishita R, Hashii M, Higashida H, Yoshii M, Nukada T. (1998). Differential interactions of the C terminus and the cytoplasmic I-II loop of neuronal Ca2+ channels with G-protein alpha and beta gamma subunits. II. Evidence for direct binding. J Biol Chem. 273(28):17595-17603.

Galante M, Marty A. (2003). Presynaptic ryanodine-sensitive calcium stores contribute to evoked neurotransmitter release at the basket cell-Purkinje cell synapse. J Neurosci. 23:11229-11234.

Gao T, Yatani A, Dell'Acqua ML, Sako H, Green SA, Dascal N, Scott JD, Hosey MM. (1997). cAMP-dependent regulation of cardiac L-type Ca2+ channels requires membrane targeting of PKA and phosphorylation of channel subunits. Neuron. 19(1): 185-196.

Gerhardstein BL, Puri TS, Chien AJ, Hosey MM. (1999). Identification of the sites phosphorylated by cyclic AMP-dependent protein kinase on the beta 2 subunit of L-type voltage-dependent calcium channels. Biochemistry. 38(32):10361-10370.

Giannini G, Conti A, Mammarella S, Scrobogna M, Sorrentino V (1995). The ryanodine receptor/calcium channel genes are widely and differentially expressed in murine and peripheral tissues. J Cell Biol. 128(5):893-904.

Glickstein M, Strata P and Voogd J. (2009). Cerebellum: history. Neuroscience. 162(3):549-559.

Glickstein M, Sultan F and Voogd J. (2011). Functional localization in the cerebellum. Cortex. 47(1): 59-80.

Glitsch M. (2006). Selective inhibition of spontaneous but not Ca2+ -dependent release machinery by presynaptic group II mGluRs in rat cerebellar slices. J Neurophysiol. 96(1):86-96.

Glitsch MD. (2008). Spontaneous neurotransmitter release and Ca2+--how spontaneous is spontaneous neurotransmitter release?. Cell Calcium. 43(1):9-15.

Glitsch M, Marty A. (1999). Presynaptic effects of NMDA in cerebellar Purkinje cells and interneurons. J Neurosci. 19(2):511-519.

Goswami SP, Bucurenciu I, Jonas P. (2012). Miniature IPSCs in hippocampal granule cells are triggered by voltage-gated Ca2+ channels via microdomain coupling. J Neurosci. 32(41):14294-14304.

Grantham CJ, Bowman D, Bath CP, Bell DC, Bleakman D. (1994). Omega-conotoxin MVIIC reversibly inhibits a human N-type calcium channel and calcium influx into chick synaptosomes. Neuropharmacology. 33(2):255-258.

Hanson JE, Smith Y. (2002). Subcellular distribution of high-voltage-activated calcium channel subtypes in rat globus pallidus neurons. J Comp Neurol. 442(2):89-98.

Harlow ML, Ress D, Stoschek A, Marshall RM, McMahan UJ. (2001). The architecture of active zone material at the frog's neuromuscular junction. Nature. 409(6819):479-484.

Hefft S, Jonas P. (2005). Asynchronous GABA release generates long-lasting inhibition at a hippocampal interneuron-principal neuron synapse. Nat Neurosci. 8(10):1319-1328.

Hell JW, Westenbroek RE, Warner C, Ahlijanian MK, Prystay W, Gilbert MM, Snutch TP, Catterall WA. (1993). Identification and differential subcellular localization of the neuronal class C and class D L-type calcium channel alpha 1 subunits. J Cell Biol. 123(4): 949-962.

Hell JW, Yokoyama CT, Breeze LJ, Chavkin C, Catterall WA. (1995). Phosphorylation of presynaptic and postsynaptic calcium channels by cAMP-dependent protein kinase in hippocampal neurons. EMBO J. 14(13):3036-3044.

Helton TD, Xu W, Lipscombe D. (2005). Neuronal L-type calcium channels open quickly and are inhibited slowly. J Neurosci. 25(44):10247-10251.
Herlitze S, Garcia DE, Mackie K, Hille B, Scheuer T, Catterall WA. (1996). Modulation of Ca2+ channels by G-protein beta gamma subunits. Nature. 380(6571): 258-262.

Herlitze S, Hockerman GH, Scheuer T, Catterall WA. (1997). Molecular determinants of inactivation and G protein modulation in the intracellular loop connecting domains I and II of the calcium channel alpha1A subunit. Proc Natl Acad Sci USA. 94(4):1512-1516.

Hescheler J, Pelzer D, Trube G, Trautwein W. (1982). Does the organic calcium channel blocker D600 act from inside or outside on the cardiac cell membrane? Pflugers Arch. 393(4):287-291.

Hess P, Lansman JB, Tsien RW. (1984). Different modes of Ca channel gating behaviour favoured by dihydropyridine Ca agonists and antagonists. Nature. 538-544.

Hillyard DR, Monje VD, Mintz IM, Bean BP, Nadasdi L, Ramachandran J, Miljanich G, Azimi-Zoonooz A, McIntosh JM, Cruz LJ, et al. (1992). A new Conus peptide ligand for mammalian presynaptic Ca2+ channels. Neuron. 9(1):69-77.

Hobom M, Dai S, Marais E, Lacinova L, Hofmann F, Klugbauer N. (2000). Neuronal distribution and functional characterization of the calcium channel alpha2delta-2 subunit. Eur J Neurosci. 12(4):1217-1226.

Hoffer BJ, Siggins GR, Oliver AP, Bloom FE. (1972). Cyclic AMP-mediated adrenergic synapses to cerebellar Purkinje cells. Adv Cyclic Nucleotide Res. 1:411-423.

Holmgaard K, Jensen K, Lambert JD. (2008). Imaging of Ca2+ responses mediated by presynaptic L-type channels on GABAergic boutons of cultured hippocampal neurons. Brain Res. 1249:79-90.

Holz GG 4th, Dunlap K, Kream RM. (1988). Characterization of the electrically evoked release of substance P from dorsal root ganglion neurons: methods and dihydropyridine sensitivity. J Neurosci. 8(2):463-471.

Hoogland TM, Saggau P. (2004). Facilitation of L-type Ca2+ channels in dendritic spines by activation of beta2 adrenergic receptors. J Neurosci. 24(39):8416-8427.

Hoppa MB, Lana B, Margas W, Dolphin AC, Ryan TA. (2012). α2δ expression sets presynaptic calcium channel abundance and release probability. Nature. 486(7401):122-125.

Huang Z, Lujan R, Kadurin I, Uebele VN, Renger JJ, Dolphin AC, Shah MM. (2011). Presynaptic HCN1 channels regulate Cav3.2 activity and neurotransmission at select cortical synapses. Nat Neurosci. 14(4):478-486.

Humeau Y, Shaban H, Bissière S, Lüthi A. (2003). Presynaptic induction of heterosynaptic

associative plasticity in the mammalian brain. Nature. 426(6968):841-845.

Ikeda SR. (1996). Voltage-dependent modulation of N-type calcium channels by G-protein beta gamma subunits. Nature. 380(6571):255-258.

Ishibashi H, Murai Y, Akaike N. (1998). Effect of nilvadipine on the voltage-dependent Ca2+ channels in rat hippocampal CA1 pyramidal neurons. Brain Res. 813(1):121-127.

Jarvis SE, Zamponi GW. (2005). Masters or slaves? Vesicle release machinery and the regulation of presynaptic calcium channels. Cell Calcium. 37(5):483-488.

Jensen K, Jensen MS, Lambert JD. (1999a). Post-tetanic potentiation of GABAergic IPSCs in cultured rat hippocampal neurones. J Physiol. 519(1):71-84.

Jensen K, Jensen MS, Lambert JD. (1999b). Role of presynaptic L-type Ca2+ channels in GABAergic synaptic transmission in cultured hippocampal neurons. J Neurophysiol. 81(3):1225-1230.

Jensen K, Mody I. (2001). L-type Ca2+ channel-mediated short-term plasticity of GABAergic synapses. Nat Neurosci. 4(10):975-976.

Jiménez C, Bourinet E, Leuranguer V, Richard S, Snutch TP, Nargeot J. (2000). Determinants of voltage-dependent inactivation affect Mibefradil block of calcium channels. Neuropharmacology. 39(1):1-10.

Jones LP, Wei SK, Yue DT. (1998). Mechanism of auxiliary subunit modulation of neuronal alpha1E calcium channels. J Gen Physiol. 112(2):125-143.

Jun K, Piedras-Rentería ES, Smith SM, Wheeler DB, Lee SB, Lee TG, Chin H, Adams ME, Scheller RH, Tsien RW, Shin HS. (1999). Ablation of P/Q-type Ca(2+) channel currents, altered synaptic transmission, and progressive ataxia in mice lacking the alpha(1A)-subunit. Proc Natl Acad Sci USA. 96(26):15245-15250.

Kameyama M, Hofmann F, Trautwein W. (1985). On the mechanism of beta-adrenergic regulation of the Ca channel in the guinea-pig heart. Pflugers Arch. 405(3):285-293.

Kang MG, Chen CC, Felix R, Letts VA, Frankel WN, Mori Y, Campbell KP. (2001). Biochemical and biophysical evidence for gamma 2 subunit association with neuronal voltage-activated Ca2+ channels. J Biol Chem. 276(35):32917-32924.

Kang S, Cooper G, Dunne SF, Dusel B, Luan CH, Surmeier DJ, Silverman RB. (2012). CaV1.3-selective L-type calcium channel antagonists as potential new therapeutics for Parkinson's disease. Nat Commun. 3:1146.

Katz B, Miledi R. (1965a). The measurement of synaptic delay, and the time course of acetylcholine release at the neuromuscular junction. Proc R Soc Lond B Biol Sci. 161:483-495.

Katz B, Miledi R. (1965b). The effect of temperature on the synaptic delay at the neuromuscular junction. J Physiol. 181(3):656-670.

Katz B, Miledi R. (1970). Further study of the role of calcium in synaptic transmission. J Physiol. 207(3): 789-801.

Kepplinger KJ, Förstner G, Kahr H, Leitner K, Pammer P, Groschner K, Soldatov NM, Romanin C. (2000). Molecular determinant for run-down of L-type Ca2+ channels localized in the carboxyl terminus of the 1C subunit. J Physiol. 529:119-130.

Kerr LM, Filloux F, Olivera BM, Jackson H, Wamsley JK. (1988). Autoradiographic localization of calcium channels with [125I]omega-conotoxin in rat brain. Eur J Pharmacol. 146(1):181-183.

Kim S, Yun HM, Baik JH, Chung KC, Nah SY, Rhim H. (2007). Functional interaction of neuronal Cav1.3 L-type calcium channel with ryanodine receptor type 2 in the rat hippocampus. J Biol. Chem. 282(45):32877-32889.

Klem MK, Weinberg RJ, Criswell HE, Breese GR. (2010). The PLC/IP 3 R/PKC pathway is required for ethanol-enhanced GABA release. Neuropharmacology. 58(7):1179-1186.

Klugbauer N, Dai S, Specht V, Lacinová L, Marais E, Bohn G, Hofmann F. (2000). A family of gamma-like calcium channel subunits. FEBS Lett. 470(2):189-197.

Klugbauer N, Lacinová L, Marais E, Hobom M, Hofmann F. (1999). Molecular diversity of the calcium channel alpha2delta subunit. J Neurosci. 19(2):684-691.

Klugbauer N, Marais E, Hofmann F. (2003). Calcium channel alpha2delta subunits: differential expression, function, and drug binding. J Bioenerg Biomembr. 35(6):639-647.

Kölliker A. (1890). Zur feineren anatomie des zentralen nervensystems. 1. Das Kleinhirn. Z. wiss. Zool. 49:663-689.

Kondo S, Marty A. (1998). Differential effects of noradrenaline on evoked, spontaneous and miniature IPSCs in rat cerebellar stellate cells. J Physiol. 509:233-243.

Konnerth A, Llano I, Armstrong CM. (1990). Synaptic currents in cerebellar Purkinje cells. Proc Natl Acad Sci USA. 87(7):2662-2665.

Kosaka T, Kosaka K, Nakayama T, Hunziker W, Heizmann CW. (1993). Axons and axon terminals of cerebellar Purkinje cells and basket cells have higher levels of parvalbumin immunoreactivity than somata and dendrites: quantitative analysis by immunogold labeling. Exp Brain Res. 93(3):483-491.

Koschak A, Reimer D, Huber I, Grabner M, Glossmann H, Engel J, Striessnig J. (2001). alpha 1D (Cav1.3) subunits can form l-type Ca2+ channels activating at negative voltages. J biol Chem. 276(25):22100-22106.

Kulik A, Nakadate K, Hagiwara A, Fukazawa Y, Luján R, Saito H, Suzuki N, Futatsugi A, Mikoshiba K, Frotscher M, Shigemoto R. (2004). Immunocytochemical localization of the alpha 1A subunit of the P/Q-type calcium channel in the rat cerebellum. Eur J Neurosci. 19(8):2169-2178.

Kunze DL & Rampe D. (1992). Characterization of the effects of the new Ca2+ channel activator, FPL 64176, in GH3 cells. Mol Pharmacol. 42(4):666-670.

Kuwajima G, Futatsugi A, Niinobe M, Nakanishi S and Mikoshiba K. (1992). Two types of ryanodine receptors in mouse brain: skeletal muscle type exclusively in Purkinje cells and cardiac muscle type in various neurons. Neuron. 9(6):1133-1142.

Lainé J, Axelrad H. (1998). Lugaro cells target basket and stellate cells in the cerebellar cortex. Neuroreport. 9(10):2399-2403.

Lambert RC, Bessaïh T, Crunelli V, Leresche N. (2013). The many faces of T-type calcium channels. Pflugers Arch.

Lauri SE, Bortolotto ZA, Nistico R, Bleakman D, Ornstein PL, Lodge D, Isaac JT, Collingridge GL. (2003). A role for Ca2+ stores in kainate receptor-dependent synaptic facilitation and LTP at mossy fiber synapses in the hippocampus. Neuron. 39(2):327-341.

Lee JH, Daud AN, Cribbs LL, Lacerda AE, Pereverzev A, Klöckner U, Schneider T, Perez-Reyes E. (1999). Cloning and expression of a novel member of the low voltage-activated T-type calcium channel family. J Neurosci. 19(6):1912-1921.

Lee JH, Gomora JC, Cribbs LL, Perez-Reyes E. (1999). Nickel block of three cloned T-type calcium channels: low concentrations selectively block alpha1H. Biophys. 77(6):3034-3042.

Leitch B, Szostek A, Lin R, Shevtsova O. (2009). Subcellular distribution of L-type calcium channel subtypes in rat hippocampal neurons. Neuroscience. 164(2):641-657.

Levine JM, Card JP. (1987). Light and electron microscopic localization of a cell surface antigen (NG2) in the rat cerebellum: association with smooth protoplasmic astrocytes. J Neurosci. 7(9):2711-2720.

Li L, Bischofberger J, Jonas P. (2007). Differential gating and recruitment of P/Q-, N-, and R-type Ca2+ channels in hippocampal mossy fiber boutons. J Neurosci. 27(49):13420-13429.

Li C, Davletov BA, Südhof TC. (1995b). Distinct Ca2+ and Sr2+ binding properties of synaptotagmins. Definition of candidate Ca2+ sensors for the fast and slow components of neurotransmitter release. J Biol Chem. 270(42):24898-24902.

Li C, Ullrich B, Zhang JZ, Anderson RG, Brose N, Südhof TC. (1995a). Ca(2+)-dependent and -independent activities of neural and non-neural synaptotagmins. Nature. 375(6532):594-599.

Lipscombe D, Helton TD, Xu W. (2004). L-type calcium channels: the low down. J Neurophysiol. 92(5):2633-2641.

Liu H, De Waard M, Scott VE, Gurnett CA, Lennon VA, Campbell KP. (1996). Identification of three subunits of the high affinity omega-conotoxin MVIIC-sensitive Ca2+ channel. J Biol Chem. 271(23): 13804-13810.

Liu Z, Ren J and Murphy TH. (2003). Decoding of synaptic voltage waveforms by specific classes of recombinant high-threshold Ca(2+) channels. J Physiol. 553:473-488.

Llano I, Gerschenfeld HM. (1993a). Inhibitory synaptic currents in stellate cells of rat cerebellar slices. J Physiol. 468:177-200.

Llano I, Gerschenfeld HM. (1993b). Beta-adrenergic enhancement of inhibitory synaptic activity in rat cerebellar stellate and Purkinje cells. J Physiol. 468:201-224.

Llano I, González J, Caputo C, Lai FA, Blayney LM, Tan YP, Marty A. (2000). Presynaptic calcium stores underlie large-amplitude miniature IPSCs and spontaneous calcium transients. Nat Neurosci. 3(12):1256-1265.

Llano I, Marty A, Armstrong CM, Konnerth A. (1991). Synaptic- and agonist-induced excitatory currents of Purkinje cells in rat cerebellar slices. J Physiol. 434:183-213.

Llano I, Tan YP, Caputo C. (1997). Spatial heterogeneity of intracellular Ca2+ signals in axons of basket cells from cerebellar slices. J Physiol. 502:509-519.

Llinás R, Sugimori M, Hillman DE, Cherksey B. (1992). Distribution and functional significance of the P-type, voltage-dependent Ca2+ channels in the mammalian central nervous system. Trends Neurosci. 15(9):351-355.

Llinás R, Sugimori M, Lin JW, Cherksey B. (1989). Blocking and isolation of a calcium channel from neurons in mammals and cephalopods utilizing a toxin fraction (FTX) from funnel-web spider poison. Proc Natl Acad Sci USA. 86(5):1689-1693.

Lory P, Chemin J. (2007). Towards the discovery of novel T-type calcium channel blockers. Expert Opin Ther Targets. 11(5):717-722.

Luciani L. (1891) *Il cervelletto: nuovi studi di fisiologia normale e patologica*, Le Monnier. German translation (1893), E. Besold.

Ludwig A, Flockerzi V, Hofmann F. (1997). Regional expression and cellular localization of the alpha1 and beta subunit of high voltage-activated calcium channels in rat brain. J Neurosci. 17(4):1339-1349.

Marcantoni A, Baldelli P, Hernandez-Guijo JM, Comunanza V, Carabelli V, Carbone E. (2007). L-type calcium channels in adrenal chromaffin cells: role in pace-making and secretion. Cell Calcium. 42(4-5):397-408.

Mark MD, Maejima T, Kuckelsberg D, Yoo JW, Hyde RA, Shah V, Gutierrez D, Moreno RL, Kruse W, Noebels JL, Herlitze S. (2011). Delayed postnatal loss of P/Q-type calcium channels recapitulates the absence epilepsy, dyskinesia, and ataxia phenotypes of genomic Cacna1a mutations. J Neurosci. 31(11):4311-4326.

Martin RL, Lee JH, Cribbs LL, Perez-Reyes E, Hanck DA. (2000). Mibefradil block of cloned T-type calcium channels. J Pharmacol Exp Ther. 295(1):302-308.

Maximov A, Tang J, Yang X, Pang ZP, Südhof TC. (2009). Complexin controls the force transfer from SNARE complexes to membranes in fusion. Science. 323(5913): 516-521.

McDonough SI, Boland LM, Mintz IM, Bean BP. (2002). Interactions among toxins that inhibit N-type and P-type calcium channels. J Gen Physiol. 119(4):313- 328.

McDonough SI, Mintz IM, Bean BP. (1997). Alteration of P-type calcium channel gating by the spider toxin omega-Aga-IVA. Biophys J. 72(5):2117-2128.

McDonough SI, Swartz KJ, Mintz IM, Boland LM, Bean BP. (1996). Inhibition of calcium channels in rat central and peripheral neurons by omega-conotoxin MVIIC. J Neurosci. 16(8):2612-2623.

McKay BE, McRory JE, Molineux ML, Hamid J, Snutch TP, Zamponi GW, Turner RW. (2006). Ca(V)3 T-type calcium channel isoforms differentially distribute to somatic and dendritic compartments in rat central neurons. Eur J Neurosci. 24(9):2581-2594.

McKinney RA, Capogna M, Dürr R, Gähwiler BH, Thompson SM. (1999). Miniature synaptic events maintain dendritic spines via AMPA receptor activation. Nat Neurosci. 2(1):44-49.

Middleton FA, Strick PL. (2001). Cerebellar projections to the prefrontal cortex of the primate. J Neurosci. 21(2):700-712.

Milner B, Squire LR, Kandel ER. (1998). Cognitive neuroscience and the study of memory. Neuron. 20(3):445-468.

Milstein AD, Nicoll RA. (2009). TARP modulation of synaptic AMPA receptor trafficking and gating depends on multiple intracellular domains. Proc Natl Acad Sci USA. 106(27):11348-11351.

Mintz IM, Sabatini BL, Regehr WG. (1995). Calcium control of transmitter release at a cerebellar synapse. Neuron. 15(3):675-688.

Mitchell KJ, Lai FA, Rutter GA. (2003). Ryanodine receptor type I and nicotinic acid adenine dinucleotide phosphate receptors mediate Ca2+ release from insulin-containing vesicles in living pancreatic beta-cells (MIN6). J Biol Chem. 278(13):11057-11064.

Miyazaki T, Fukaya M, Shimizu H, Watanabe M. (2003). Subtype switching of vesicular glutamate transporters at parallel fibre-Purkinje cell synapses in developing mouse cerebellum. Eur J Neurosci. 17(12):2563-2572.

Mochida S, Sheng ZH, Baker C, Kobayashi H, Catterall WA. (1996). Inhibition of neurotransmission by peptides containing the synaptic protein interaction site of N-type Ca2+ channels. Neuron. 17(4):781-788.

Molineux ML, Fernandez FR, Mehaffey WH, Turner RW. (2005). A-type and T-type currents interact to produce a novel spike latency-voltage relationship in cerebellar stellate cells. J Neurosci. 25(47):10863-10873.

Monteil A, Chemin J, Bourinet E, Mennessier G, Lory P, Nargeot J. (2000). Molecular and functional properties of the human alpha(1G) subunit that forms T-type calcium channels. J Biol Chem. 275(9):6090-6100.

Moosmang S, Lenhardt P, Haider N, Hofmann F, Wegener JW. (2005). Mouse models to study L-type calcium channel function. Pharmacol Ther. 106(3):347-355.

Morgans CW. (2001). Localization of the alpha(1F) calcium channel subunit in the rat retina. Invest Ophthalmol Vis Sci. 42(10): 2414-2418.

Mori F, Fukaya M, Abe H, Wakabayashi K, Watanabe M. (2000). Developmental changes in expression of the three ryanodine receptor mRNAs in mouse brain. Neurosci Lett. 285(1):57-60.

Mouton J, Marty I, Villaz M, Feltz A, Maulet Y. (2001). Molecular interaction of dihydropyridine receptors with type-1 ryanodine receptors in rat brain. Biochem J. 354:597-603.

Murakami N, Ishibashi H, Katsurabayashi S, Akaike N. (2002). Calcium channel subtypes on single GABAergic presynaptic terminal projecting to rat hippocampal neurons. Brain Res. 951(1):121-129.

Myoga MH, Regehr WG. (2011). Calcium microdomains near R-type calcium channels control the induction of presynaptic long-term potentiation at parallel fiber to purkinje cell synapses. J Neurosci. 31(14):5235-5243.

Naguro I, Nagao T, Adachi-Akahane S. (2001). Ser(1901) of alpha(1C) subunit is required for the PKA-mediated enhancement of L-type Ca(2+) channel currents but not for the negative shift of activation. FEBS Lett. 489(1): 87-91.

Neher E, Sakaba T. (2008). Multiple roles of calcium ions in the regulation of neurotransmitter release. Neuron. 59(6):861-872.

Newcomb R, Szoke B, Palma A, Wang G, Chen Xh, Hopkins W, Cong R, Miller J, Urge L, Tarczy-Hornoch K, Loo JA, Dooley DJ, Nadasdi L, Tsien RW, Lemos J, Miljanich G. (1998). Selective peptide antagonist of the class E calcium channel from the venom of the tarantula Hysterocrates gigas. Biochemistry. 37(44):15353-15362.

Nicoll RA, Tomita S, Bredt DS (2006) Auxiliary subunits assist AMPA-type glutamate receptors. Science. 311:1253–1256.

Nicolson RI, Fawcett AJ. (2005). Developmental dyslexia, learning and the cerebellum. J Neural Transm Suppl. 69:19-36.

Nowycky MC, Fox Ap and Tsien RW. (1985). Long-opening mode of gating of neuronal calcium channels and its promotion by the dihydropyridine calcium agonist Bay K 8644. Proc Natl Acad Sci USA. 82(7):2178-2182.

Nusser Z, Cull-Candy S, Farrant M. (1997). Differences in synaptic GABA(A) receptor number underlie variation in GABA mini amplitude. Neuron. 19(3):697-709.

Obermair GJ, Szabo Z, Bourinet E, Flucher BE. (2004). Differential targeting of the L-type Ca2+ channel alpha 1C (CaV1.2) to synaptic and extrasynaptic compartments in hippocampal neurons. Eur J Neurosci. 19(8): 2109-2122.

Okita M, Watanabe Y, Taya K, Utsumi H, Hayashi T. (2000). Presynaptic L-type Ca(2)+ channels on excessive dopamine release from rat caudate putamen. Physiol Behav. 68(5):641-649.

Olschowka JA, Molliver ME, Grzanna R, Rice FL, Coyle JT. (1981). Ultrastructural demonstration of noradrenergic synapses in the rat central nervous system by dopamine-beta-hydroxylase immunocytochemistry. J Histochem Cytochem. 29(2):271-280.

Olson L, Fuxe K. (1971). On the projections from the locus coeruleus noradrenaline neurons: the cerebellar innervations. Brain Res. 28(1):165-171.

Ono K, Fozzard HA. (1992). Phosphorylation restores activity of L-type calcium channels after rundown in inside-out patches from rabbit cardiac cells. J Physiol. 454:673-688.

Orduz D, Llano I. (2007). Recurrent axon collaterals underlie facilitating synapses between cerebellar Purkinje cells. Proc Natl Acad Sci USA. 104(45):17831-17836.

Osterrieder W, Brum G, Hescheler J, Trautwein W, Flockerzi V, Hofmann F. (1982). Injection of subunits of cyclic AMP-dependent protein kinase into cardiac myocytes modulates Ca2+ current. Nature. 298(5874):576-578.

Ouardouz M, Nikolaeva MA, Coderre E, Zamponi GW, McRory JE, Trapp BD, Yin X, Wang W, Woulfe J, Stys PK. (2003). Depolarization-induced Ca2+ release in ischemic spinal cord white matter involves L-type Ca2+ channel activation of ryanodine receptors. Neuron. 40(1):53-63.

Palay SL, Chan-Palay V. (1974). Cerebellar cortex: cytology and organization. New York: Springer.

Pan ZH, Hu HJ, Perring P, Andrade R (2001) T-type Ca(2+) channels mediate neurotransmitter release in retinal bipolar cells. Neuron. 32(1):89–98.

Parajuli LK, Nakajima C, Kulik A, Matsui K, Schneider T, Shigemoto R, Fukazawa Y. (2012). Quantitative regional and ultrastructural localization of the Ca(v)2.3 subunit of R-type calcium channel in mouse brain. J Neurosci. 32(39):13555-67.

Pérez-Alvarez A, Hernández-Vivanco A, Caba-González JC, Albillos A. (2011) Different roles attributed to Cav1 channel subtypes in spontaneous action potential firing and fine tuning of exocytosis in mouse chromafin cells. J Neurochem. 116(1): 105-121.

Pickel VM, Segal M, Bloom FE. (1974a). A radioautographic study of the efferent pathways of the nucleus locus coeruleus. J Comp Neurol. 155(1):15-24.

Pickel VM. Segal M, Bloom FE. (1974b). Axonal proliferation following lesions of cerebellar peduncles. A combined fluorescence microscopy and radioautographic study. J Comp Neurol.

155(1):43-60.

Platzer J, Engel J, Schrott-Fischer A, Stephan K, Bova S, Chen H, Zheng H, Striessnig J. (2000). Congenital deafness and sinoatrial node dysfunction in mice lacking class D L-type Ca2+ channels. Cell. 102(1):89-97.

Pouzat C, Hestrin S. (1997). Developmental regulation of basket/stellate cell--Purkinje cell synapses in cerebellum. J Neurosci. 17(23):9104-9112.

Puopolo M, Raviola E, Bean BP. (2007). Roles of subthreshold calcium current and sodium current in spontaneous firing of mouse midbrain dopamine neurons. J Neurosci. 27(3):645-656.

Purkinje J. (1838) Versammlung der Naturforscher und Aertze zur Prag. Isis von Oken 7: 581.

Qin N, Yagel S, Momplaisir ML, Codd EE, D'Andrea MR. (2002). Molecular cloning and characterization of the human voltage-gated calcium channel alpha(2)delta-4 subunit. Mol Pharmacol. 62(3):485-496.

Rakic P. (1972). Extrinsic cytological determinants of basket and stellate cell dendritic pattern in the cerebellar molecular layer. J Comp Neurol. 146(3):335-354.

Ramón y Cajal (1911). Histologie du système nerveux de l'homme et des vertébrés. A Maloine.

Rampe D, Lacerda AE. (1991). A new site for the activation of cardiac calcium channels defined by the nondihydropyridine FPL 64176. J Pharmacol Exp Ther. 259(3):982-987.

Ramsey IS, Delling M, Clapham DE. (2006). An introduction to TRP channels. Annu Rev Physiol. 68:619-647.

Randall A, Tsien RW. (1995). Pharmacological dissection of multiple types of Ca2+ channel currents in rat cerebellar granule neurons. J Neurosci. 15(4):2995-3012.

Randall A, Tsien RW. (1997). Contrasting biophysical and pharmacological properties of T-type and R-type calcium channels. Neuropharmacology. 36(7):879-893.

Rettig J, Sheng ZH, Kim DK, Hodson CD, Snutch TP, Catterall WA. (1996). Isoform-specific interaction of the alpha1A subunits of the brain Ca2+ channels with the presynaptic proteins syntaxin and SNAP-25. Proc Natl Acad Sci USA. 93(14):7363-7368.

Ribrault C, Sekimoto K, Triller A. (2011). From the stochasticity of molecular processes to the variability of synaptic transmission. Nat Rev Neurosci. 12(7):375-387.

Richards MW, Butcher AJ, Dolphin AC. (2004). Ca^{2+} channel beta-subunits: Structural insights AID our understanding. Trends Pharmacol Sci. 25(12):626-632.

Riva D, Giorgi C. (2000). The cerebellum contributes to higher functions during development: Evidence from a series of children surgically treated for posterior fossa tumours. Brain. 123:1051-1061.

Rolando L. (1809) Saggio sopra la vera struttura del cervello dell'uomo e degli animali e sopra le funzioni del sistema nervosa. Stamperia da S.S.R.M. Privilegiata, Sassari.

Rossi B, Maton G, Collin T. (2008). Calcium-permeable presynaptic AMPA receptors in cerebellar molecular layer interneurones. J Physiol. 586:5129-5145.

Sabatini BL, Regehr WG. (1996). Timing of neurotransmission at fast synapses in the mammalian brain. Nature. 384(6605): 170-172.

Saitow F, Satake S, Yamada J, Konishi S. (2000). Beta-adrenergic receptor-mediated presynaptic facilitation of inhibitory GABAergic transmission at cerebellar interneuron-Purkinje cell synapses. J Neurosphysiol. 84(4):2016-2025.

Sammet K. (2007). Luigi Rolando (1773-1831). J Neurol. 254(3):404-405.

Sawada K, Hosoi E, Bando M, Sakata-Haga H, Lee NS, Jeong YG and Fukui Y. (2008). Differential alterations in expressions of ryanodine receptor subtypes in cerebellar cortical neurons of an ataxic mutant, rolling mouse Nagoya. Neuroscience. 152(3):609-617.

Schramm M, Thomas G, Towart R, Franckowiak G. (1983). Novel dihydropyridines with positive inotropic action through activation of Ca^{2+} channels. Nature. 303(5917):535-537.

Schweighofer N, Doya K, Kuroda S. (2004). Cerebellar aminergic neuromodulation: towards a functional understanding. Brain Res Brain Res Rev. 44(2-3):103-116.

Seagar M, Lévêque C, Charvin N, Marquèze B, Martin-Moutot N, Boudier JA, Boudier JL, Shoji-Kasai Y, Sato K, Takahashi M. (1999). Interactions between proteins implicated in exocytosis and voltage-gated calcium channels. Philos Trans R Soc Lond B Biol Sci. 354(1381):289-297.

Shahrezaei V, Cao A, Delaney KR. (2006). Ca2+ from one or two channels controls fusion of a single vesicle at the frog neuromuscular junction. J Neurosci. 26(51):13240-13249.

Sheng ZH, Rettig J, Takahashi M, Catterall WA. (1994). Identification of a syntaxin-binding site on N-type calcium channels. Neuron. 13(6):1303-1313.

Sheng ZH, Westenbroek RE, Catterall WA. (1998). Physical link and functional coupling of presynaptic calcium channels and the synaptic vesicle docking/fusion machinery. J Bioenerg Biomembr. 30(4):335-345.

Sheng ZH, Yokoyama CT, Catterall WA. (1997). Interaction of the synprint site of N-type Ca2+ channels with the C2B domain of synaptotagmin I. Proc Natl Acad Sci USA. 94(10):5405-5410.

Shinnick-Gallagher P, McKernan MG, Xie J, Zinebi F. (2003). L-type voltage-gated calcium channels are involved in the in vivo and in vitro expression of fear conditioning. Ann NY Acad Sci. 985:135-149.

Shipe WD, Barrow JC, Yang ZQ, Lindsley CW, Yang FV, Schlegel KA, Shu Y, Rittle KE,

Bock MG, Hartman GD, et al. (2008) Design, synthesis, and evaluation of a novel 4 aminomethyl-4-fluoropiperidine as a T-type Ca2+ channel antagonist. J Med Chem 51(13):3692–3695.

Shistik E, Ivanina T, Puri T, Hosey M, Dascal N. (1995). Ca2+ current enhancement by alpha 2/delta and beta subunits in Xenopus oocytes: contribution of changes in channel gating and alpha 1 protein level. J Physiol. 489:55-62.

Shu Y, Hasenstaub A, Duque A, Yu Y, McCormick DA. (2006). Modulation of intracortical synaptic potentials by presynaptic somatic membrane potential. Nature. 441(7094):761-765.

Simat M, Parpan F, Fritschy JM. (2007). Heterogeneity of glycinergic and gabaergic interneurons in the granule cell layer of mouse cerebellum. J Comp Neurol. 500(1):71-83.

Sinnegger-Brauns MJ, Hetzenauer A, Huber IG, Renström E, Wietzorrek G, Berjukov S, Cavalli M, Walter D, Koschak A, Waldschütz R, Hering S, Bova S, Rorsman P, Pongs O, Singewald N, Striessnig J Jö. (2004). Isoform-specific regulation of mood behavior and pancreatic beta cell and cardiovascular function by L-type Ca 2+ channels. J Clin Invest. 113(10):1430-1439.

Sotelo C. (2008). Development of "Pinceaux" formations and dendritic translocation of climbing fibers during the acquisition of the balance between glutamatergic and gamma-aminobutyric acidergic inputs in developing Purkinje cells. J Comp Neurol. 506(2):240-262.

Sotelo C. (2010). Camillo Golgi and Santiago Ramon y Cajal: The anatomical organization of the cortex of the cerebellum. Can the neuron doctrine still support our actual knowledge on the cerebellar structural arrangement?. Brain Res Rev. 66(1-2):16-34.

Soto D, Coombs ID, Kelly L, Farrant M, Cull-Candy SG. (2007). Stargazin attenuates intracellular polyamine block of calcium-permeable AMPA receptors. Nat Neurosci. 10(10): 1260-1267.

Spafford JD, Zamponi GW. (2003). Functional interactions between presynaptic calcium channels and the neurotransmitter release machinery. Curr Opin Neurobiol. 13(3):308-314.

Stea A, Soong TW, Snutch TP. (1995). Determinants of PKC-dependent modulation of a family of neuronal calcium channels. Neuron. 15(4):929-940.

Stephens GJ, Morris NP, Fyffe RE, Robertson B. (2001). The Cav2.1/alpha1A (P/Q-type) voltage-dependent calcium channel mediates inhibitory neurotransmission onto mouse cerebellar Purkinje cells. Eur J Neurosci. 13(10):1902-1912.

Striessnig J, Grabner M, Mitterdorfer J, Hering S, Sinnegger MJ, Glossmann H. (1998). Structural basis of drug binding to L Ca2+ channels. Trends Pharmacol Sci. 19(3):108-115.

Subramanian J, Dye L, Morozov A. (2013). Rap1 signaling prevents L-type calcium channel-dependent neurotransmitter release. J Neurosci. 33(17):7245-7252.

Subramanian J, Morozov A. (2011). Erk1/2 inhibit synaptic vesicle exocytosis through L-type calcium channels. J Neurosci. 31(12):4755-4764.

Südhof TC. (2004). The synaptic vesicle cycle. Annu rev Neurosci. 27:509-547.

Südhof TC. (2013). A molecular machine for neurotransmitter release: synaptotagmin and beyond. Nat Med. 19(10):1227-1231.

Sultan F, Bower JM. (1998). Quantitative Golgi study of the rat cerebellar molecular layer interneurons using principal component analysis. J Comp Neurol. 393(3):353-373.

Sutton MA, Wall NR, Aakalu GN, Schuman EM. (2004). Regulation of dendritic protein synthesis by miniature synaptic events. Science. 304(5679):1979-1983.

Swartz KJ. (1993). Modulation of Ca2+ channels by protein kinase C in rat central and peripheral neurons: disruption of G protein-mediated inhibition. Neuron. 11(2):305-320.

Swartz KJ., Merritt A, Bean BP, Lovinger DM. (1993). Protein kinase C modulates glutamate receptor inhibition of Ca2+ channels and synaptic transmission. Nature. 361(6408):165-168.

Takahashi T, Momiyama A. (1993). Different types of calcium channels mediate central synaptic transmission. Nature. 1993. 366(6451):156-158.

Takayama C, Inoue Y. (2004). Extrasynaptic localization of GABA in the developing mouse cerebellum. Neurosci Res. 50(4):447-458.

Takemura M, Kiyama H, Fukui H, Tohyama M, Wada H. (1988). Autoradiographic visualization in rat brain of receptors for omega-conotoxin GVIA, a newly discovered calcium antagonist. Brain Res. 451(1-2):386-389.

Tan YP, Llano I. (1999). Modulation by K+ channels of action potential-evoked intracellular Ca2+ concentration rises in rat cerebellar basket cell axons. J Physiol. 520:65-78.

Tanabe T, Takeshima H, Mikami A, Flockerzi V, Takahashi H, Kangawa K, Kojima M, Matsuo H, Hirose T, Numa S. (1987) Primary structure of the receptor for calcium channel blockers from skeletal muscle. Nature 328(6128):313-318.

Tang AH, Karson MA, Nagode DA, McIntosh JM, Uebele VN, Renger JJ, Klugmann M, Milner TA, Alger BE. (2011). Nerve terminal nicotinic acetylcholine receptors initiate quantal GABA release from perisomatic interneurons by activating axonal T-type (Cav3) Ca^{2+} channels and Ca^{2+} release from stores. J Neurosci. 31(38):13546-13561.

Tedford HW, Zamponi GW. (2006). Direct G protein modulation of Cav2 calcium channels. Pharmacol Rev. 58(4):837-862.

Tippens AL, Pare JF, Langwieser N, Moosmang S, Milner TA, Smith Y, Lee A. (2008). Ultrastructural evidence for pre- and postsynaptic localization of Cav1.2 L-type Ca2+ channels in the rat hippocampus. J Comp Neurol. 506(4):569-583.

Todorovic SM, Lingle CJ. (1998). Pharmacological properties of T-type Ca2+ current in adult rat sensory neurons: effects of anticonvulsant and anesthetic agents. J Neurophysiol. 79(1):240-252.

Tomita S, Chen L, Kawasaki Y, Petralia RS, Wenthold RJ, Nicoll RA, Bredt DS. (2003). Functional studies and distribution define a family of transmembrane AMPA receptor regulatory proteins. J Cell Biol. 161(4): 805-816.

Triggle DJ. (1992). Calcium-channel antagonists: mechanisms of action, vascular selectivities, and clinical relevance. Cleve Clin J Med. 59(6):617-627.

Tunwell RE, Wickenden C, Bertrand BM, Shevchenko VI, Walsh MB, Allen PD, Lai FA. (1996). The human cardiac muscle ryanodine receptor-calcium release channel: identification, primary structure and topological analysis. Biochem J. 318:477-487.

Vandael DH, Marcantoni A, Mahapatra S, Caro A, Ruth P, Zuccotti A, Knipper M, Carbone E. (2010). Ca(v)1.3 and BK channels for timing and regulating cell firing. Mol Neurobiol. 42(3):185-198.

Vendel AC, Terry MD, Striegel AR, Iverson NM, Leuranguer V, Rithner CD, Lyons BA, Pickard GE, Tobet SA, Horne WA. (2006). Alternative splicing of the voltage-gated Ca2+ channel beta4 subunit creates a uniquely folded N-terminal protein binding domain with cell-specific expression in the cerebellar cortex. J Neurosci. 26(10):2635-2644.

Vincent P, Marty A. (1996). Fluctuations of inhibitory postsynaptic currents in Purkinje cells from rat cerebellar slices. J Physiol. 494(1):183-199.

Wakamori M, Mikala G, Mori Y. (1999). Auxiliary subunits operate as a molecular switch in determining gating behaviour of the unitary N-type Ca2+ channel current in Xenopus oocytes. J Physiol. 517:659-672.

Watanabe T, Kalasz H, Yabana H, Kuniyasu A, Mershon J, Itagaki K, Vaghy PL, Naito K, Nakayama H, Schwartz A. (1993). Azidobutyryl clentiazem, a new photoactivatable diltiazem analog, labels benzothiazepine binding sites in the alpha 1 subunit of the skeletal muscle calcium channel. FEBS Lett. 334(3):261-264.

Watanabe Y, Lawlor GF, Fujiwara M. (1998). Role of nerve terminal L-type Ca2+ channel in the brain. Life Sci. 62(17-18):1671-1675.

Watanabe Y, Wang ZM, Rhee JS, Lawlor GF, Ishibashi H, Akaike N. (2002). Inhibitory effects of 1,4-DHP antagonists on synaptic GABA release modulated by BAY-K 8644 in mechanically dissociated rat substantia innominata. Life Sci. 71(10):1103-1113.

Waters J, Smith SJ. (2000). Phorbol esters potentiate evoked and spontaneous release by different presynaptic mechanisms. J Neurosci. 20(21):7863-7870.

Weiss N, Hameed S, Fernández-Fernández JM, Fablet K, Karmazinova M, Poillot C, Proft J, Chen L, Bidaud I, Monteil A, Huc-Brandt S, Lacinova L, Lory P, Zamponi GW, De Waard M. (2012). A Ca(v)3.2/syntaxin-1A signaling complex controls T-type channel activity and low-threshold exocytosis. J Biol Chem. 287(4):2810-2818.

Westenbroek RE, Ahlijanian MK, Catterall WA. (1990). Clustering of L-type Ca2+ channels at the base of major dendrites in hippocampal pyramidal neurons. Nature. 347(6290):281-284.

Westenbroek RE, Hell JW, Warner C, Dubel SJ, Snutch TP, Catterall WA. (1992). Biochemical properties and subcellular distribution of an N-type calcium channel alpha 1 subunit. Neuron. 9(6):1099-1115.

Westenbroek RE, Sakurai T, Elliott EM, Hell JW, Starr TV, Snutch TP, Catterall WA. (1995). Immunochemical identification and subcellular distribution of the alpha 1A subunits of brain calcium channels. J Neurosci. 15(10):6403-6418.

Williams C, Chen W, Lee CH, Yaeger D, Vyleta NP, Smith SM. (2012). Coactivation of multiple tightly coupled calcium channels triggers spontaneous release of GABA. Nat Neurosci. 15(9):1195-1197.

Williams ME, Feldman DH, McCue AF, Brenner R, Velicelebi G, Ellis SB, Harpold MM. (1992). Structure and functional expression of alpha 1, alpha 2, and beta subunits of a novel human neuronal calcium channel subtype. Neuron. 8(1):71-84.

Williams S, Serafin M, Mühlethaler M, Bernheim L. (1997). Facilitation of N-type calcium current is dependent on the frequency of action potential-like depolarizations in dissociated cholinergic basal forebrain neurons of the guinea pig. J Neurosci. 17(5):1625-1632.

Williams SR, Stuart GJ. (2000). Action potential backpropagation and somato-dendritic distribution of ion channels in thalamocortical neurons. J Neurosci. 20(4):1307-1317.

Wiser O, Cohen R, Atlas D. (2002). Ionic dependence of Ca2+ channel modulation by syntaxin 1A. Proc Natl Acad Sci. USA. 99(6):3968-3973.

Wiser O, Trus M, Hernández A, Renström E, Barg S, Rorsman P, Atlas D. (1999). The voltage sensitive Lc-type Ca2+ channel is functionally coupled to the exocytotic machinery. Proc Natl Acad Sci USA. 96(1):248-253.

Witcher DR, De Waard M, Sakamoto J, Franzini-Armstrong C, Pragnell M, Kahl SD, Campbell KP. (1993). Subunit identification and reconstitution of the N-type Ca2+ channel complex purified from brain. Science. 261(5120):486-489.

Wu LG, Saggau P. (1995). Block of multiple presynaptic calcium channel types by omega-conotoxin-MVIIC at hippocampal CA3 to CA1 synapses. J Neurophysiol. 73(5):1965-1972.

Wu LG, Westenbroek RE, Borst JG, Catterall WA, Sakmann B. (1999). Calcium channel types with distinct presynaptic localization couple differentially to transmitter release in single calyx-type synapses. J Neurosci. 19(2):726-736.

Wycisk KA, Budde B, Feil S, Skosyrski S, Buzzi F, Neidhardt J, Glaus E, Nürnberg P, Ruether K, Berger W. (2006). Structural and functional abnormalities of retinal ribbon synapses due to Cacna2d4 mutation. Invest Ophthalmol Vis Sci. 47(8):3523-3530.

Xu W, Lipscombe D. (2001). Neuronal Ca(V)1.3alpha(1) L-type channels activate at relatively hyperpolarized membrane potentials and are incompletely inhibited by dihydropyridines. J Neurosci. 21(16):5944-5951.

Yamazaki K, Shigetomi E, Ikeda R, Nishida M, Kiyonaka S, Mori Y, Kato F. (2006). Blocker-resistant presynaptic voltage-dependent Ca2+ channels underlying glutamate release in mice nucleus tractus solitarii. Brain Res. 1104(1): 103-113.

Yang J, Tsien RW. (1993). Enhancement of N- and L-type calcium channel currents by protein kinase C in frog sympathetic neurons. Neuron. 10(2):127-136.

Zamponi GW. (2003). Regulation of presynaptic calcium channels by synaptic proteins. J Pharmacol Sci. 92(2):79-83.

Zamponi GW, Bourinet E, Snutch TP. (1996). Nickel block of a family of neuronal calcium channels: subtype- and subunit-dependent action at multiple sites. J Membr Biol. 151(1):77-90.

Zander JF, Münster-Wandowski A, Brunk I, Pahner I, Gómez-Lira G, Heinemann U, Gutiérrez R, Laube G, Ahnert-Hilger G. (2010). Synaptic and vesicular coexistence of VGLUT and VGAT in selected excitatory and inhibitory synapses. J Neurosci. 30(22):7634-7645.

Zhang Y, Chen YH, Bangaru SD, He L, Abele K, Tanabe S, Kozasa T, Yang J. (2008). Origin of the voltage dependence of G-protein regulation of P/Q-type Ca2+ channels. J Neurosci. 28(52): 14176-14188.

Zhang L, Goldman JE. (1996). Developmental fates and migratory pathways of dividing progenitors in the postnatal rat cerebellum. J Comp Neurol. 370(4):536:550.

Zhang JF, Randall AD, Ellinor PT, Horne WA, Sather WA, Tanabe T, Schwarz TL, Tsien RW. (1993). Distinctive pharmacology and kinetics of cloned neuronal Ca2+ channels and their possible counterparts in mammalian CNS neurons. Neuropharmacology. 32(11):1075-1088.